Delft University of Technology
MSc Sustainable Energy Technology

Master Thesis

Comparison of Different Engagement and Dispatch Protocols applied to the Units Responsible of Charging and Discharging an Ocean Battery System: Simulation-based Study to Evaluate the Efficiency and Performance of the System

---

Author:
Luca Pasqualini - 4830156

Supervisors:
dr. Laura Ramirez Elizondo
Marijn van Rooij – Co-founder & CTO – Ocean Grazer BV

January 25, 2021

Abstract

The company Ocean Grazer BV is interested in launching to the market a novel storage technology: the Ocean Battery. Such battery will be installed under the sea with the purpose to store the surplus power produced by wind turbines in the form of potential energy by filling an elastic bladder, exposed to the ocean pressure, with water.

This piece of work has two purposes: the first is to create in Simulink a model which can simulate the dynamic behavior of the hydraulic and electric components used for the filling and draining process of the bladder. The second, is to study how the engagement and dispatch protocol of the Battery Management System, applied to different configurations of the electric components, changes the efficiency and the performance of the system. Ultimately, the optimal configuration and protocol are evaluated and decided.

The method that has been used is a simulation-based study. Mainly two electric components have been considered: a fixed operation one, the Three-phase Asynchronous machine, and a variable operation one, the Brushless Direct Current machine. These machines have been stacked up and put into work as parallel operating units at groups of five. Different configurations are considered and studied, each of them has its own protocol. The produced Simulink program has been used to simulate different situations and the responses of the stacks have been compared.

From these simulations it emerged that the early activated Three-phase Asynchronous Machine stack is the optimal solution for this type of problem. This configuration, which does not allow variable speed operation, performs surprisingly well in all the simulations run and, while keeping the efficiency always high, its protocol is also prone to be slightly changed to cope with the needs of different situations.

The study solves the problems of the company which now has a dynamic model able to simulate the behavior of the power exchanging parts of the Ocean Battery and knows what the strengths and the weaknesses of the different configurations and protocols are. An optimal solution for the considered case has been found.

Nevertheless, this study does not include the possibility of having more storage units communicating among them which remains an unsolved problem for the company. This further work could possibly be implemented starting from this thesis and using the created Simulink program, which is a new useful tool the company now possesses to progress in its growth.

Table of Contents

List of Figures

List of Tables

1. Introduction

1.1. Problem analysis

The main objective of this thesis is to investigate on how the engagement and dispatch protocol of the battery management system of the Ocean Battery influences the efficiency and performance of the whole system. This research is also intended to create a dynamic model for the hydraulic and electric elements constituting the Ocean Battery which will be used to run simulations. Such elements that need to be put at work together are the ones designated to the charging and discharging process. Once conclusions are drawn, the created program, which is the deliverable of this work, could be used by the company Ocean Grazer BV to run further simulations in the future.

1.1.1. Problem background

Ocean Grazer BV is interested in launching a product. Their focus at the moment is the Ocean Battery, an innovative storage system which is based on the possibility of storing water at high pressure on the seabed.

The water stored is confined by an elastic bladder which will push it outside the battery through a turbine when power is to be delivered. If Ocean Grazer BV succeeds to launch this product to the market and to fully integrate this product, it can be considered a novel technology that efficiently reuses the area between neighboring wind turbines and that can be a valuable addition to wind farms. Storage systems are the bottleneck of the renewable energy transition. The added value of coupling a storage technology to a renewable energy generator is the fact that the intermittent nature of the renewable energy source, which is the main drawback of these technologies, can be avoided by storing energy when a production surplus is available and delivering the energy previously stored when there is an high demand.

The scientific contribution of this piece of work, resides on the fact that multiple pump and turbine units in parallel as the power exchanging element for the Ocean Battery have not been studied before and the results coming from this thesis will be used as a baseline in the future to do further research on the topic and also to implement the already existing studies the company has.

Moreover, this thesis elaborates on another important aspect that has never been studied on the Ocean Battery: the relationship protocol used by the storage technology, and the efficiency of the storage system itself. Knowing the aspects of this relationship is essential to determine the best protocol to implement in the system.

Being still in the research and development phase of the project, it is very challenging to retrieve information that are certain and have not changed over time: studies done two years ago by the company on this topic are already considered obsolete and some of the data used in these works have changed and are no longer considered reliable. Furthermore, not so many publications can be found about this topic on the Ocean Battery and there are not many benchmarks from which it is possible to continue researching from.

One of the few it was possible to take inspiration from, is a master thesis project done by the student Kirsten Niekolaas from the University of Groningen named "Revenue maximization of distributed Ocean Battery systems through Model Predictive Control". She modeled a control mechanism which aimed at revenue maximization for a distributed system of Ocean Batteries all connected by themselves and to a wind farm.

Not all features though could be considered in this latter work: the main part that is missing is a thorough dynamic model of the storage technology. The dynamic model of the storage technology not only concerns the electric parts (electric machines) but also the hydraulic parts (pumps and turbines) which are to be coupled to the first ones. Having this dynamic model handy, will allow the company to implement it in the previous work to see if the revenue maximizing configuration changes and, if so, to find the new one. Moreover, the other deliverable of this thesis, the Simulink program, will be a useful tool for Ocean Grazer BV to simulate new scenarios for the Ocean Battery and see how it reacts.

1.1.2. Problem statement

From the problem background, the problem statement is defined as follow:

"The problem is that the relationship between the engagement and dispatch protocol governing the Battery Management System and the efficiency and performance of the whole system is unknown, also a dynamic model of the hydraulic and electric parts of the Ocean Battery working as parallel units has not been studied before."

Such topics are of great interest for the company since they could implement the solutions to these problems found in this work in their future research.

1.2. Scope of the research

The Ocean Battery is a battery that can store mechanical energy in the form of water under pressure: the water pressure at a given depth. It is composed of many parts such as: the concrete structure, the elastic bladder, the atmospheric pressure water tanks, electric components, hydraulic components et cetera. When the energy produced by the wind turbines connected to the battery is abundant and cannot be completely delivered to the grid, such energy is used to run the motors. The motors are connected to the pumps which move water from the atmospheric pressure tank inside the elastic bladder. The bladder is subjected to high pressure caused by the weight of the ocean water surrounding it, so when more energy is needed on the demand side, the water is pushed from the bladder to the atmospheric pressure tank by the pressure difference via hydraulic turbines. The turbines are connected to generators which will convert the mechanical rotational energy of the turbines into electrical energy to be delivered to the grid.

The whole system is quite complicated and broad hence the scope of the research is limited to the following. The hydraulic and electric components will be dimensioned, put together and dynamically tested to study how the efficiency varies. Also, efficiency related parameters will be studied by changing the engagement and dispatch protocol governing the BMS and the configuration of the system.

The main parts of the scope of the research can be categorized as follow.

- **Pump and Turbine dimensioning.** First, the dimensioning of the hydraulic elements needs to be performed in accordance with the company needs.
- **Electric Motors and Generators.** Different models of electric machine will be studied and then coupled with the hydraulic part of the system.
- **Coupling of the hydraulic and electric system.** These elements present some peculiarities, and it is important to study them and to find how the efficiency varies according to them.
- **Efficiency.** Finding a way to state whether one configuration is more suitable than another can be done by comparing the efficiencies of the system, defined as the ratio between the energy output and input.
- **Simulations.** Many simulations will be run to study the behavior of the change in of the system when using a different engagement and dispatch protocol for the BMS.

Other parameters such as closeness to ideal behavior and efficacy will also be studied during the simulations.

1.3. Research goal

First the goal statement is formulated, then the research questions are presented and finally the operationalization is explained.

1.3.1. Goal statement

The goal statement is defined as follow.

"The goal is to develop different engagement and dispatch protocols for the battery management system and to study how they affect the efficiency and the performance of the system, so that a suitable configuration of the hydraulic and electric components used to charge and discharge the Ocean Battery can be designed for a further installation."

This project covers different topics, the ones previously presented. To address them all some literature review on these topics needs to be done firstly, later all the information can be put at work in Simulink to create a dynamic model. This leads to a better understanding of what are the main parts of the system and where it is possible to intervene to obtain the desired result.

It is important to state that this work has a double valence: the first part is intended to be more useful to the company since the already existing knowledge on the subject is used to dimension and create the dynamic model, and literature is used to justify the choices taken to make the model work. The second part, the one concerning the development of the different engagement and dispatch protocols, the simulations, and the results, besides being of great interest for the company is also the part that accounts more for the scientific contribution of this work since, has previously stated, multiple pump and turbine units in parallel working as the power exchanging element for the Ocean Battery have not been studied before. Proposing this novel set-up, opens the door to a whole new field of interest orbiting around this topic which is the dependency of the efficiency and the performance of the Ocean Battery on the protocol governing the battery management system which is entrusted of charging and discharging the storage technology.

To find such dependency critical thinking, experience and simulations will be used. As already mentioned, once this problem has been solved and a suitable configuration found, these

results could be used by the company and implemented in all their previous studies, among them especially the above-mentioned revenue maximizing program.

1.3.2. Research questions

The main research question that serves as a basis throughout this research to achieve the goal which is shortly formulated as follows.

"How do changes in the engagement and dispatch protocol of the battery management system influence the efficiency and the performance of the Ocean Battery?"

To answer the main question, some sub-questions need to be answered first. The sub-questions are formulated as follow:

1) *Which pump and turbine model should be used?*
2) *How can the hydraulic part be dimensioned?*
3) *Which electric motors and generators models are suitable for the Ocean Battery?*
4) *What are their characteristics and limitations?*
5) *Can the hydraulic and electric components be easily coupled?*
6) *Which configurations should be taken into consideration?*
7) *Which parameters should be considered when running the simulations?*
8) *How can I state whether one configuration is better than another?*

1.3.3. Operationalization

Based on the aforementioned sub-questions, the steps to answer these sub-questions are listed in this section. These steps will ultimately lead to answering the main research question.

1) The suitable hydraulic parts can be chosen by doing some literature research according to the constraints given by the company.
2) The hydraulic part can be dimensioned by studying papers and overall performing some literature review. Furthermore, personal previous knowledge will help.
3) Some requirements on the motor and generator type are given by the company. Finding electric components that can fulfill them can be done by doing research and also studying pre-set models in Simulink.
4) The characteristics and limitations of the motors and generators can be known by performing studies on the models and simulation in Simulink so to obtain the motor and generator characteristics. Once these are known, mathematical knowledge, critical

thinking and literature research can be used to find these parts' limitations and main features.

5) Some conditions need to be respected when coupling the hydraulic and electric parts. If these constraints are not taken into consideration, some redesigning needs to be performed.
6) The configurations that will be studied and compared, are decided by myself alongside with the company supervisor. Experience and intuition are a good way to decide which configurations are worth mentioning and studying.
7) Some parameters to be studied are straight-forward, like the efficiency. Others are decided while running the simulations to highlight some strengths and weaknesses of the different engagement and dispatch protocols and configuration. Experience from the company and critical thinking are key to decide such parameters.
8) It is possible to state if one configuration is better than another by analyzing the results coming from the simulations. Such results will be compared and ranked. The higher the ranking, the better the

1.4. Conceptual Model

As previously explained, the goal of this research is to find how the engagement and dispatch protocols of the battery management system affects the efficiency and the performance of the system, so that the optimal configuration of the hydraulic and electric components working in parallel and used to charge and discharge the Ocean Battery can be decided and installed. This work is more focused on the technical side of the Ocean Battery rather than its economics. In fact, the variables that will be considered in the system are the power exchanged by the electric components and the flowrate processed by the hydraulic components. The fact that it is possible to perform a study on the optimization of the efficiency and the performance starting from the previously mentioned variables, comes from the idea of putting more units in parallel. If only one motor, one pump, one turbine and one generator were to be installed there would have not been need for an optimization.

The objective of these thesis is to find the engagement and dispatch protocol of the BMS such that the efficiency, and other parameters related to it, are optimized. The configuration that leads to the best trade-off between high efficiency, closeness to the ideal behavior, efficacy and reliability among the proposed ones will be the optimal.

Figure 1 shows the schematic of the conceptual model: on top of it there is the objective of the thesis, which is to find the optimal configuration for the system. This must be done merging the outcomes of the study of two parallel works. The first outcome that must be achieved is the creation of the system stacks, meaning the cluster of modules of coupled hydraulic and electric units. One hydraulic unit (pump or turbine) coupled with an electric unit (motor or generator respectively) for a module. More modules (a cluster) for a stack. Every stack is governed by its own engagement and dispatch protocol. Such stacks are represented and studied in Simulink. A good Simulink model is crucial since it will be used to calculate all the efficiency related parameters of the system. The creation of a Simulink model comes from the possibility of coupling hydraulic and electric components of the system in such a way that they can communicate together, as explained in the paper "Modelling and simulation of micro hydro power plant using matlab simulink" [1]. These components that are to be coupled together are, respectively, pumps and turbines, and motors and generators. These parts are the foundation of the system, therefore choosing them wisely is the very first step of the research. This whole process is checked before assembling the stacks.

The second outcome that will be used to reach the goal of the thesis is the analysis of the simulations and the ranking of the efficiency related parameters coming from every simulation.

1.4.1. Conceptual Model Recap

To summarize it can be understood that:

- Two different topics need to be studied and treated differently.
- Starting from the choice of the hydraulic and electric components, the modules are formed coupling them together.
- A Simulink model that calculates the efficiency of the modules is needed.
- Stacks made of different configurations between components and modules are to be created and put in operation in the program.
- Once the stacks are formed, simulations can be run, and the efficiency related parameters can be studied and ranked.
- Finally, the configuration that uses the engagement and dispatch protocol which optimizes the efficiency related parameters of the system can be found and eventually improved.

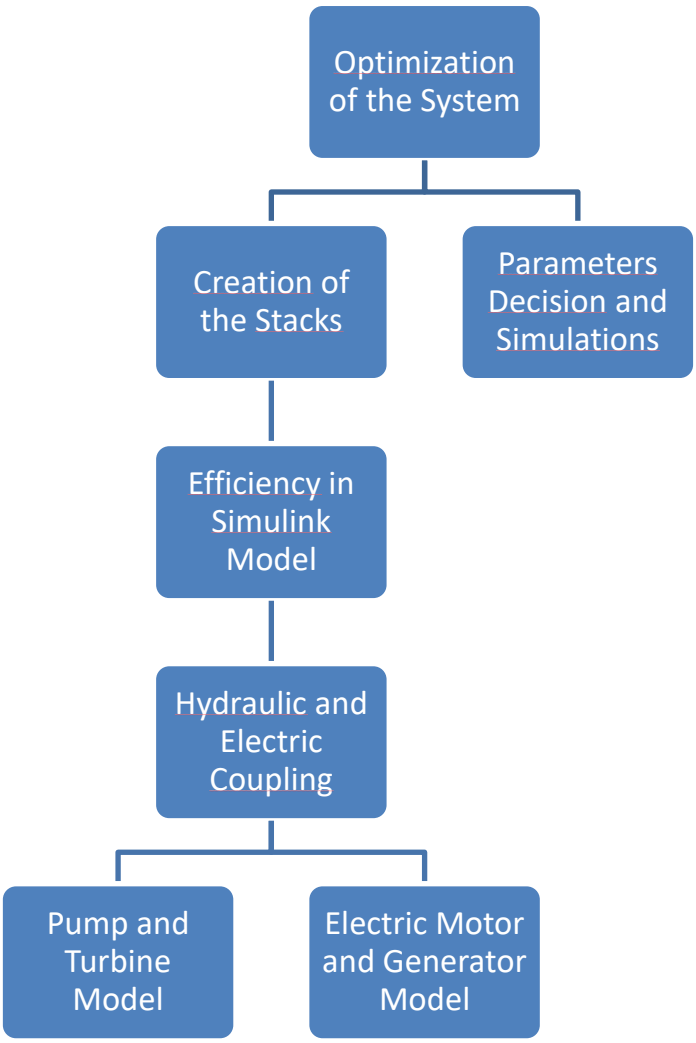

Figure 1 - Conceptual Model

1.4.2. Methodology

This subchapter explains more in detail the methods used to follow step by step the conceptual model.

1.4.2.1. Hydraulic system

Firstly, the hydraulic system will be chosen and dimensioned using mathematical formulas and the bibliography. Starting from the needs of the company (power requirement and available head, mainly) the pump and turbine model can be decided. Such model has its advantages, disadvantages and characteristics that will be discussed referring to the used bibliography. The dimensioning is done gleaning information from the cited bibliography. Graphs made with Matlab will be presented and explained. Also, a mathematical method called 'linear extrapolation' is explained and used. Lastly, it will be explained how the efficiency varies at different flowrate processing conditions.

1.4.2.2. Electric system

As for the hydraulic system, the choice of the electric components (motors and generators) comes from the needs of the company. Bibliography is essential to understand which type of machines are suitable to be installed in the system. It goes without saying that critical thinking is a key part in the choice. Simulink is used to gain the motor and generator characteristics of the machines and their specifics. The acquired data have been later processed in Matlab to produce graphs. Bibliography has been consulted throughout the whole process.

1.4.2.3. Hydraulic and electric coupling

The process of coupling these two systems might seem straight forward but it is not. Mathematical thinking and bibliography are essential to perform such action and finally determine whether the coupling is stable or unstable. The paper "Modelling and simulation of micro hydro power plant using matlab simulink" [1] has been used to justify the way the two systems have been put to work together in Simulink.

1.4.2.4. Efficiency in the Simulink model

Once assembled the Simulink model, the way the efficiency has been calculated comes from the mathematical definition of efficiency: the ratio between the energy delivered to its end user, the grid while discharging and the battery while charging, and energy supplied by the generation side, this time the battery while discharging and the grid while charging. The amount of energy is simply calculated by Simulink.

1.4.2.5. Creation of the stacks

The stacks have been assembled in Simulink, and the engagement and dispatch protocol behind them comes from critical thinking and from the suggestions of the company. Experience is what lead the company CTO to give such advice.

1.4.2.6. Parameters decision and simulations

The simulations have been carried out in Simulink and have been either requested by the company or discussed among the company and the writer. Every simulation is intended to determine the behavior of a particular efficiency related parameter which will be ranked to determine the optimal protocol and configuration of the system. Experience and foresight are what drove the company requests; intuition, previous knowledge and literature studies are what drove my decisions to run such simulations and study these parameters. The results have been processes in Matlab and Excel.

1.4.2.7. Optimization of the System

Although the term optimization has been used multiple times already, it is important to make clear that an optimization problem as such has not been formulated nor solved. Since there is

a small finite number of possible solution and their outcomes are known from the simulations, the optimal solution can be discovered even without solving the optimization problem.

2. Theoretical background and modelling

2.1. Pump and Turbine model selection and dimensioning

The first thing that needed to be done to study the dynamic behavior of a motor installed in the ocean battery was to decide which pump and turbine model is to be coupled to.

In order to decide the pump and turbine model, it is important to assess the working conditions and the needs of the battery.

The nominal power that this system needs to be designed for is of around 1 MW. To have a modular system, which as previously explained is less prone to failure and gives the possibility to later perform an optimization, it has been decided to build up the system using multiple modules of maximum power output of 200 kW machines each.

The head at which the pumps and turbines are meant to work is H = 45m. Value discussed and agreed with Marijn van Rooj, Ocean Grazer CTO and supervisor of this work.

Having these two values and assuming a nominal efficiency of ηp = 0.90 for the pump and ηt = 0.90 [2], the flowrate can be calculated using this formula:

$$P * \eta = \rho * g * H * Q \tag{1}$$

where ρ=1000 kg/m^3 is the density of water, g=9.8 m/s^2 is the gravity acceleration, Q is the flowrate to be calculated and P is the nominal power of the rotating element. It is also important to specify that the previously considered values of efficiency represent the total efficiency of the pump and turbine. This means the combination of the mechanical, volumetric and hydraulic efficiency of the rotating element. The generator and the system runway hydraulic losses will later be considered and explained.

From this calculation, it appears that the pumping flowrate of one single pump is Q_p = 0.40 m^3/s. Having estimated and calculated these values, it was possible to proceed and decide which pump model was suitable for this problem.

From Figure in Appendix A, which was taken from the website of a turbine manufacturer [3], it results that the Francis pump and turbine is a suitable model for my project. That is because under the previously estimated conditions, which are H=45m and Q_p = 0.40 m^3/s represented by the red lines in the graph, it can be noticed that the intersection between these two lines falls in the region of interest of the Francis turbine. Hence the Francis turbine, according to this picture, is a suitable pump and turbine model. It is important to say that the Francis model can

be used as a Pump as Turbine [4], meaning that the same machine can be used both in pump and in turbine configuration according to the needs of the moment. So, if the comparison between a Pump as Turbine (PaT) and Pump and Turbine separate systems is to be made, there will be no need to pick a different pump model. The Francis is a very versatile centrifugal reaction machine widely used in many power generation systems, especially in hydropower application [21]. It can both be used in a vertical and horizontal axis configuration. Hence, it is wise to shape this work over the decision to install this kind of turbine [2].

Figure 2 shows a representation of a Francis Turbine.

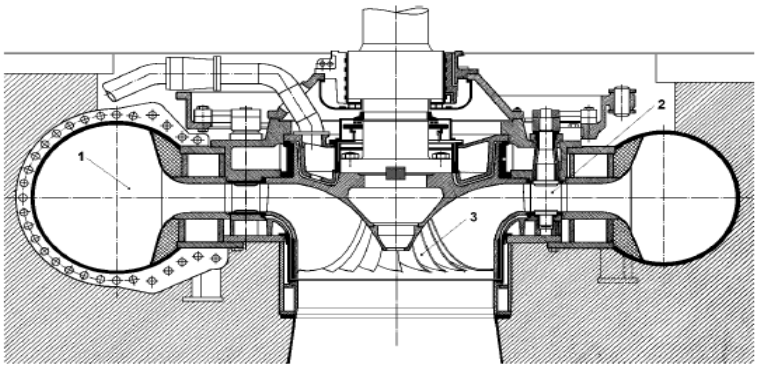

Figure 2 - Francis Turbine schematic representation [2]

Francis machines are usually operated at 80% of their maximum flowrate because the efficiency is higher around that value. Meaning that the nominal flowrate and rated power correspond to $0.8*Q_{max}$ and $0.8*P_{max}$ [2]. So $Q_{nom} = 0.32\ m^3/s$ and the nominal power output is $P_{nom} = 160\ kW$.

The fact that the nominal power of the hydraulic component is 160 kW has been thought because it corresponds to the nominal power of a pre-existing asynchronous motor model in Simulink, hence all the motor electrical characteristics will remain the same. The motor will later have to be coupled to the hydraulic part, so it is convenient to already tune the two parts choosing the same nominal power. Once the model has been selected, the dimensioning must be done. The process of the dimensioning is thoroughly explained in Appendix A. Table 1 and 2 show all the needed specifics of the hydraulic components used in the system.

Pump Type	Francis
Nominal Power (kW)	160
Nominal Head (m)	45
Nominal Efficiency (-)	0.90
Nominal Flowrate (m^3/s)	0.32
Nominal Angular velocity (RPM - rad/s)	1487 - 155.72
Specific Speed (m^3/s)	48.4
Impeller diameter (m)	0.41
Moment of Inertia ($kg*m^2$)	2.23

Table 1 - Pump Specifics

Turbine Type	Francis
Nominal Power (kW)	160
Nominal Head (m)	45
Nominal Efficiency (-)	0.90
Nominal Flowrate (m^3/s)	0.32
Nominal Angular velocity (RPM - rad/s)	1513 – 158.5
Specific Speed (m^3/s)	49.2
Impeller diameter (m)	0.3
Moment of Inertia ($kg*m^2$)	0.51

Table 2 - Turbine Specifics

2.2. Efficiency and flowrate

Once dimensioned the pump and the turbine, it is important to state the working conditions of such elements. Meaning that it is important to state how the efficiency changes while operating at different flowrates.

In order to obtain a precise efficiency-flowrate curve one would have to perform measurements on an existing installation, which was not possible. Therefore, it was found in literature a very useful paper explaining and showing the dependence of the efficiency at different flowrate for different turbines models. Once isolated the Francis curve (number 2 in Figure 3 [2]), it was just a matter of extrapolating precise numbers and putting them into Matlab to be processed. This whole process is carefully explained in Appendix B.

Figure 4 shows the efficiency-flowrate graph generated from this process. It is important to notice that, as anticipated, the maximum efficiency occurs at around 80% of the maximum allowable flowrate for the Francis machine. Also, during the start-up, some water inside the propeller of the turbine starts going in without having the machine actually producing power: this behavior can be seen at the very beginning of the curve where for flowrate smaller than 14% the efficiency is zero. This graph will be later used in a look-up table in Simulink to run the simulations.

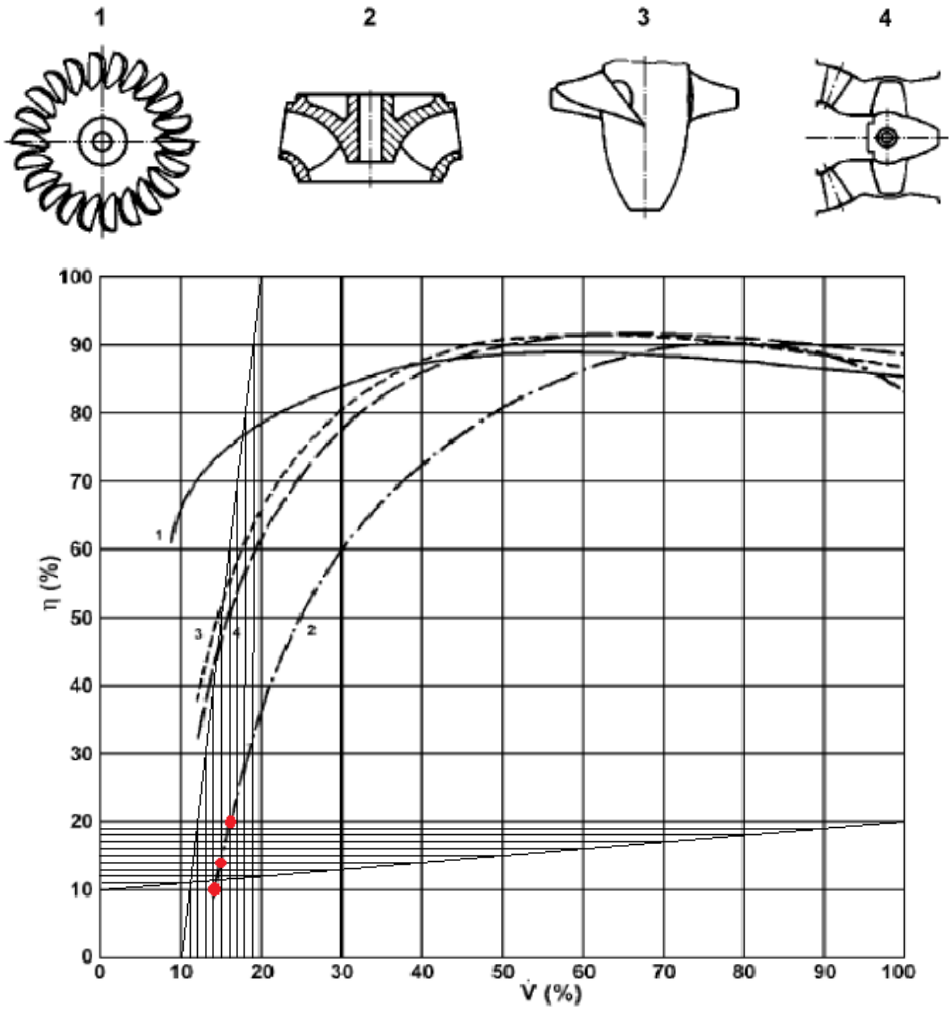

Figure 3 - Example of the extrapolation of the first operational points [2]

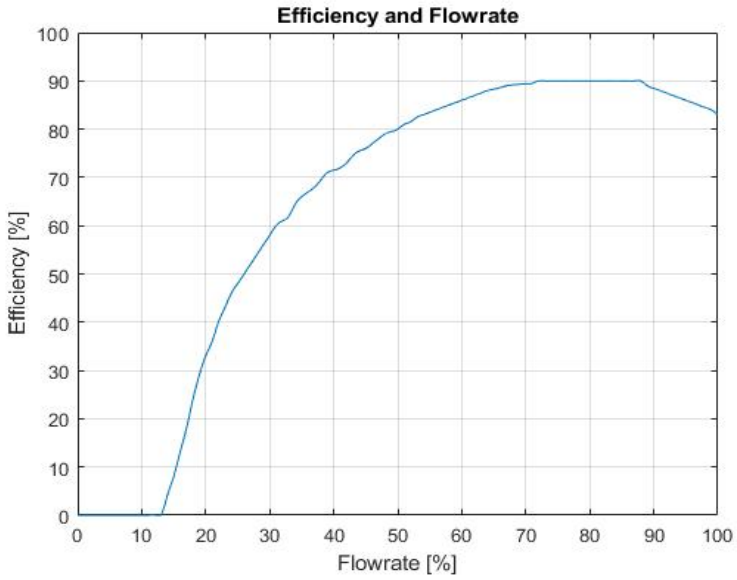

Figure 4 - Matlab Efficiency and Flowrate graph

2.3. Three-phase Asynchronous Machine SI units in Simulink

Once determined the pump and turbine specifics and their working conditions, it is now time to talk about the Motor and Generator type that will be coupled to these machines.

It was decided to use a Three-phase Asynchronous Machine (TAM) as Motor and Generator for the system. This type of machine is commonly used in power applications, especially in hydropower plants [2], besides Simulink offers a very good pre-set for this machine called "Asynchronous Machine SI unit".

The TAM is divided into two main parts: the stator, which is the fixed part connected to the grid with windings that can generate a magnetic rotating field and the rotor, which is the rotating part connected to the pump or turbine by a rigid shaft. Every winding that is present in the stator is called a pole. Two windings with opposite polarity that are put diametrically opposed in the stator are called a pole pair. This machine can both work as a motor, so extracting power from the grid and giving it to the pump, and as a generator, so converting the rotational energy of the turbine into electrical energy to supply to the grid.

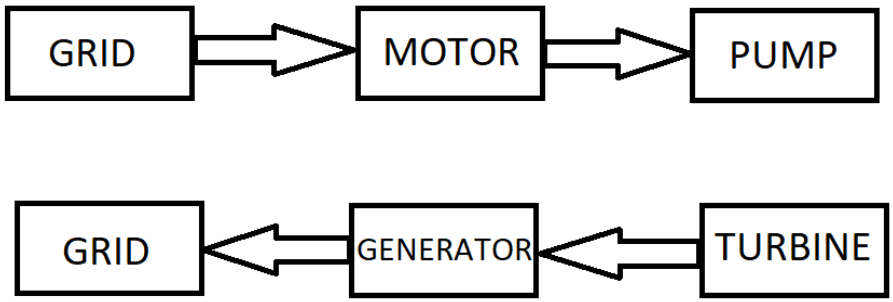

Figure 5 - Energy Flow representation used to visualize the difference between a motor and a generator

The name "Asynchronous" comes from the fact that two different angular velocities come to play: the velocity of the stator's rotating magnetic field and the rotor's magnetic field velocity. These two velocities must be different for the machine to work. When the stator's magnetic field rotates faster than the rotor's, then the TAM is in motor mode since the stator's magnetic field is "dragging" the rotor. While, if the rotor's rotating magnetic field is faster than the stator's rotating magnetic field then it is in generator mode and the rotor is "dragging" the stator's rotating filed. When the two velocities are the same then synchronism occurs and the machine is not receiving nor delivering any torque, therefore any power.

As previously mentioned, the rated power of the TAM is 160 kW. This is due to the fact that Simulink has a pre-set 160 kW TAM with the following characteristics:

Nominal Power (kW)	160
Line to line Voltage (V)	400
Frequency (Hz)	50
Rated Angular Velocity (RPM and rad/s)	1487 – 155.72
Stator Resistence (Ohm)	0.01379
Stator Inductance (H)	0.000152
Rotor Resistence (Ohm)	0.007728
Rotor Inductance (H)	0.000152
Mutual Inductance (H)	0.00769
Rotor Moment of Inertia (kg*m^2)	2.9

Table 3 - Asynchronous Machine Specifics

The motor characteristic is a graph that shows how the applied torque varies at different rotational speeds.

In order to construct such graph a simulation in Simulink had to be done. First, an infinite grid representation had to be connected to the TAM and then the machine was put at work at different velocities: from 0 to 1500 RPM, which is the synchronous velocity, hence the velocity at which the machine is not producing nor withdrawing power and torque. Adding a bus selector at the output of the machine it was possible to display the electromagnetic torque delivered by the machine.

The nominal angular velocity suggested by the Simulink block, 1487 RPM (equal to 155.7 rad/s), is for a machine with two pole pairs, therefore Figure 6 shows the motor characteristic of a 160 kW TAM, with line-to-line voltage of 400 V, frequency of 50 Hz e 2 pole pairs:

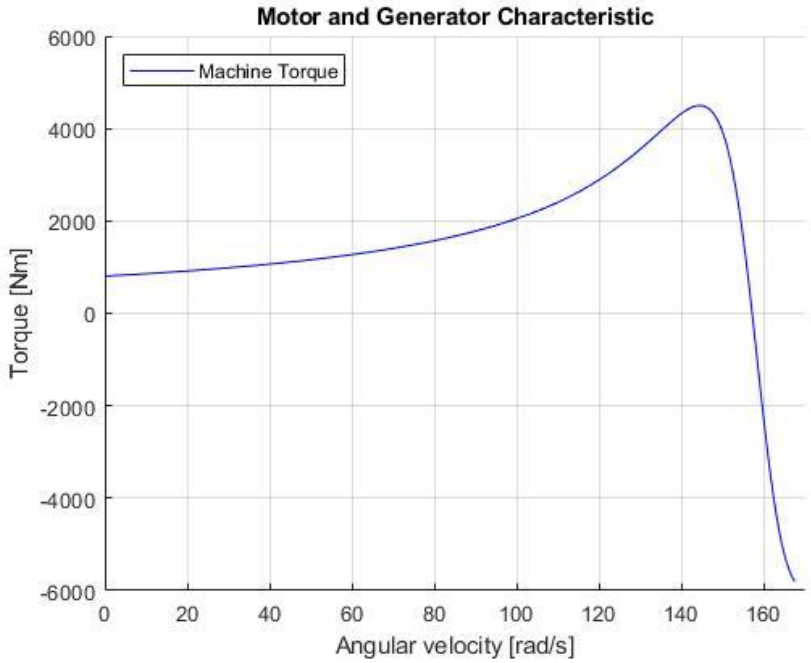

Figure 6 - Motor and Generator characteristic of a 2 pole pairs 160 kW Three-phase Asynchronous Machine

As mentioned in "Different Methods of Speed Control of Three-Phase Asynchronous Motor" [10], usually a TAM should be working at an angular velocity that is no greater nor smaller than 5% to the synchronism condition. This is since the electrical frequency is strictly dependent on the angular velocity of the machine. Of course, the smaller the variation in angular velocity, the closer to 50 Hz the electrical frequency of the machine will be. Equation 2 shows the relation between the angular velocity of a TAM and the electrical frequency output:

$$f = \frac{p * \omega}{2\pi} \tag{2}$$

Where *f* is the frequency, ω is the angular velocity and *p* is the number of pole pairs, which is 2 in this case.

In the case of the selected machine, a percentual variation of -0.9% of the synchronous velocity corresponds the nominal working condition in motor mode: this means that at an angular velocity of 155.7 rad/s (99.1% of 157.1 rad/s, the synchronism velocity) the motor produces the nominal torque.

For the machine to work in generator more, as can be seen in Figure 6, it would be enough to work past the synchronism velocity, 157.1 rad/s, so that the rotor would drag the stator rotating magnetic field.

Past the maximum torque point, occurring at around 145 rad/s, TAMs' torque is designed to decrease following the behavior of a straight line. So, varying the angular velocity the same

amount past the synchronism velocity, the machine is supposed to deliver a negative torque of the same magnitude as in motor mode.

A variation of +0.9% of 157.1 rad/s, corresponds to 158.5 rad/s. Operating the TAM at this angular velocity, indeed, it is possible to obtain the nominal torque in generator mode.

As anticipated, to calculate the power exchanged by the machine, one needs to multiply the electromagnetic torque value by the angular velocity.

$$P = T * \omega \tag{3}$$

Figure 7 shows the power produced by the motor over imposed the motor characteristic for the 2 pole pairs TAM:

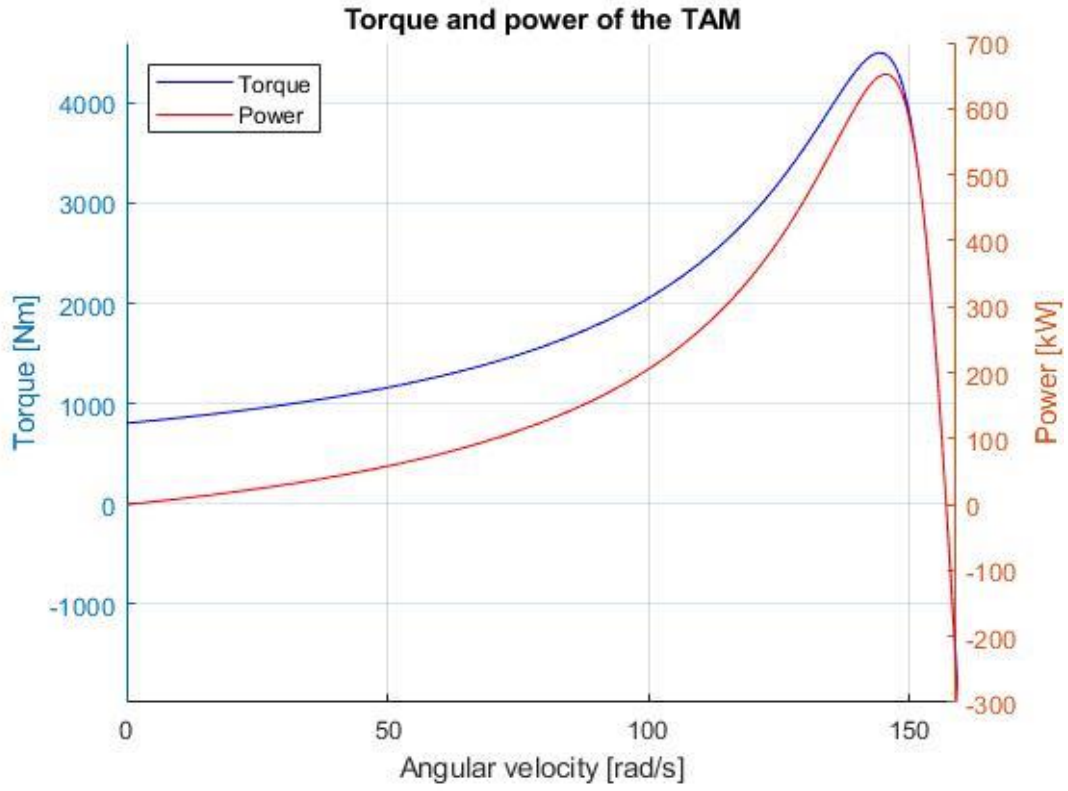

Figure 7 – Torque and Power generated by a 160 kW 2 pole pairs TAM

It is important to notice how, even if the rated power if the motor is 160 kW, as can be seen in Figure 7, in theory this motor would be able to deliver a maximum power of around 600 kW. The fact that the maximum applicable torque is way higher than the nominal is a desirable characteristic. The reason for this is that TAMs need to be working in stability conditions, which will be later explained, and stability happens when the motor characteristic is represented by a decreasing line.

Furthermore, it is important to notice that a slight change in angular velocity will considerably change the torque output and the power produced. From this consideration, it is possible to better understand what has been previously anticipated: this type of machines needs to be operated at constant speed. Angular velocity variations are not desirable and should be avoided with this type of motor and generator.

2.4. Centrifugal machine and motor coupling

Now that the pump, turbine and TAMs' behaviors have been described, it is time to couple them together. As explained in Figure 5, the pump is to be coupled to the TAM operating in motor mode, while the turbine is to be coupled to the TAM operating in generator mode.

2.4.1. Pump-Motor coupling

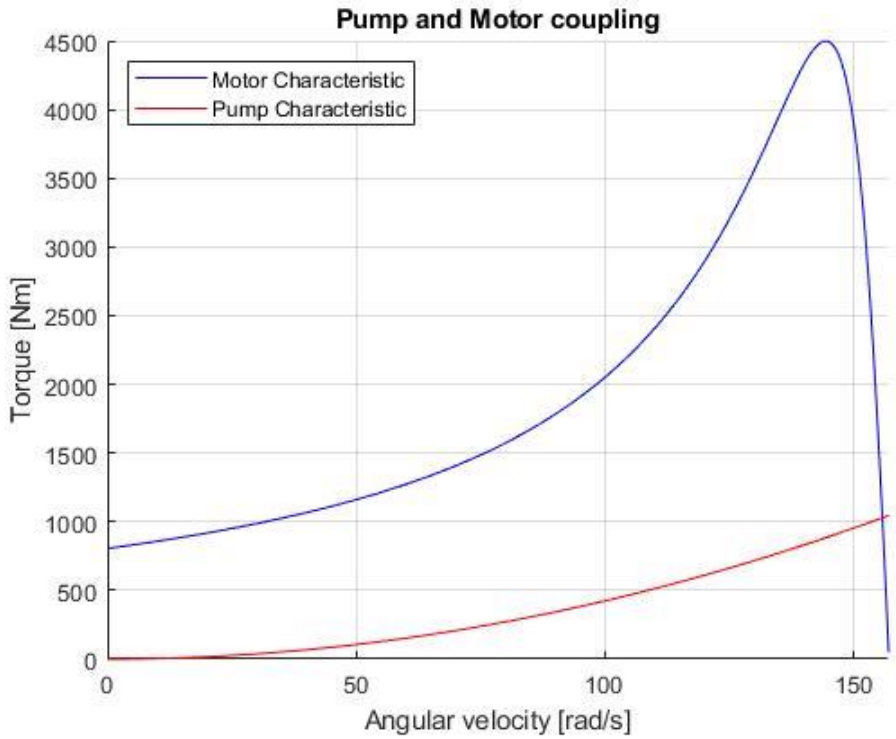

Figure 8 - Pump and Motor Characteristics coupled

Figure 8 shows the pump and the motor characteristic coupled together. The intersection between the two curves is the operational point, which is given by the angular velocity and the torque applied by the pump and the motor. Once these two values are known, the power exchanged can easily be calculated.

It is important now to stop and discuss about stability. Stability is the situation in which something is not likely to move or change. In other words: how can one be sure that this operational point is not going to change should any small perturbation occur?

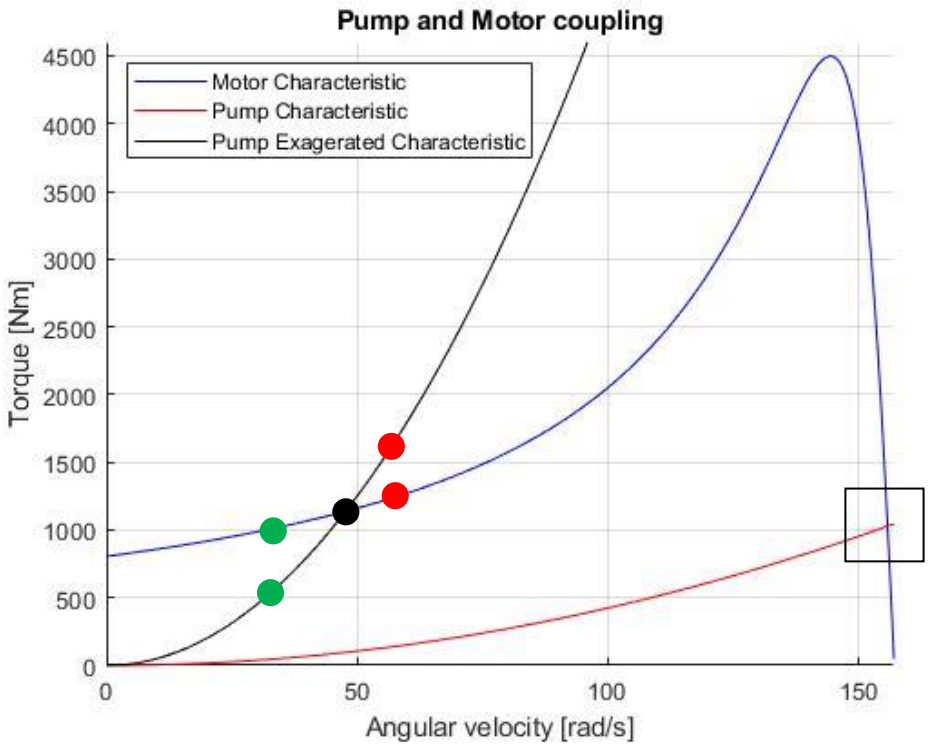

Figure 9 – Motor Characteristic coupled with two different pumps

Let us suppose that the pump characteristic was represented by the steeper black curve and that the operational point, in this situation, is represented by the black circle. If, due to a perturbation during operation which is likely to occur, the angular velocity of the motor increases, then also the torque that the motor can deliver would increase. If the angular velocity increases for the motor, it will also increase for the pump since the two elements are connected via a rigid shaft. And if the angular velocity of the pump increases, then also its required torque does. This situation is represented by the red circles in Figure 9. If this happens the motor will have to deliver more torque to cope with the load's need. And the only way the motor can do that is by accelerating. If the motor accelerates also the pump will, increasing again the torque it needs. This results in a situation of instability since the initial operational condition will never be reached again. The motor and the pump will continue accelerate until they can reach a stability point, if this does not happen then the system is shut down by a control mechanism or it breaks.

If, instead of increasing the angular velocity, the perturbation makes the motor slow down, it will be able to deliver less torque. Similarly, if the pump slows down as well, it will need less torque applied. At that point the motor control strategy will make the motor decelerate even more since the load's demand is lower than what it is currently delivering. This situation is

represented by the green circles in Figure 9. This is also a situation of instability where the pump will need less and less torque as it slows down, and the motor will keep on decreasing its angular velocity in order to supply just the torque is being demanded by the pump until it shuts down. In conclusion, the black circle in Figure 9, is said to be a non-stable operational point. Table 4 shows the schematic of the black circle just discussed.

Perturbation	**Consequence on the motor torque**	**Reaction of the pump**	**Consequence on the pump torque**	**Reaction of the motor**	**Conclusion of the cycle**
ω motor increases	T delivered by the motor increases	ω of the pump increases	T required by the pump increases to a higher value than the T delivered by the motor	The motor keeps on increasing its speed to cope with the pump needs and the cycle restarts	The cycle is iterated until the system either finds a stability point, or it is shut down or it breaks
ω motor decreases	T delivered by the motor decreases	ω of the pump decreases	T required by the pump decreases to a lower value than the T delivered by the motor	The motor keeps on decreasing its speed to cope with the pump needs and the cycle restarts	The cycle is iterated until the system either finds a stability point, or it shuts down automatically

Table 4 - Schematic of the instability point represented by the black circle in Figure 9

Figure 10 will now be analyzed. It is just a zoomed in representation of the box present in Figure 10. The black circle in Figure 10 is the actual operational point of the previously described system. The same discussion as before will be done for this operational point so to demonstrate that stability is reached during operation of the machine. Let us start by assuming that, due to a possible perturbation, the angular velocity of the motor increases. Similarly, the angular velocity of the pump will increase. Situation represented, again, by the red circles in Figure 10. When this happens, the torque required by the pump will increase, while the torque that the motor can deliver will decrease. In order to cope with the load's need, the motor will have to slow down to increase its deliverable torque. When the motor slows down, so the pump will, hence going back to the operational point: the black circle. If, on the contrary, due to a possible perturbation the motor slows down, likewise will the pump: the pump required torque will decrease while the motor deliverable torque will increase. Situation represented by the green circles in Figure 10. The pump requires a lower torque, so the motor will speed up in

order to deliver less torque. The pump will speed up as well until they both go back to the starting point: the black circle representing the operational point.

In conclusion, it can be said that the coupling of this motor and this pump can be made and can be operated in stable conditions as demonstrated.

Perturbation	**Consequence on the motor torque**	**Reaction of the pump**	**Consequence on the pump torque**	**Reaction of the motor**	**Conclusion of the cycle**
ω motor increases	T delivered by the motor decreases	ω of the pump increases	T required by the pump increases to a higher value than the T delivered by the motor	The motor decreases its speed to deliver more torque as required by the pump	A situation of stability is reached
ω motor decreases	T delivered by the motor increases	ω of the pump decreases	T required by the pump decreases to a lower value than the T delivered by the motor	The motor increases its speed to deliver less torque as required by the pump	A situation of stability is reached

Table 5 - Schematic of the stability point represented by the black circle in Figure 15

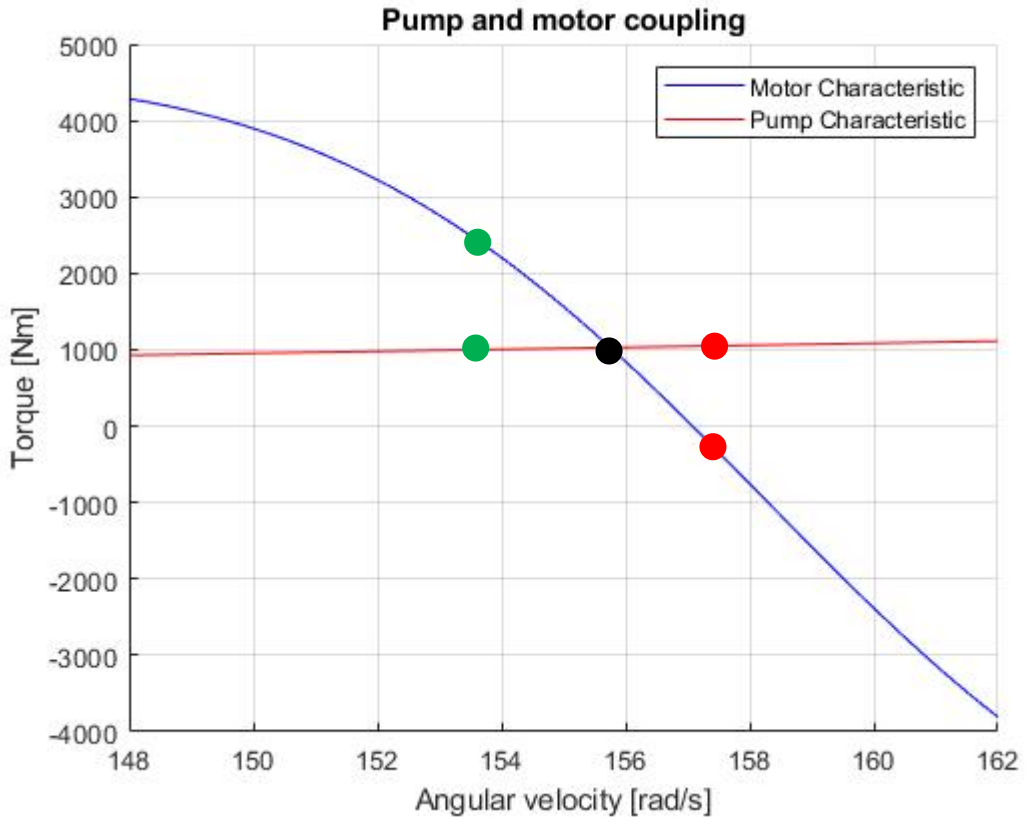

Figure 10 - Detail inside the box of Figure 9

2.4.2. Turbine-Generator coupling

It is important now to mention the fact that, while it is essential to speak about stability and instability for the coupling of a motor and a pump, this can be ignored in a turbine-generator system. The motor can withdraw as much energy from the grid as required by the pump: the motor responds to the pump needs. In a more colloquial way: the pump is the one that calls the shots, so if the rotating element is working at a certain rotational speed and its characteristic demands a high value of torque, the motor must respond to this by delivering such torque. A turbine, instead, will only exchange the energy that is supposed to produce regardless the generator characteristic. If the nominal power of the turbine is 160 kW, it shall not deliver more than that, not even if the generator is working at an operational point that demands a higher torque and so a higher power. For this reason, it does not make sense to talk about stability and instability since the turbine will work as supposed to and the generator will receive only as much power as the turbine delivers. Once again, the rotating element is calling the shots.

Figure 11 shows the coupling of the turbine with the generator.

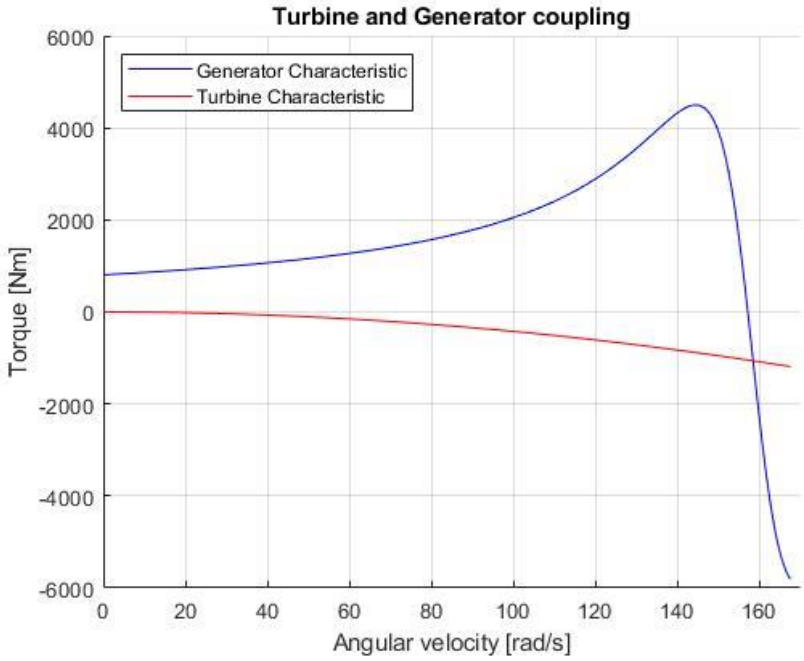

Figure 11 - Turbine and Generator characteristics coupled

For clarity's sake, Figure 12 shows the characteristics of the TAM, the pump and the turbine all in the same graph. It is important to notice that the operational point of the pump-motor coupling gives a positive torque and, as previously explained, is a stable point, while the torque delivered by the turbine-generator coupling gives a negative torque. The two operational points are very close to the synchronism velocity so the frequency variations will end up being extremely small and therefore acceptable.

Referring to Equation 2, the electrical frequencies during steady state for the two systems are:

$$f_{\text{PM system}} = 49.57\ Hz \qquad ; \qquad f_{\text{TG system}} = 50.39\ Hz$$

The two frequencies are, as desired, very close to 50 Hz so the systems can easily be integrated in the grid.

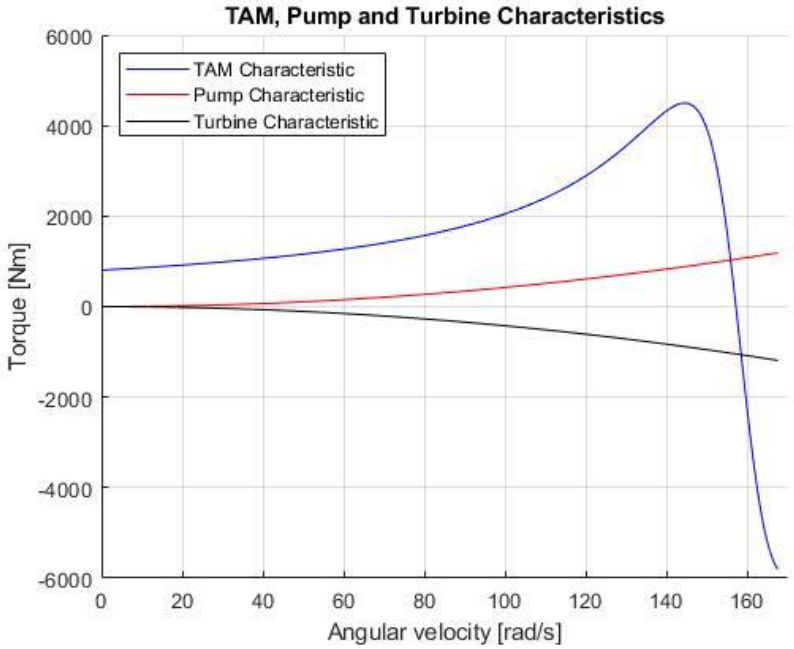

Figure 12 – TAM, pump, and turbine characteristics all in the same graph

2.5. Transient behavior of the system

Every mechanical system needs a certain amount of time to reach its nominal state speed-wise, such time period is called the transient time. Being the velocity a state variable a continuous function describes its behavior and its change over time when subject to certain conditions. Such conditions are explained in the Appendix D, from which it was possible to obtain the following equation.

$$\omega(t) = \omega_{\text{nom}} * (1 - e^{-\frac{t}{\tau}}) \tag{4}$$

In this equation τ represents the time constant of the system and has been calculated to be equal to:

$$\tau_{\text{pump}} = 0.777\ seconds \quad ; \quad \tau_{\text{turbine}} = 0.517\ seconds$$

Once the time constants are known, it is possible to proceed to calculate the transient time. The TAMs are very sensible to speed variations, meaning that the slightest perturbation in speed will make the machine supply or receive a very different torque value than the nominal one. Due to the high level of precision required by the system, it is possible to consider the transient over once the value of the angular velocity is equivalent to 99.7% of the nominal angular velocity. This condition is reached after six τs have passed as the exponential formula confirms:

$$\frac{\omega(6\tau)}{\omega_{\text{nom}}} = \left(1 - e^{-\frac{6\tau}{\tau}}\right) = 0.997$$

It is possible to say that the time required for the system to finish its transient it equal to 6τ. So:

$$\Delta t_{\text{pump}} = 4.66\ seconds \quad ; \quad \Delta t_{\text{turbine}} = 3.12\ seconds$$

These results are confirmed in "*Estimating reversible pump-turbine characteristics* " [4].

Figure 13 shows and compare the transients of the two systems. As previously demonstrated, the PM system takes more time than the TG since it has a bigger moment of inertia.

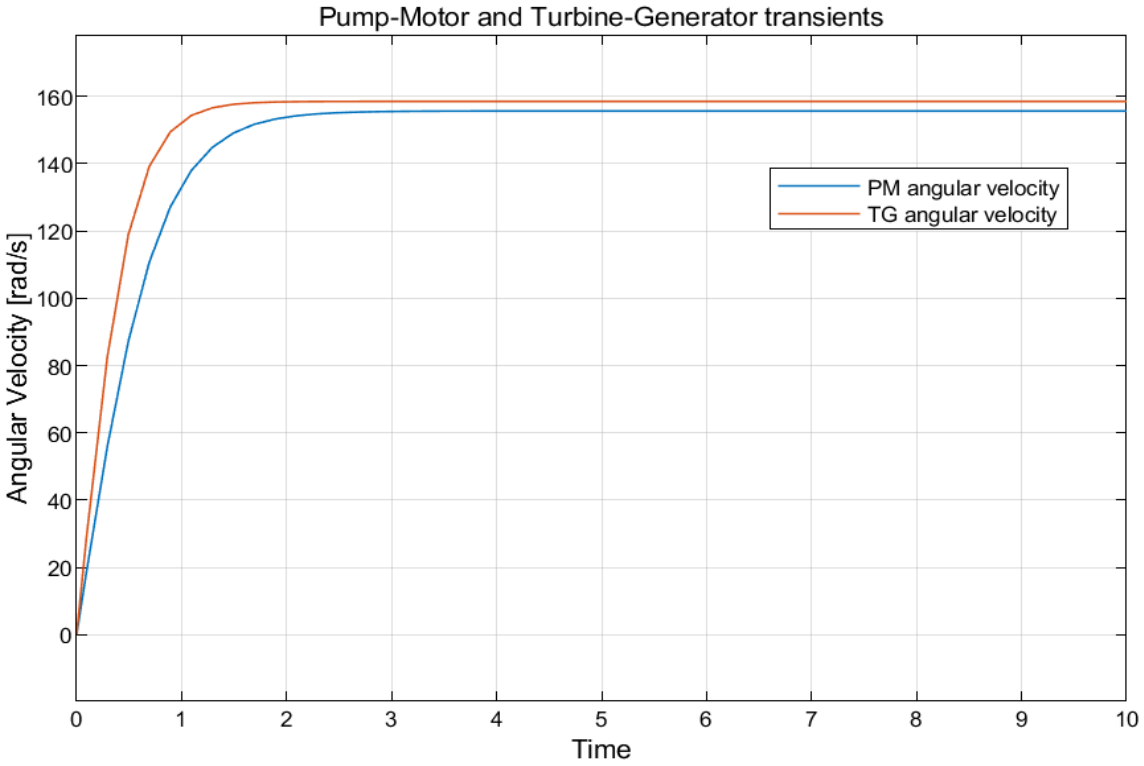

Figure 13 - Transients of the PM and TG system

Even if the previous discussion was focused on the start-up time of the system, it is important to say that the behavior of the system during the ramp-down is the same: it will decelerate following the same exponential function since the time constants τ are the same and so are the necessary Δt.

2.6. Simulink model

It is now time to merge all the previous information together to create a Simulink model that will describe the two systems: one for the PM system, and one for the TG system. The two systems are very similar to one another, they are both made of five main parts which are:

- pump and turbine model
- asynchronous machine blocks
- losses
- total energy calculation
- overall efficiency calculation

2.6.1. Pump and turbine model

The pump and turbine model are described in the insight in Appendix C and D, and so has the asynchronous machine block in section 2.3., what is very important to say is that, the input given to the PM system, is the angular velocity. This input value is given such that the electromagnetic torque generated by the TAM, is the nominal torque the system should deliver, therefore producing nominal power. On the contrary, the input given to the TG system, is the mechanical torque that the turbine is supposed to deliver, which will be converted by the transfer function in the angular velocity signal. This signal is the input given to the asynchronous machine block. It is possible to say that the main difference in the two systems, is the fact that in the PM system the grid is the first element that comes into play, which can directly and perfectly control the TAM.

2.6.2. Asynchronous machine block

The asynchronous machine is the second element involved whose output is the input of the third element: the pump. For the TG system is the other way around: the input given is the nominal torque the turbine can produce. This value is controllable. The output of the turbine is the rotor angular velocity which is the input of the second element that comes into play, the asynchronous machine. The outputs of the TAM block are used to calculate the power produced and the energy supplied to the third element of the system: the grid.

2.6.3. Losses

About the losses, they are calculated and added before the power is supplied to the final users of both systems. Meaning that the losses are accounted when calculating the energy supplied to the water in the pump system and when calculating the energy supplied to the grid by the generator. The losses that have been considered are: the varying of the efficiency of the rotating element with varying flowrate, as described in section 2.2., the motor efficiency,

supposed to be constant and equal to 97.3% (calculated from the Simulink block and confirmed by literature [8]) and the water runway losses. Since the runway geometry of the Ocean Grazer is yet not known, the value assumed for modelling this type of losses is an efficiency of 99%. This value is completely arbitrary at this stage. It has been put there to remind that, as explained in "Revenue optimization for the Ocean Grazer wave energy converter through storage utilization" [9], these losses are present and will need to be accounted for more thoroughly once the geometry of the systems is known.

2.6.4. Total energy and overall efficiency calculations

The total energy exchanged is very straight-forward to calculate in Simulink: once the power delivered to the final user (the water in the PM system, and the grid in the TG one) including all the previously explained losses has been calculated, a simple integrator block will do to calculate the total energy delivered. There are two integrator blocks for each system: one calculates the energy delivered to the final user, hence the energy output, while one calculates the energy input. It is easy to calculate the overall system efficiency just by taking the ratio between these two values.

Another important thing to state is the fact that, as previously explained, in the PM system the motor precedes the pump and losses are all accounted for after this element. The decisional input is the rotor-imposed speed which is to be delivered to the asynchronous machine. In the TG system on the contrary the turbine precedes the generator, and the decisional input is the turbine-imposed deliverable torque. As well as the PM system, losses are accounted for after the second element, which in this latter case is the generator. In both subsystems, the integrator blocks used to calculate the total energy exchanged are put one after the first element, and one after the losses' calculation part of the program.

Also the flowrate that is being processed has to be calculated. In the PM system the flowrate is calculated after all the losses have been considered: the output power signal is converted into the flowrate. On the other hand, in the TG system, the flowrate processed by the turbine is what put in action the whole discharging process, therefore the flowrate is calculated at the very beginning before the losses are considered.

3. Simulations

3.1. Simulations to calculate the efficiency of the systems with TAMs

Once described the Simulink code, it is now possible to run simulations to calculate the efficiency of the charging and discharging process for different operational time.

More effects are over-imposed during the start-up and the shut-down of the systems: variable efficiency of the pump and turbine, singular behavior of the TAMs at different angular velocities and the inertia of the rotating elements that will make the system still produce energy for some seconds after the system is turned off.

At the beginning of the simulation the two systems are at rest. They are run for different operational times ranging from 0.2 seconds up to 1800 seconds (30 minutes) in order to find how the efficiency changes and to determine its asymptotic value. The simulation runs longer than the actual operational time so that the anticipated effect of the inertia of the machine can be accounted for: once the machine is turned off, it will still be producing power since it will still be spinning.

As can be seen in Figure 14, the efficiency of the filling process, so the efficiency of the PM system, has an asymptotic value of 82%, while the one of the draining process, which corresponds to the TG system has a final efficiency value of 76%.

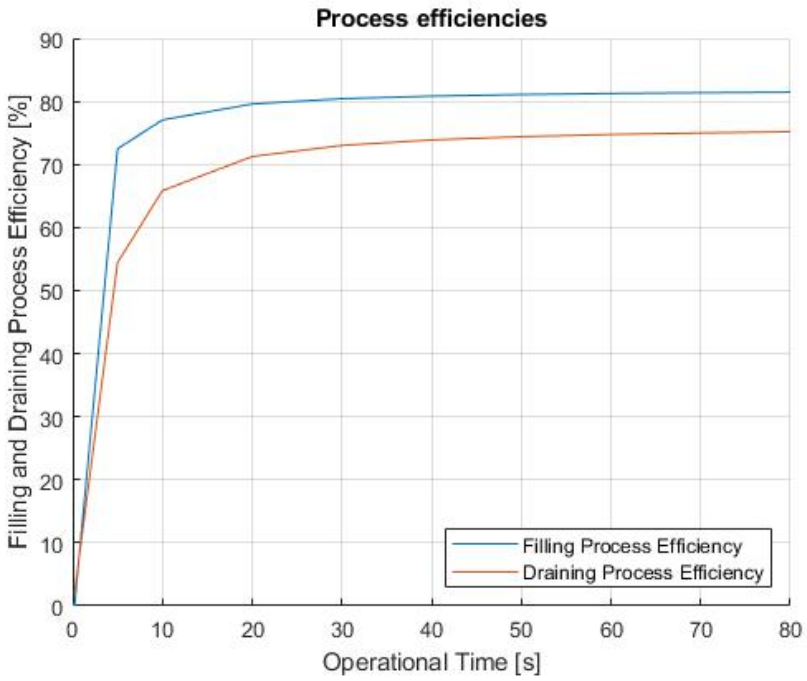

Figure 14 - Efficiencies of the process of filling and draining the tank for different operational times

As expected, the two curves are increasing. They start from 0, which means that for low operational times the two systems are not efficient. This is because the systems spend time processing a small flowrate which, as explained in section 2.2., is not efficient for the pump and the turbine. Also, it is important to notice that the PM system is more efficient than the TG system. This can be understood by looking at Figure 15 and 16:

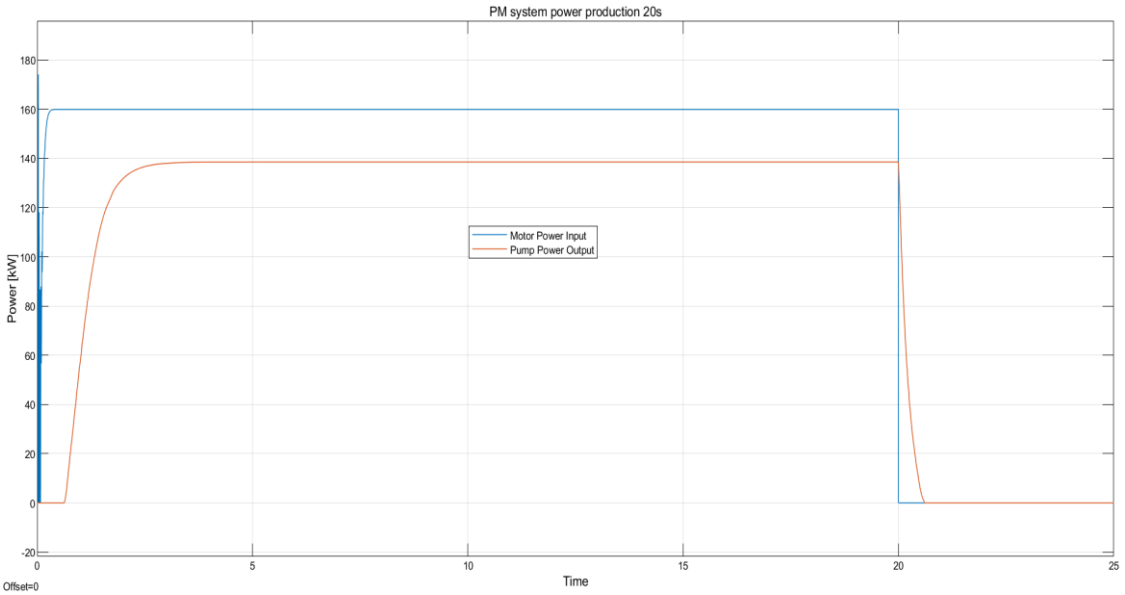

Figure 15 - Motor power input and pump power output for an operational time of 20 seconds

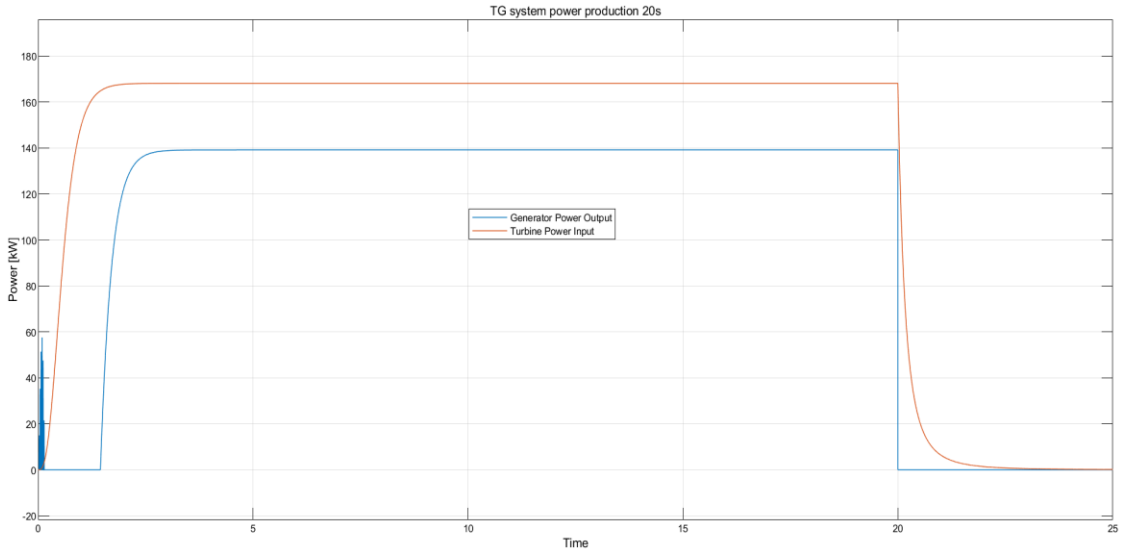

Figure 16 - Turbine power input and generator power output for an operational time of 20 seconds

During the start-up of the PM and TG system, both the pump and the generator need some time before they can start delivering energy to the battery and to the grid, respectively. At the very beginning of operations both the pump and the generator are not exchanging any energy. They reason why the pump is not exchanging any, or low, energy relies on its flowrate-efficiency dependency. If the flowrate is low, which it is during the start-up time, the energy delivered will be very low. For the generator, as explained in section 2.3., before the TAM starts operating in generator mode, it must pass the synchronism velocity. Before this happens, the TAM would be working in motor mode. Since the generator is not supposed to be withdrawing power from the grid, instead of having a negative value for the power production curve in Figure 16, it is enough to say that the generator is not producing any power. Hence, during start up, even if the turbine is delivering energy to the generator, the electric element is not able to deliver power to the grid, hence the efficiency is low.

Let us now analyze what happens during shut down. In the PM system, when the motor is switched off, no power is being withdrawn from the grid, but, due to inertia effects, the pump will still be spinning pumping some water inside the battery, therefore exchanging energy. This effect does increase the efficiency. On the contrary, in the TG system, the turbine does require some time before it comes to a stop so it will keep spinning for some time while consuming water not effectively used to produce electricity. In fact, this energy is not being delivered to the grid by the generator since the low rotational speed of the rotor will not allow generator operation. This energy is lost. This effect does decrease the efficiency.

The above-described effects are relevant when the transients have not negligible weight on the overall operation. This means that, as can be understood from Figures 17 and 18, the longer the operational time, the less important are the losses that occur during transients. From these figures it can also be understood how the ratio between the output power and the input power exchanged in steady state is equal to the asymptotic value of the efficiency.

It has to be said that for both systems, the behavior of the curves during start-up and shutdown is the same no matter the operational time, hence, the area underneath the curves, which represents mathematically the energy exchanged, is always the same during transient operations.

The reason why the filling efficiency is higher than the draining efficiency even when the losses occurring during transients are negligible, can be understood by looking at Figure 12 in section 2.4. and Figure 16 and 18 in this section. The rated power of the turbine is higher than 160 kW. That is because the turbine and the generator characteristics meet beyond the synchronism

velocity. The electric components though, have the same rater power this way. Having the TG system a greater power input than the PM with the same power output, results in a higher efficiency for the PM system.

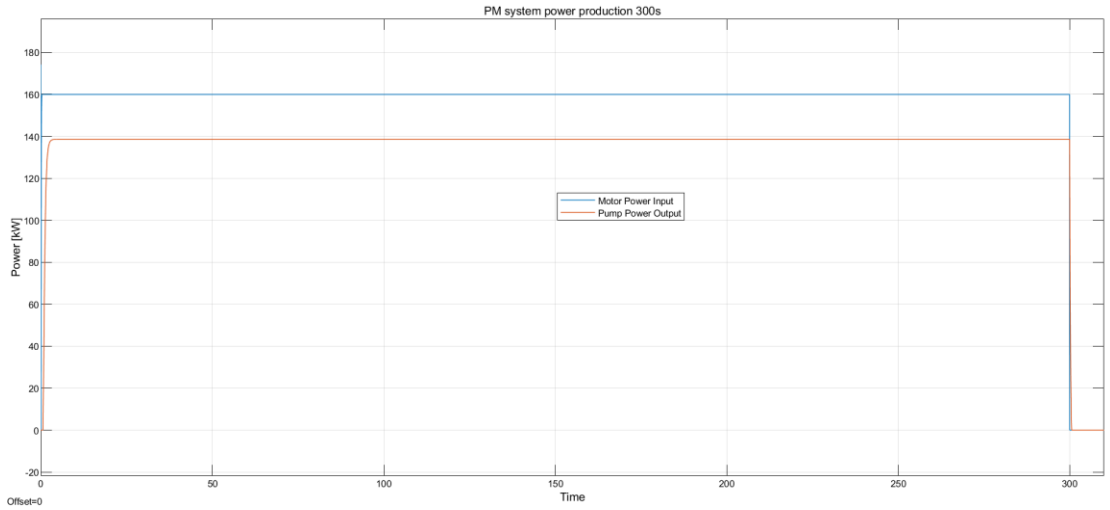

Figure 17 - Motor power input and pump power output for an operational time of 300 seconds

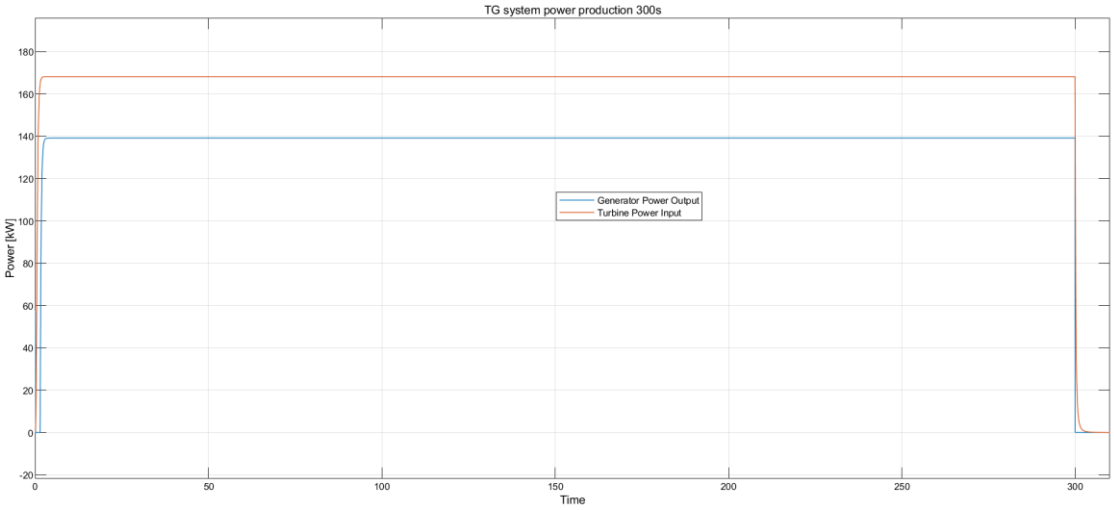

Figure 18 - Turbine power input and generator power output for an operational time of 300 seconds

3.2. Simulations to calculate the efficiency of the systems with DCMs

In this section the results of the simulations to calculate the process efficiencies of the DC systems will be presented and discussed. As explained in Appendix F, the system is the same as for the TAMs and the process efficiency is calculated the same way. If the obtained results are comparable to the TAMs one, the model can be considered validated.

At the beginning of the simulation the two systems are at rest. They are run for different operational times ranging from 0.2 seconds up to 1800 seconds (30 minutes) in order to find how the efficiency changes and to determine its asymptotic value. The simulation runs longer than the actual operational time so that the anticipated effect of the inertia of the machine can be accounted for: once the machine is turned off, it will still be producing power since it will still be spinning.

As can be seen in Figure 19, the efficiency of the filling process, so the efficiency of the PM system, has an asymptotic value of 87.0 %, while the one of the draining process, which corresponds to the TG system has a final efficiency value of 86.7%.

The values are higher than those for the TAMs, that is mainly because the fact that the DCM does not have a fixed characteristic, but it can easily change its behavior; this makes possible to better follow the behavior of the hydraulic part especially in the first part of the simulation where more losses are present in the TAM system. Also, in the TG contrarily of what happened in the TAM system, the turbine can work at 160 kW and the generator will simply tune in with it to deliver the rater power before losses.

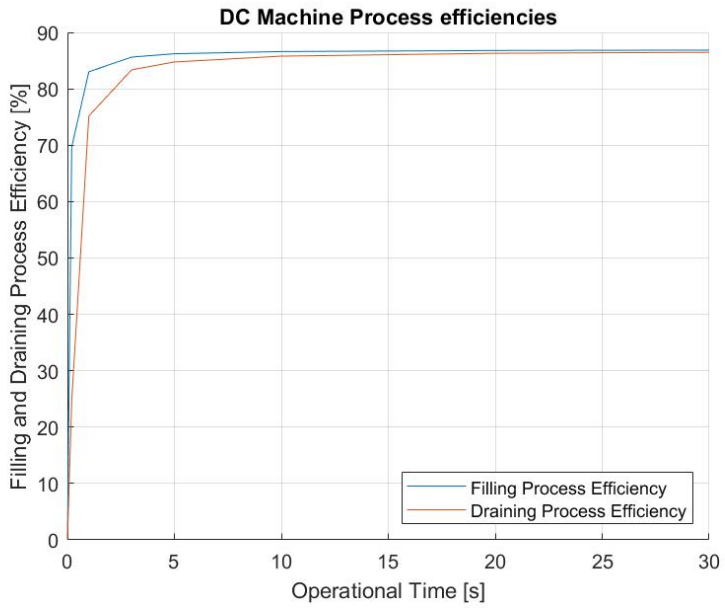

Figure 19 - Efficiencies of the process of filling and draining the tank for different operational times with the DCMs

Figure 19 only shows efficiencies for operational times up to 30 seconds to better represent the curves before they reach their asymptotical values. As expected, the two curves are increasing. They start from 0, which means that for low operational times the two systems are not very efficient. This is because the systems spend time processing a small flowrate which, as explained in section 2.2., is not efficient for the pump and the turbine. Also, it is important to notice that the PM system is more efficient than the TG system.

Similarly to what has been done for the two systems with the TAMs, the power input and output of the rotating element and the DCM throughout operation will now be shown in Figures 20 to 23. That bump occurring during the first seconds of the simulation in Figure 20 and 22 is because for low operational velocities the output of the DCM is very high being its characteristic a decreasing line, this is true until the load and motor characteristics meet and start having a normal behavior.

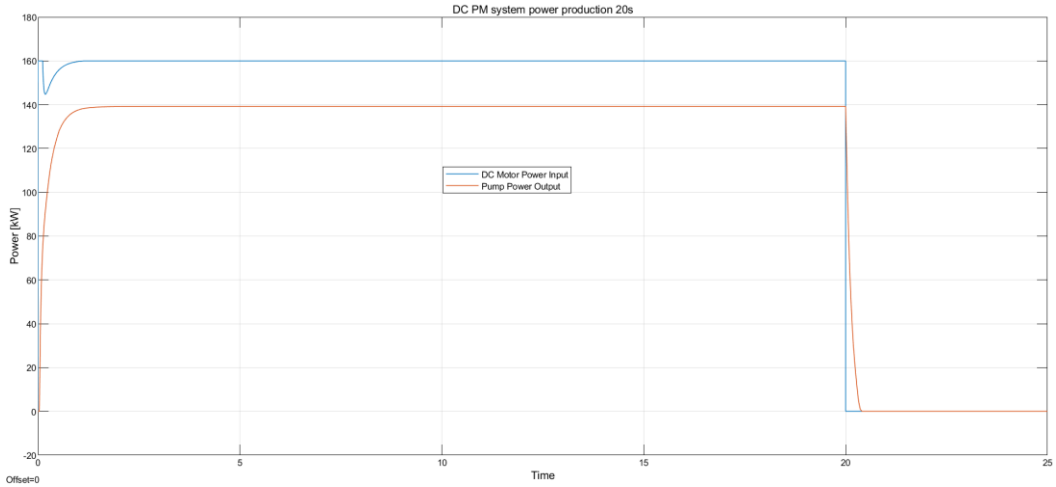

Figure 20 – DC Motor power input and pump power output for an operational time of 20 seconds

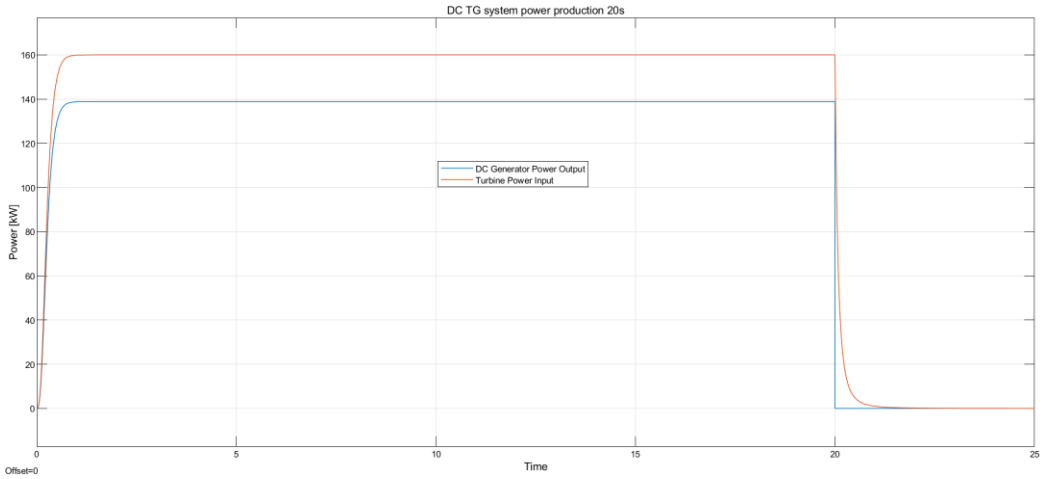

Figure 21 - Turbine power input and DC generator power output for an operational time of 20 seconds

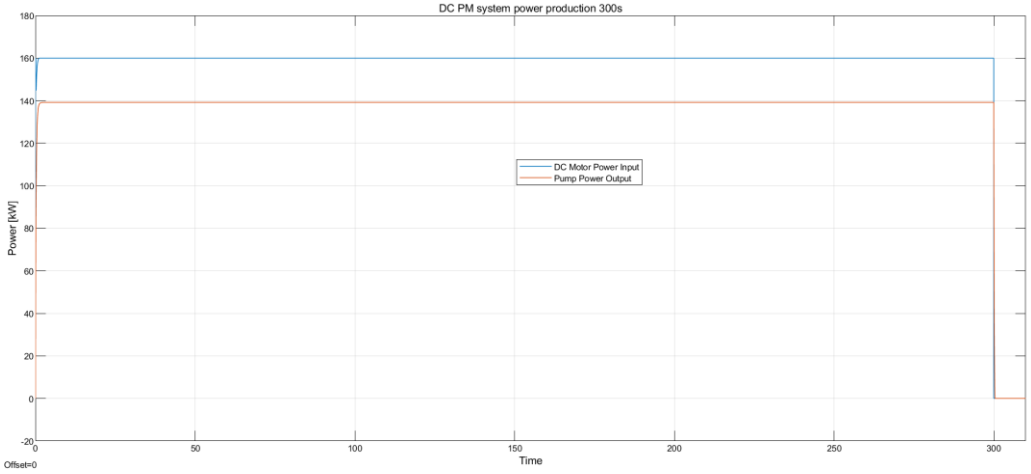

Figure 22 – DC Motor power input and pump power output for an operational time of 300 seconds

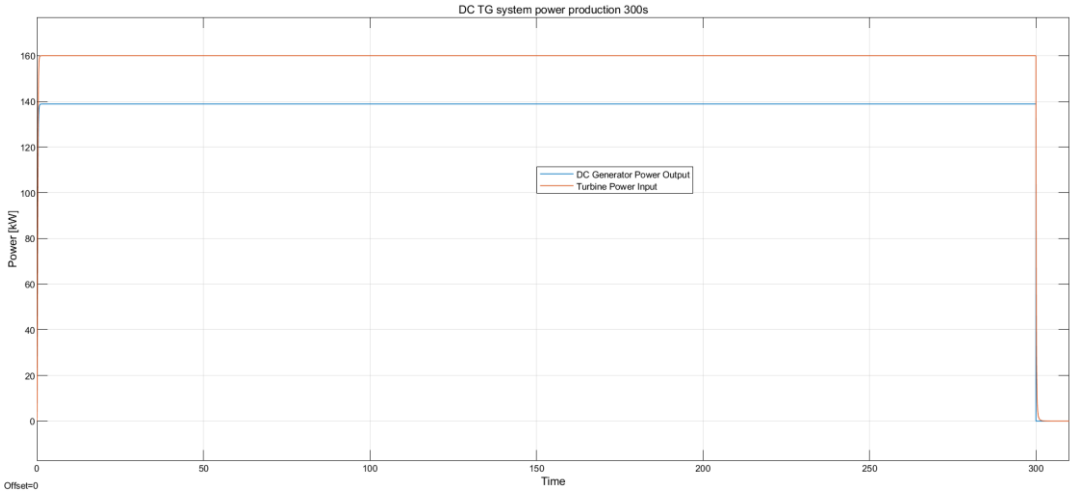

Figure 23 - Turbine power input and generator power output for an operational time of 300 seconds

It can easily be noticed that these behaviors are similar to the ones of the TAMs.

3.3. Storage system model in Simulink

Before diving into the storage system model in Simulink, it is very important to remark what power flows are being considered. The ocean battery does not store energy like other conventional batteries in the form of electrical or chemical potential energy. The ocean battery stores water. Such volume of water is subject to a certain constant pressure applied by the surrounding water of the ocean. Since the fluid inside the inflatable pouches of the battery is not moving, it is possible to talk about potential mechanical energy. The potential energy deriving from this situation can be calculated as follow:

$$E_{\text{Stored}} = \rho * V * g * H \tag{6}$$

Where ρ is the density of water, V is the volume of water stored inside the battery, g is the acceleration of gravity and H is the nominal head which is assumed to be constant. What is important to understand from this equation, is the fact that every term on the right side is constant except for the volume of water stored inside the battery. Therefore, the State of Charge (SoC) of the battery can and will be calculated keeping track of the volume of water inside the water tank.

To have a clearer overview it is possible to say that electrical power is used to operate the motor which drives the pump. This hydraulic element charges the battery by storing water inside the ocean battery. The reverse process consists in running the turbine by draining water from the battery. The turbine is connected to the generator which delivers electricity to the grid.

Figure 24 - Different types of power flows

This introduction is essential to understand how the storage system has been modeled in Simulink.

The input given to the battery is obviously the flowrate that goes inside the battery at which is subtracted the flowrate exiting the battery: logically the battery either charges or discharges, it cannot do both unless it is due to an effect of inertia. The flowrate is then integrated to be able to work with the water volume. A delay block is used to have the battery process the differential of the water volume. Every calculation cycle processes the difference between the

previous water volume and the new one. Such value is divided by the total volume of the battery so that it is possible to calculate the percentual change of the charge of the battery. This value is than added to the previous SoC of the battery coming from the red delay block. The choice of making it red comes from the necessity to recognize it from the others since, changing one of the parameters of that block, it is possible to start the simulation with a different SoC. In other words, at the beginning of the simulation, the battery could be fully charged, fully discharged or at 50% of the full capacity. The red block is the one that allow to make such change.
Once the new SoC has been calculated there are three options:

1. The new SoC is greater than 0% and less than 100%
2. The new SoC is less than 0%
3. The new SoC is greater than 100%

Option one represents regular operation, so the new is SoC of the battery simply corresponds to that value. Option two corresponds to the situation where the battery is empty, but the demand is still higher than the generation. In this case the new SoC will be 0% and the “grid” output of that block corresponds to the loss of load failure mode. Meaning that some power, needed by the grid, is not able to be delivered, at least from that specific storage unit. More storage units will be present once the installation is done so that power could be retrieved from a different battery, but this is beyond the scope of this research.
Option three is the specular situation of option 2: the battery is full, and the generation is still higher than the demand. In this case the new SoC of the battery is 100%. In this situation some of the energy or all the energy produced is not processed by the battery but is promptly delivered to the grid which will take care of its management. In other words, the management of this energy is not an issue concerning the Ocean Battery system. This represents another failure mode of the dimension of the battery. As for option two, more storage units will be present once the installation is done so that power could be delivered to a different battery, but this is beyond the scope of this research.
For both the latter cases, if the battery is on the threshold of being fully charged or discharged and the volume processed is more than needed, only the exact water volume will be processed while the rest of the energy will be either dumped or not supplied.

Reconnecting with the first part of this chapter, once the SoC is known, it is possible to calculate both the water volume inside the tank and the total energy available.

The battery volume used in this calculation is V = 116.5 m^3 (corresponding to 14.3 kWh). This is not the exact volume of the Ocean Battery, it is smaller. Nevertheless, a bigger volume would have made all the following simulations extremely more time consuming. Furthermore, the accuracy of these simulations using a reduced volume is still good.

3.4. Round-Trip Efficiency (RTE)

To compare one storage system to another the parameter that is used is the Round-Trip Efficiency (RTE). The battery round-trip efficiency is "the round-trip DC-to-storage-to-DC energy efficiency of the storage bank" [17], in this case it can be considered the Generation-to-storage-to-Grid energy efficiency. In other words, the RTE represents the fraction of the electrical energy from the generation side put into the storage, in the form of water, that can be retrieved and delivered to the grid in form of electricity.

To calculate the RTE of the ocean battery Simulink was used. The simulation was run feeding the system with the maximum power supply bearable by the PM systems: all the five PM units will work in nominal condition pumping the nominal flowrate inside the battery bank. The simulation starts with a completely empty battery: SoC = 0%. Once the battery reaches SoC equal to 100%, meaning that it is fully charged, the sign of the input variable is reversed so that all the PM machines will slow down and eventually stop, meanwhile all five TG units will be activated working in nominal condition discharging the battery by draining water outside of it. The simulation stops when the battery is empty (SoC = 0%).

As previously described, while charging the battery there are some losses: the energy stored inside the battery, proportional to the volume of water contained in the tank, is less than the electrical energy used to run the motors that drive the pumps. The ratio of these two values is the charging efficiency. Likewise, while discharging the battery, the maximum amount of energy that can be retrieved from it corresponds to the total volume of water stored. While using this water to activate the turbine, which drives the generator, some energy is lost in the process of transforming the potential energy of the water in electrical energy to deliver to the grid. The ratio of these two values is the discharging efficiency.

The RTE then corresponds to the ratio between the electricity delivered to the grid by the generators and the electrical energy used by the motors to fill the ocean battery with water. From this reasoning, it is also understandable that the RTE corresponds to the filling efficiency times the draining efficiency.

$$RTE = \frac{E_{\text{delivered to the grid}}}{E_{\text{withdrawn from the generation side}}} = \eta_{\text{filling}} * \eta_{\text{draining}} \quad (7)$$

Looking at Figure 25 in the next page, the top graph in the picture shows the behavior of the SoC of the battery, while the bottom graph represents the energy exchanged during the simulation by every part of the system: the top yellow curve shows the energy withdrawn from

the generation source to run the motor. When the battery is fully charged the motor is shut down, in fact the yellow line stops growing and remains constant until the end of the simulation. The blue line, which represents the energy corresponding to the water stored inside the battery shows the same behavior: increasing at first and then constant. The difference in the slope with yellow curve is caused by the fact that losses have been considered, hence the total energy stored is less than the total energy withdrawn from the grid. The ratio between the maxima values of the blue and yellow lines is the filling efficiency ($\eta_{filling}$). Likewise, the draining efficiency is calculated. As expected, the TG systems are started once the battery is fully charged and needs to be discharged. The red curve represents the energy corresponding to the water drained from the battery. Trivial to say that the water that can be drained cannot be more nor less than what is already there: in fact, the final value of the red curve coincides with the blue's final value. Losses are present in the TG system as well as in the PM. As a matter of fact, the green curve's final value, which represents the total energy delivered to the grid by the generator, is less than the blue one. The ratio between the green and red constant lines is the draining efficiency ($\eta_{draining}$). Having the values of these two efficiencies, one would simply have to multiply them by themselves to calculate the value of the RTE, as stated in Equation 7.

Also, since the RTE is the fraction of the electrical energy withdrawn from generation source that is later delivered to the grid, another way to calculate such RTE from Figure 25 is directly taking the maximum value of the green line, which corresponds to the energy exchanged to the grid, and divide it by the maximum value of the yellow line, which is the energy produced by the source. The numerical value of this division equals the multiplication of the filling and draining efficiency values.

Increasing or decreasing the volume of the battery bank, it is possible to notice that, running the RTE calculation simulation, the time of the simulation increases or decreases respectively: the bigger the volume, the longer it will take to completely fill the Ocean battery. What remains almost constant though, is the calculated value of the RTE. Small variations can be noticed on the RTE if simulations are carried out with different volumes because of the inertia of the rotating components. Such variations are basically negligible given the good accuracy of the system. Moreover, since many simulations need to be done, a fast-responsive system which is slightly less accurate, is more desirable than a slow-responsive one that can reach a moderately better level of accuracy.

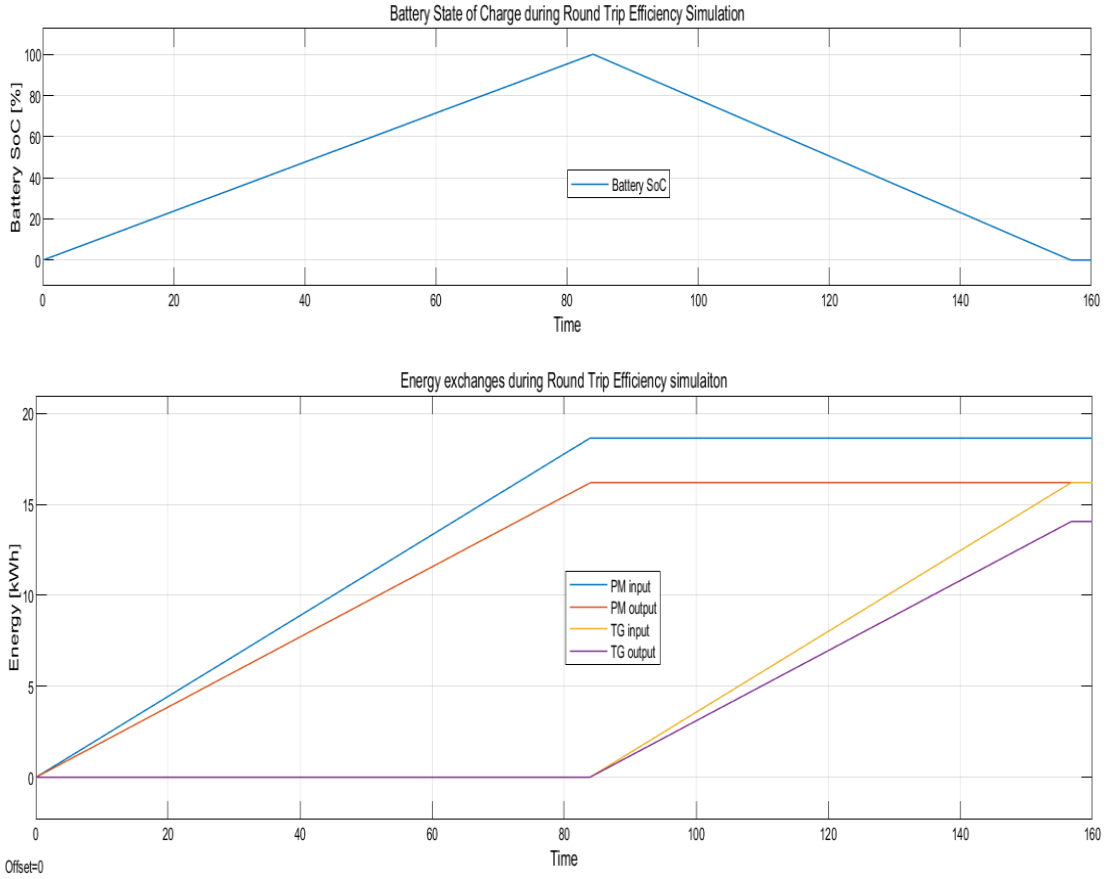

Figure 25 - Energy exchanges and SoC variation during the RTE simulation

3.5. Stack of multiple systems

This model is meant to be used to simulate the charging and discharging process of the Ocean Battery. It has been decided in the beginning with the company supervision and approval to only work with five systems stacked together to have a cumulative rated power input of 800 kW. The reason why it is more convenient to have more machines stacked together rather than a single machine of rated power 800 kW, is due to the possibility of occurrence of failure in the machine. Should one system break, there would still be power exchange in stack configuration, even if smaller than rated, whilst if only one big machine is connected to the battery and it fails, the whole system would not be operating until the problem is fixed. It would be interesting to study how much more convenient is one configuration than another. Also because, as previously explained, having more units running in parallel to charge and discharge the battery will allow to study how the protocol governing the activation of each unit will affect the efficiency and the performance of the whole system.

The engagement and dispatch protocol behind every stacks is different, since more configuration can be evaluated and every type of motor and generator that can be studied has its own peculiarity: TAMs are meant to operate in nominal conditions only, and DCMs can also work in partial load but at a lower efficiency.

In Simulink, the stacks are fed with the power demand signal, given in kW, since later on the program will be used to run other simulations which input is the mismatch between generation and consumption, also measured in kW. The output signals of the stacks in Simulink are: the power flows into the systems in kW, the power flows out of the systems in kW, the energy exchanged between the different element of the stack, and the flowrates processed by every unit in the stack. All these signals can be used to calculate the efficiency and the performance of the different systems and to later compare them together.

3.5.1. Machine engagement and dispatch protocols

After the definition of “Machine Engagement and Dispatch Protocol” is given, the following sub-sections will present and explain all the stacks that have been created and their engagement and dispatch protocols.

By “Machine Engagement and Dispatch protocol” it is meant the procedure adopted to determine how many, which and how the units forming the different stacks should be activated and operated given a certain power demand value. The protocols created will indeed communicate the system how many and which machines should operate in full load conditions and how much power the ones operated in partial load should exchange at any instant of time.

3.5.1.1. TAM Stack

The engagement and dispatch protocol behind the TAM stack it is quite straight forward: if the power that needs to be exchanged is greater or equal to the rated power of an integer multiple of the rated power of one module of the stack, the same number of modules are operated. Table 6 shows some examples of the TAM stack engagement and dispatch protocol. It is important to keep in mind that the rated power of each module is 160 kW and that in the table is considered the absolute value of the power that needs to be exchanged, even if for the convention that has been used negative power is the one exchanged by the TG system:

Power Demand [kW]	Power exchanged by the stack [kW]	Power that cannot be exchanged [kW]	Number of operating modules [-]
80	0	80	0
320	320	0	2
670	640	30	4
1000	800	200	5

Table 6 - Examples of the output power of the engagement and dispatch protocol of the TAM stack

The outcome of this type of engagement and dispatch protocol is constrained by the impossibility of the TAMs to work in partial load, hence in many cases some power cannot be exchanged, as can be seen from the third column of the previous table. The pro about this system is the fact that the machines are always operated in nominal conditions.

3.5.1.2. DC Stack

The engagement and dispatch protocol of the DC stack is different than the TAM stack's protocol since DCMs can and will operate in partial load. The bottom arrow coming out from the grey boxes represent the number of machines that have to be operating to sustain a given power demand, while the top one, "*Power remainder",* represents the power that needs to be exchanged by the one machine working in partial load. Inside the orange boxes there are the actual modules forming the stacks.

Keeping in mind the same warnings as for the previous table, Table 7 below shows some examples of the engagement and dispatch protocol outcome for the DC stack:

Power Demand [kW]	Number of operating modules in nominal conditions [-]	Number of operating modules in partial load [-]	Power exchanged by the stack [kW]	Power by the partial load module [kW]
80	0	1	80	80
320	2	0	320	0
670	4	1	670	30
1000	5	0	800	0

Table 7 - Examples of the output power of the engagement and dispatch protocol of the DCM stack

The main pro of this type of stack is the fact that unless the power demand is higher than the rated power of the stack, no power is technically ever lost by the engagement and dispatch protocol itself (thing that happened in the previous case e.g.: Power demand of 670 kW, 640 kW exchanged by the stack and 30 kW not possible to be exchanged since constrained by the protocol of the TAMs). Unfortunately, though, operating a DCM module in partial condition could result in tremendously low efficiency and, therefore, system power loss. This will be explained in the next chapters.

3.5.1.3. Mixed Stack

By saying Mixed Stack, it is meant to put at work together four TAMs and one DC machine. All five machines are governed by the same engagement and dispatch protocol. This configuration has been thought to find a solution to the protocol losses in the TAM stack. Unless the power required is exactly a multiple of the nominal power of one machine, some energy will always not be delivered either to the battery or to the grid causing a failure mode of the Ocean Battery.

This stack has the advantage of being able to use the power that cannot be exchanged by the TAM stack and having one DC machine processing such signal.

Power Demand [kW]	Number of TAMs operating at 160 kW [-]	Number of operating DCM [-]	Power processed by the DCM [kW]	Power not delivered [kW]
80	0	1	80	0
320	2	0	0	0
670	4	1	30	0
1000	4	1	160	200

Table 8 - Examples of the output power of the engagement and dispatch protocol of the Mixed stack

The advantage of this stack is the fact that unless the power demand is above rated, no energy is lost by the engagement and dispatch protocol as can be seen in the last column of Table 8.

The drawback of this stack is that, as previously mentioned, the DC machine as a low efficiency while working at low partial load.

3.5.1.4. Split DC Stack

The Split DC stack is the same as the DC one, the difference among those relies in the engagement and dispatch protocol of the second: whilst the stack described in sub-section 3.5.2., operates one machine at the time, the Split stack's protocol operates all five machines in any circumstance. All five will operate in partial load condition dividing equally among them the power demand unless it is greater or equal to 800 kW as can be seen in Table 9:

Power Demand [kW]	Number of operating modules in nominal conditions [-]	Number of operating modules in partial load [-]	Power exchanged by the stack [kW]	Power exchanged by each module [kW]
80	0	5	80	16
320	0	5	320	64
670	0	5	670	134
1000	5	0	800	160

Table 9 - Examples of the output power of the engagement and dispatch protocol of the Split DC stack

As for the previous stack, unless the power demand is above rated no energy is lost by this engagement and dispatch protocol. The fact that all machines operates at the same time in partial load is not convenient efficiency wise since, as has already made clear, losses are more relevant when the DC is operated at low partial load conditions. The purpose of studying this stack, is to show that besides the possibility of failure occurrence, more modules stacked together are a better option than just a single module of the size of 800 kW. Also, as will be later shown, while studying this stack it is possible to better investigate on the behavior of a single DC machine operated at different partial loads.

3.5.1.5. 125% Nominal Power Output DC Stack

Hydraulic components are usually run at 80% of their maximum allowable flowrate [3] since the efficiency at that point is maximum as explained in section 2.2. and seen in Figure 4. This configuration wants to explore the possibility of having one DC machine, if needed, operating a greater flowrate of its nominal such that the power output will be of 200 kW instead of 160 kW. This is made possible for only one DC machine at the time. E.g.: if the power demand is 190 kW, instead of having two DC machines running, only one will be activated; but if the power demand grows to be 210 kW, the over-nominal machine will slow down to nominal

condition delivering 160 kW, while the second one will be activated delivering the remaining 50 kW to match de demand.

Table 10 shows what happens using this configuration:

Power Demand [kW]	Number of operating modules in nominal conditions [-]	Number of operating modules in partial load [-]	Number of operating modules in partial load [-]	Power exchanged by the stack [kW]	Power by the partial load module [kW]	Power by the above nominal module [kW]
80	0	1	0	80	80	0
320	2	0	0	320	0	0
670	3	0	1	670	0	190
750	4	1	0	750	110	0
1000	4	0	1	840	0	200

Table 10 - Examples of the output power of the engagement and dispatch protocol of the 100% Flowrate DC stack

The advantage of this configuration relies on the possibility to deliver more than the maximum power output and that very low efficiency partial load operations can be avoided. On the other hand, more accelerations and decelerations are required to run such configuration.

3.5.1.6. 50% Margin TAM Stack

As explained in sub-section 3.5.1., there are cases when the TAM stack is not able to deliver the required power since, in order for one machine to be activated, the energy demand needs to be higher than the rated power of one module. Doing so, much energy is not effectively exchanged. The goal of this stack is to study what happens when a new machine is activated when the power demand is 50% lower than its rated power.

Table 11 shows some examples of it:

Power Demand [kW]	Power exchanged by the stack [kW]	Power that cannot be exchanged [kW]	Number of operating modules [-]
85	160	-75	1
320	320	0	2
420	480	-60	3
670	640	30	4
1000	800	200	5

Table 11 - Examples of the output power of the engagement and dispatch protocol of the TAM stack

This is the only configuration that allows a negative value of failure mode, as can be noticed in the third column of Table 10. This means that the system is delivering more energy than what

the grid is demanding. The rationale behind this choice, relies on the fact that multiple ocean batteries will be connected together. Delivering more power might be convenient since, not only the power demand is met, but some of the surplus could be used to charge other batteries or for other purposes inside the cluster.

3.5.1.7. 10 seconds TAM Stack

This configuration has been thought to have less switching on and off of the machine. A very responsive input signal, i.e. one that is updated every second, might not be efficient. This Stack is equivalent to the TAM stack explained in sub-section 3.5.1. with the only difference that the input signal is taken once every ten seconds instead of every second.

3.6. RTE simulations

Once the concept of Round-Trip Efficiency has been explained and the different types of stacks have been presented, the two things will now be combined.

The simulation to calculate the RTE can be done with different power input: it is possible to calculate the RTE either by supplying maximum power (having all five machines working in nominal condition) or by supplying a fraction of the maximum power input which will make only a lower number of modules charging and discharging the battery. For instance, if the simulation is run at 55%, only 3 modules will be used during this simulation: two of which are working in nominal condition, and one at 75% of its rated power (this example does not apply for the Split Stack). It is important to understand how the RTE changes while changing the fraction of the maximum power input to later be able to optimize the system.

3.6.1. TAM Round-Trip Efficiency graph

Figure 26 shows the behavior of the RTE of the TAM stack when the simulation is run with different fraction of the power input. Every 20 percentual points, a new machine is activated and as can be seen in the graph, the RTE drops a bit every time more machines are at work. This trend is occurrent in every simulation that has been run so far. The reason for it is that when more machines are working instead of only one, the simulation time is shorter, the battery fills and drains faster, hence the transients of all the machines are more relevant compared to situation when only one machine is working and the simulation time is longer. The simulations that have been run are many so, as also previously stated, the advantage of having a smaller battery that fills and drains faster outdoes the disadvantages of the situation where the inertia effects are more visible as in this case.

The efficiency of this configuration is pretty much constant and quite high throughout the whole simulation, the drawback is the fact the no power is exchanged when the power demand is below 20%. The maximum reachable RTE for the TAM stack is 75.08%, between 20% and 39% of the power input.

It is important to state that in this graph, all the results happening between one multiple of 20% and another are referred to the only working efficiency of the TAM. When the demand corresponds, for instance, to 30%, as previously explained, the TAM is only delivering power corresponding to 20% of the demand at an efficiency of 75.08%, the remaining 10% is not delivered. This type of loss is accounted for in the Efficacy section. This type of reasoning is true for all the TAM based stacks that will be used in the further explanations.

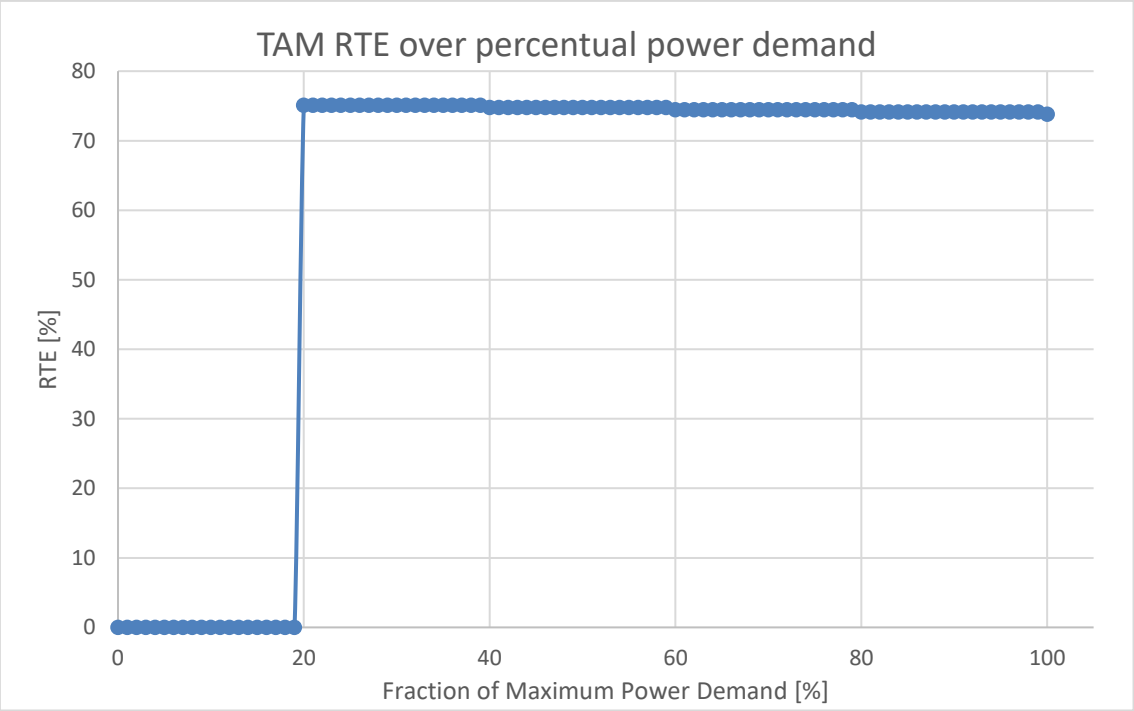

Figure 26 – TAM RTE over percentual power demand

3.6.2. DC Round-Trip Efficiency graph

Figure 27 shows the behavior of the RTE of the DC stack when the simulation is run with different fraction of the power input. This configuration has a wider range of application compared to the previous one, since it has non-zero RTE if the power demand is above or equal 15%. Overall, the efficiency of the stack fluctuates when nominal conditions are not met. Maximum RTE for the DC Stack occurring at 100% is 75.43%. So, it is a bit more efficient than the TAM Stack.

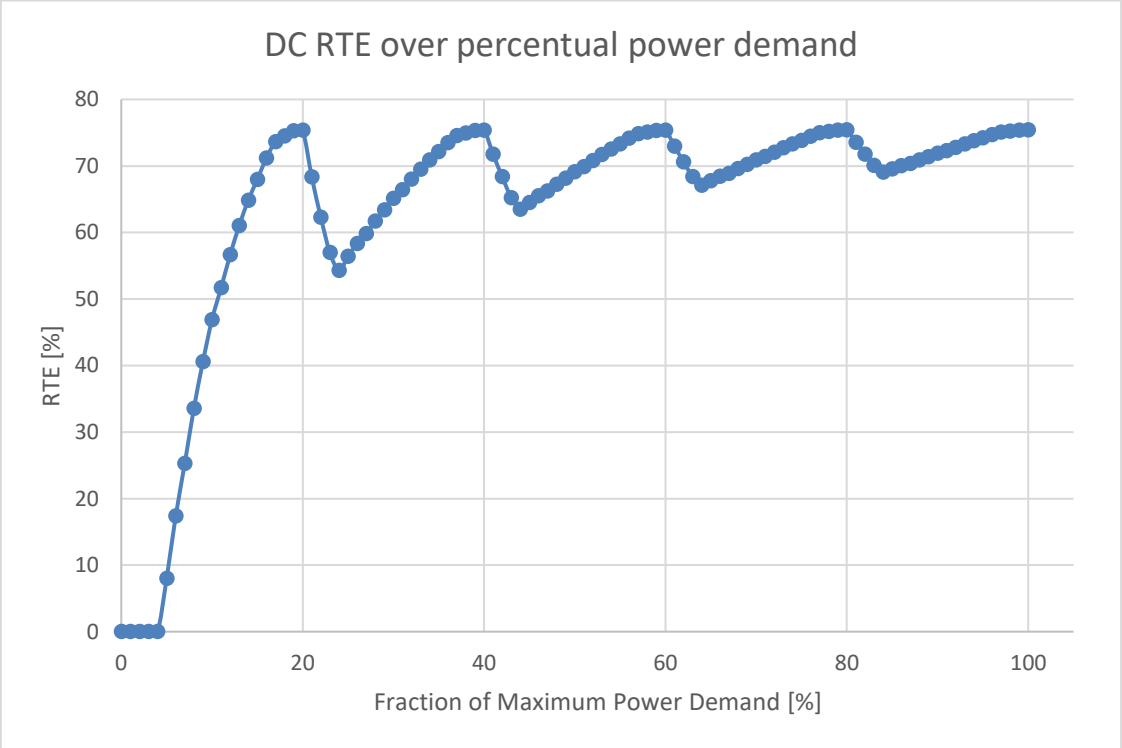

Figure 27 - DC RTE over percentual power demand

3.6.3. Mixed Round-Trip Efficiency graph

Figure 28 shows the behavior of the RTE of the Mixed stack when the simulation is run with different fraction of the power input. Although the behavior is similar to the DC one, RTE values are a bit lower. The maximum reachable RTE occurs at 19% and is 75.29%, in fact, this situation corresponds to having only the DC module working in almost nominal condition. As previously explained the DC module is a bit more efficient than the TAM.

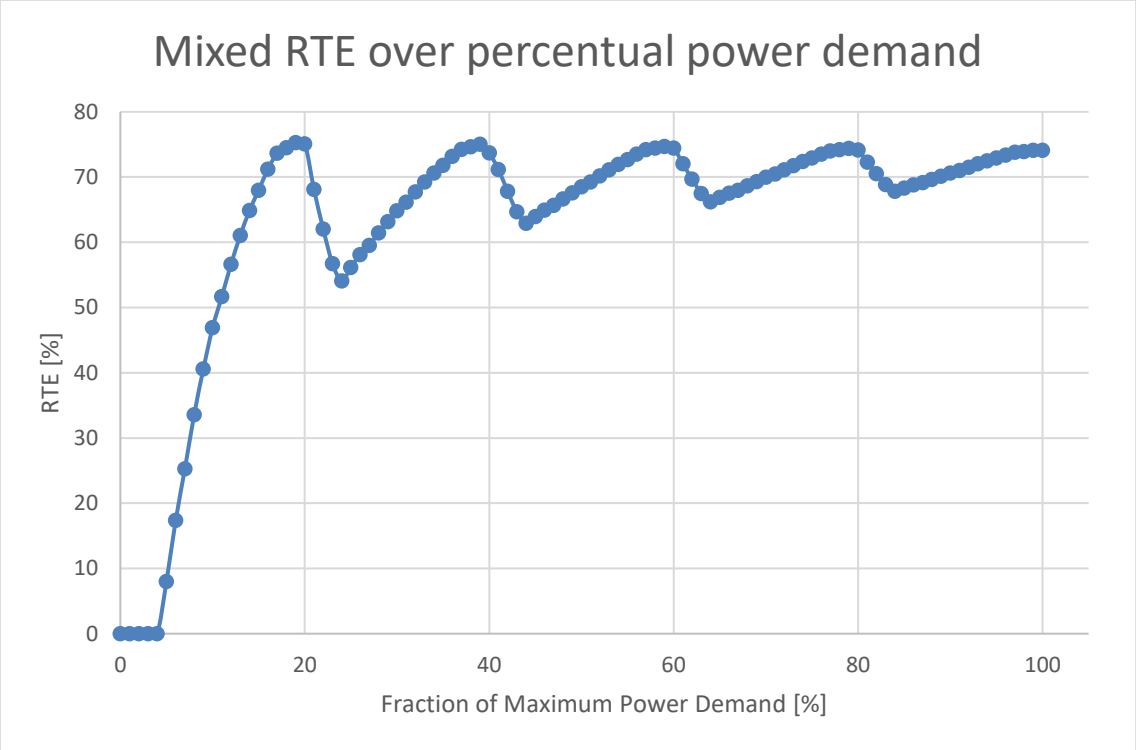

Figure 28 - Mixed RTE over percentual power demand

3.6.4. Split DC Round-Trip Efficiency graph

Figure 29 shows the behavior of the RTE of the Split DC stack when the simulation is run with different fraction of the power input. As anticipated in section 3.5.4., this stack is interesting to study since it could be compared to the situation of a single module of rated power 800 kW: the behavior would be the same. The maximum RTE is 75.43% corresponding to the full load situation (same RTE value of the DC stack performing in full load). The curve is strictly increasing after 29% but, unfortunately, a good efficiency is found only above 80%. From this graph, it is possible to have another insight on why more parallel working units are a better option than having one single machine. Not only for a probability of failure point of view, but also efficiency wise it can be noticed that more units are a better choice than just a single big one.

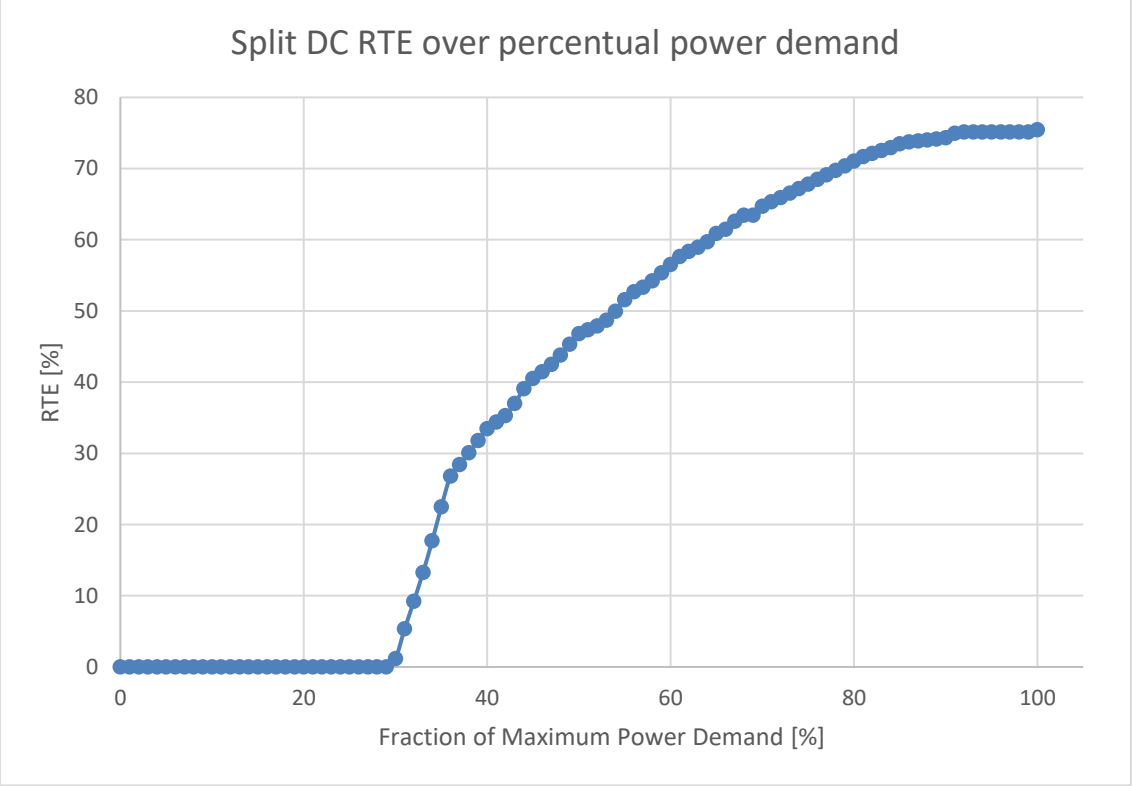

Figure 29 – Split DC RTE over percentual power demand

3.6.5. 125% Nominal Power Output DC Round-Trip Efficiency graph

Figure 30 shows the behavior of the RTE of the 125% power output DC stack when the simulation is run with different fraction of the power input. The maximum RTE of this configuration is 75.43%. Also, from this simulation, it is possible to notice that, as explained in section 2.2., the highest efficiency of the hydraulic components occurs at 80% of their maximum power output. In fact, the nominal power of the hydraulic parts is 160 kW buy they have been dimensioned to deliver 200 kW: this simulation explores that possibility.

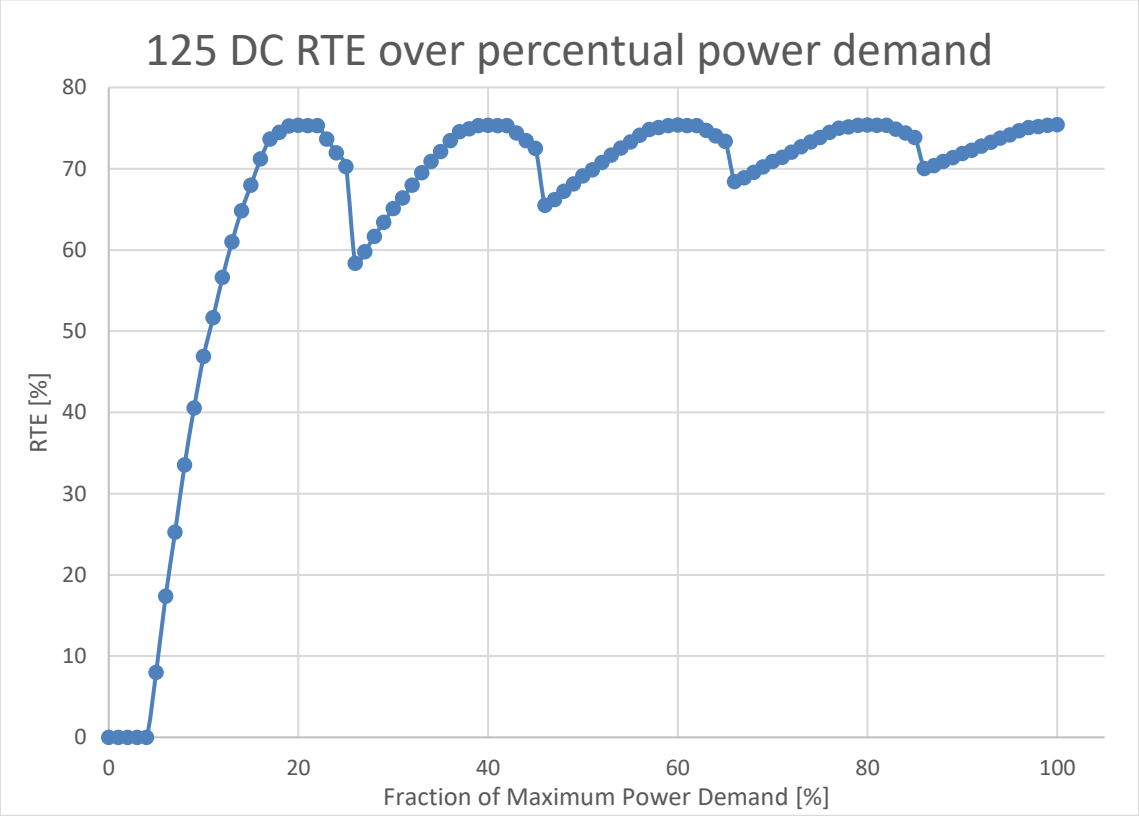

Figure 30 – 125% power output DC RTE over percentual power demand

3.6.6. 50% Margin TAM Round-Trip Efficiency graph

Figure 31 shows the behavior of the RTE of the 50% margin TAM stack when the simulation is run with different fraction of the power input. This graph is substantially the same as in sub-section 3.6.1., the main difference is the fact that the range application is now increased: in fact, the RTE starts being non-zero at 10% instead of 20%. The RTE values are the same as TAM stack ones.

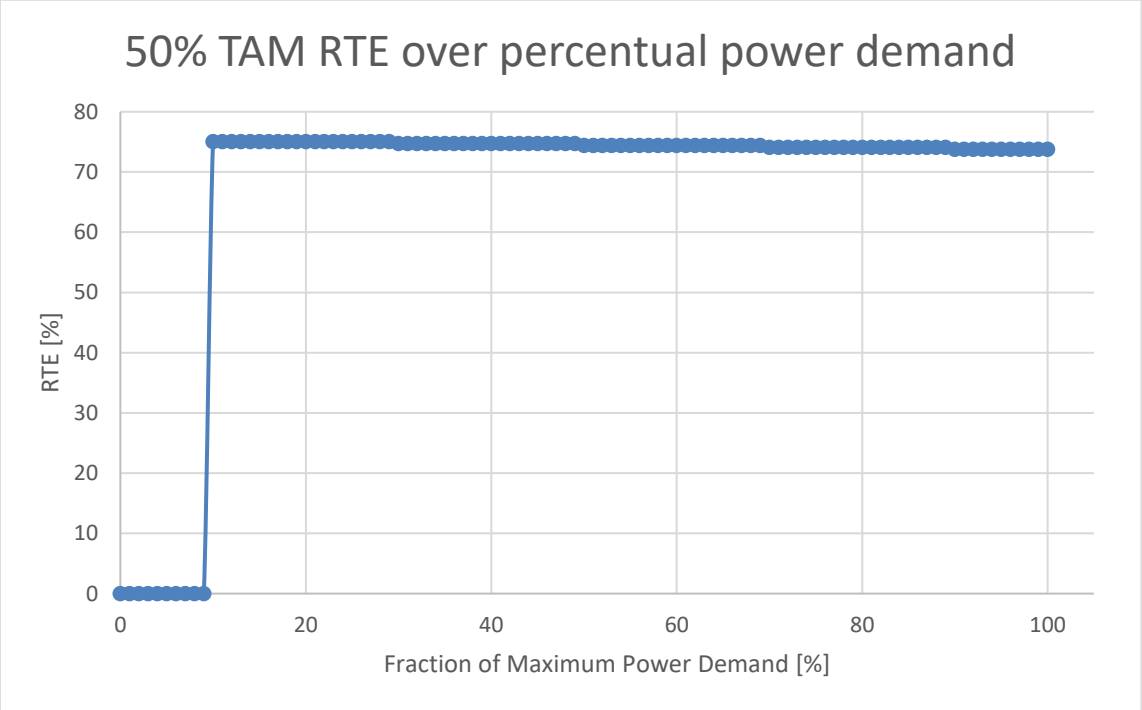

Figure 31 – 50% margin TAM RTE over percentual power demand

3.6.7. Comparison of the RTEs

Figure 32 shows in one graph a comparison between all the RTEs for the different stacks.

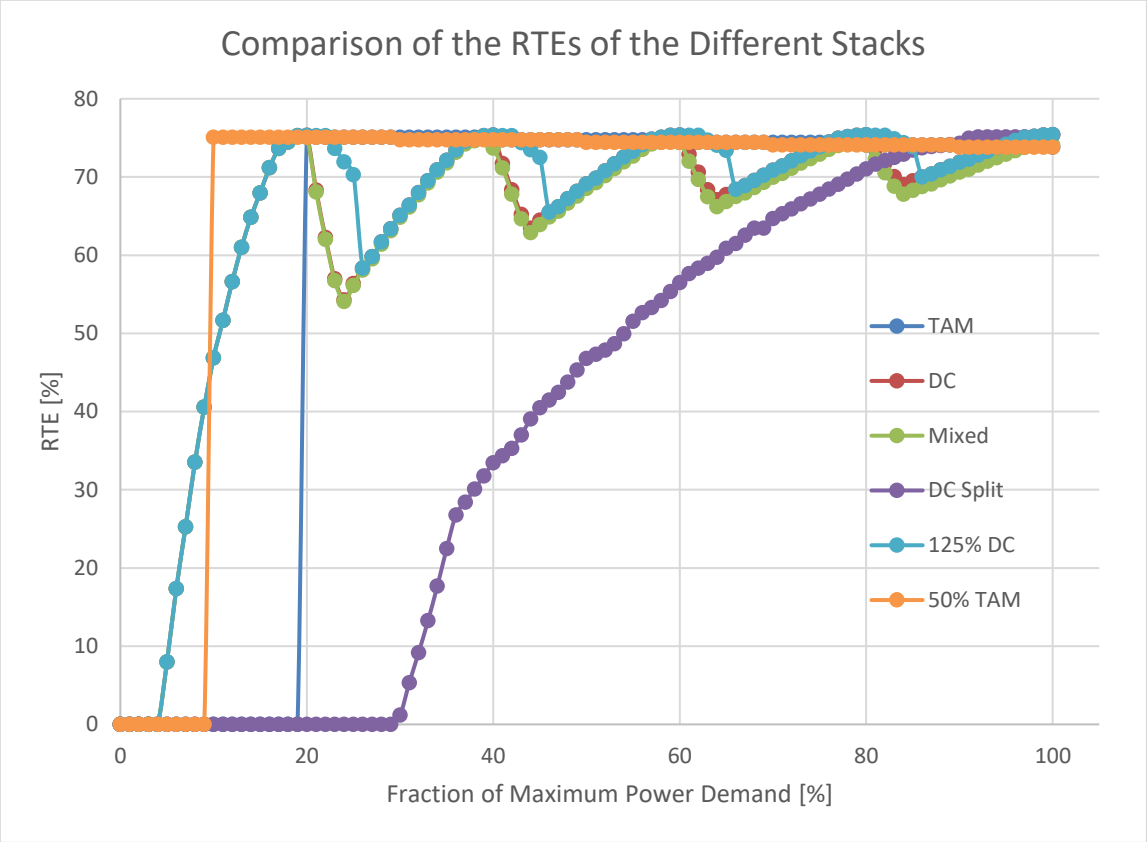

Figure 32 - Comparison of the RTEs for the different stacks

3.7. Preparation to the simulation of the Battery State of Charge

Once the storage system has been presented and explained and the configurations that are needed to be studied have been presented, it is now possible to run a simulation to determine the performance of the battery.

Batteries are the bottleneck of the renewable energy transition. The purpose of a battery is storing energy when the demand is lower than the production and delivering energy to the grid when the situation is reversed. The working logic of a battery is then triggered by the mismatch between production and demand. The definition of mismatch is the instantaneous difference between power production and power demand, in other words the difference, positive or negative, between the power generated by the energy source and the load demanded by the grid. Hence, to run the simulation, it is mandatory to come up with a mismatch profile that will be fed to the battery system to be processed.

As anticipated, to come up with the mismatch timeseries, a load profile and a generation profile are needed. The load profile has been retrieved from a document made available by TU Delft and used for a past project [18]. The load was given per minute, but to run this simulation it was mandatory to interpolate it and make it vary every second. This was made possible by using the Matlab function “Interp1”. The load profile looks as presented in Figure 33:

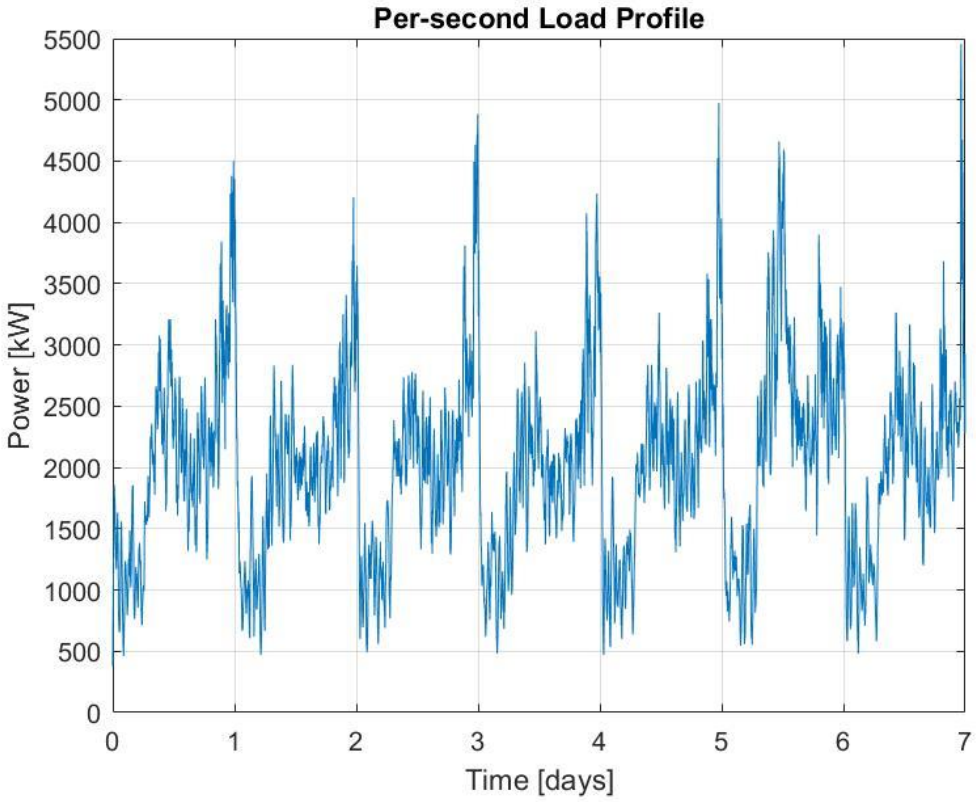

Figure 33 - Weekly load profile per second

The Ocean Battery is meant to be built within the offshore wind turbine therefore the generation profile used in the following simulation is the one coming from the power production calculation having the wind data of an offshore wind park. The wind data have been retrieved from another document also made available by TU Delft and used for a past project [19]. The wind speed data can easily be converted in power data using the formula in Equation 8:

$$P_{\text{wind turbine}} = 0.5 * \rho_{\text{air}} * \eta * A * v^3 \quad (8)$$

Where $P_{\text{wind turbine}}$ is the power produced by the wind turbine, ρ_{air} is the air density, η is the global efficiency of the wind turbine, A is the area swept by the wind turbine's blades and v is the wind speed [19].

Using these data, the generation profile per second looks as shown in Figure 34:

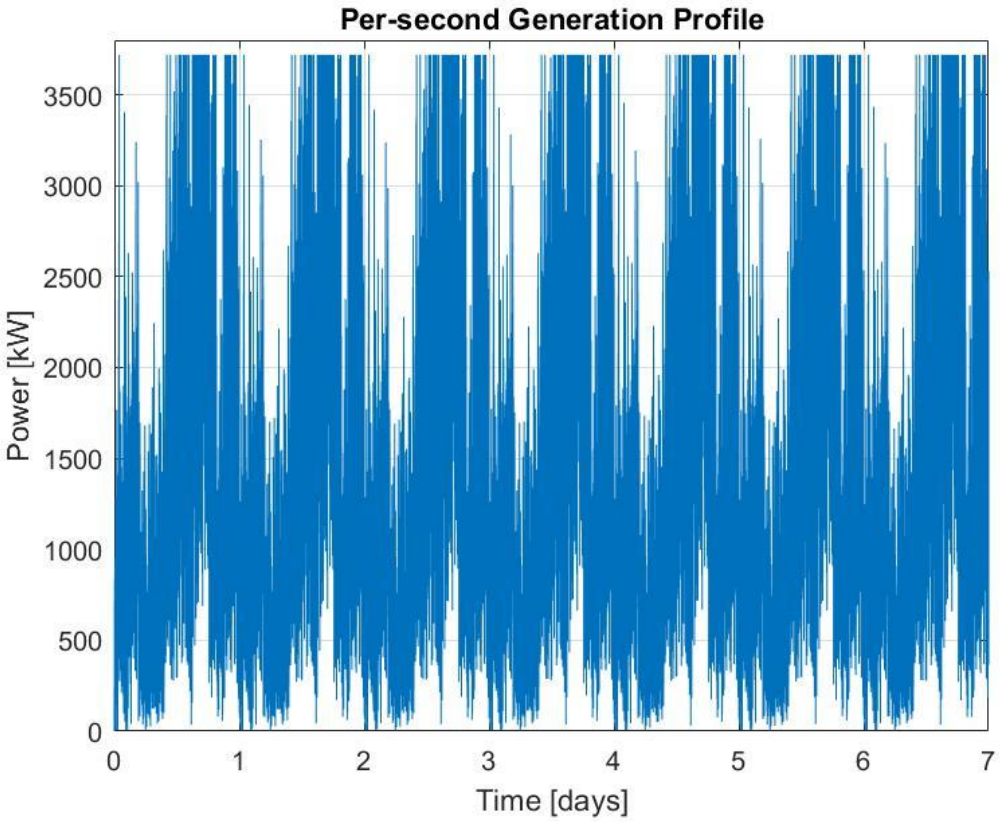

Figure 34 - Weekly load profile per second

Once both the load and the generation profiles are known, calculating the mismatch is a straight-forward process since there is just a difference to perform. The mismatch looks as presented in Figure 35 in the next page.

There is one last remark to make about Figure 35 and 36. These profiles have been multiplied by a coefficient to make them suitable to work with the predetermined size of the Ocean Battery. When designing an energy system, the process is usually reversed: first the load profile is obtained, then the generation source is sized and finally the battery is dimensioned. In this case though since the size of the battery was already decided as explained in section 3.3. (V = 116.5 m^3) it was more convenient to dimension the mismatch according to the size of the battery. The rationale behind this reasoning is the fact that the goal of this work is to find the optimal configuration for the system, not to properly dimension the system such that, for instance, the revenues are maximized. Therefore, having a larger or smaller battery, or a more or less large demand is not really the scope of this research.

The simulations run will be thoroughly explained in the next section, anyway it is important to show the actual mismatch input used to run the simulation. This can be seen in Figure 35 in the next page.

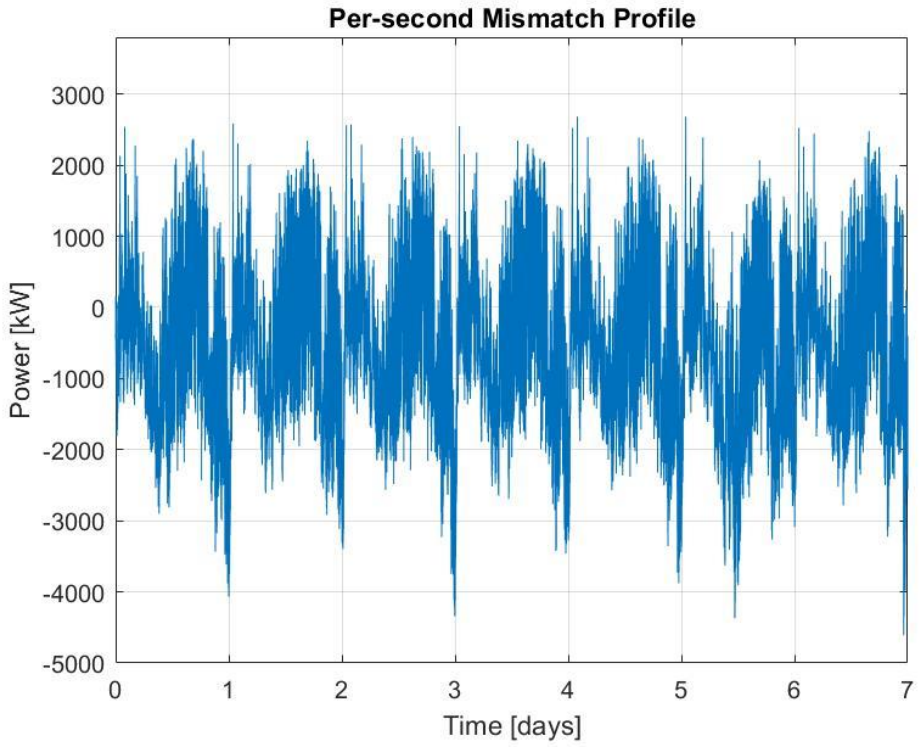

Figure 35 - Weekly mismatch profile per second

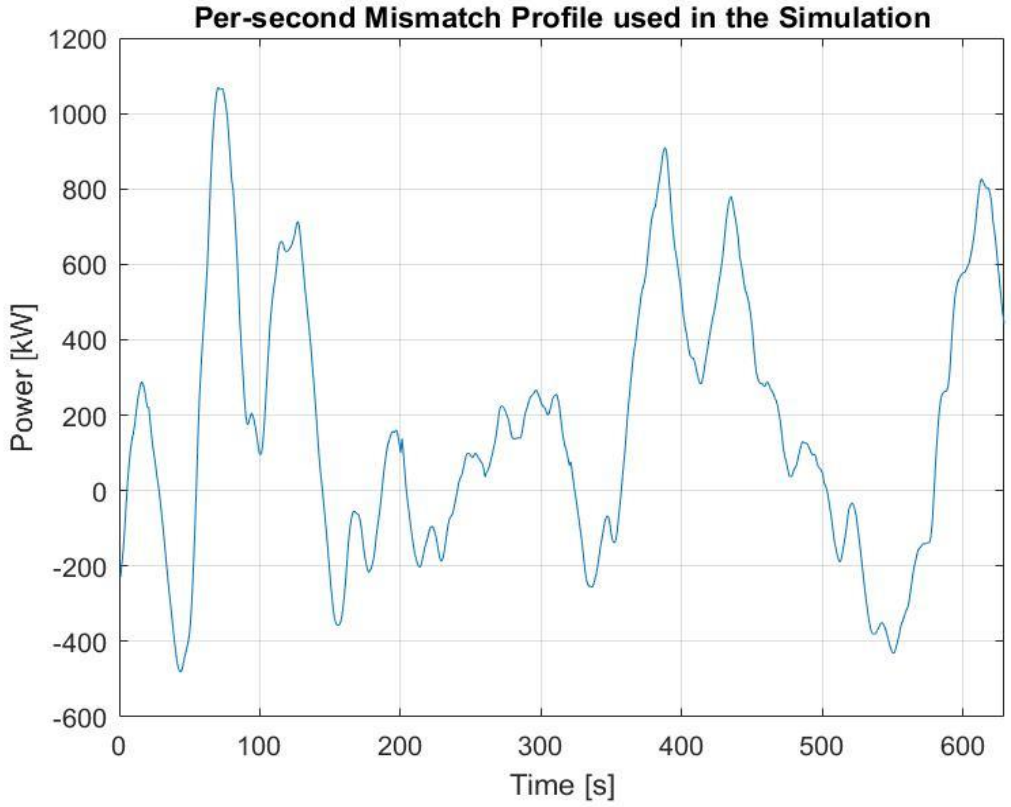

Figure 36 - Mismatch input signal used in the simulation

4. Results and discussion

4.1. Simulations on the Ocean Battery SoC using different configurations

Once every element is present in the system and has been described, it is time to put into work all the pieces together. In this section, firstly the ideal behavior of the Ocean Battery SoC will be presented and discussed, then all the above-mentioned configurations will be described as they have been implemented in the system.

What is common to all the following simulations, is the fact that the supplied input, which is the mismatch, is the same in all circumstances; also, the initial SoC of the battery is 50%. Choosing this value as the initial SoC is a common practice when studying a battery. The SoC, being given as a percentage, can easy be converted either in energy or volume of water. This two are completely equivalent as explained in section 3.3.

4.1.1. Ideal SoC

Ideal behavior of a battery means that the response of the battery to the mismatch signal is not subjected to losses and delays. The available power is instantly transferred to or from the battery without any losses. For instance, if the mismatch at a certain instant of time is -500 kW, then this exact amount of power would be able to be stored as energy inside the battery instantly. Of course, the due conversion needs to be made: -500 kW of power that has to be supplied for one second equals to -0.1389 kWh of energy, meaning that the battery will be discharged by this amount of energy after that second. The only limitation that has been put to this simulation, is fact that no more than ±800 kW can be exchanged since this is the rated power output of the system. The result of the simulation of the ideal SoC behavior can be seen in Figure 37. The mismatch input signal is also shown in the top graph of Figure 37.

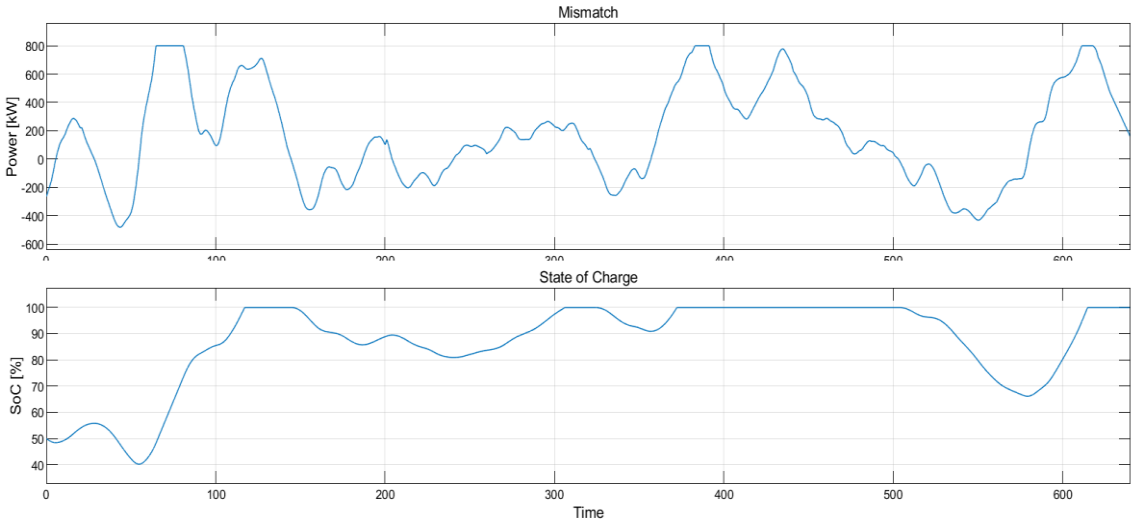

Figure 37 - Mismatch [kW] and SoC [%] over the time of the simulation

As it is visible from the previous figure, when the mismatch is positive, the battery charges unless it is already full, when it is negative the battery gets discharged and the SoC value goes down. As anticipated, the initial SoC of the battery is 50% and the power exchanged is limited to ±800 kW.

This graph will be used now on as a benchmark for all the simulations. The closer the SoC produced by one stack is to this line, the better the stack will be. In the next subchapters, the ideal SoC curve will be compared to the other stacks' SoC lines.

4.1.2. TAM SoC

The first comparison, to follow the logical order, is the one between the Ideal curve and the one generated by the TAM stack. It is easy to notice by looking at Figure 38 that depending on the power demand only some TAM modules, if any, are activated. This can be understood by noticing how the slopes of the red curve are always the same and that, when the curve is stationary, means that the mismatch is not big enough to activate even one TAM module, either motor or generator.

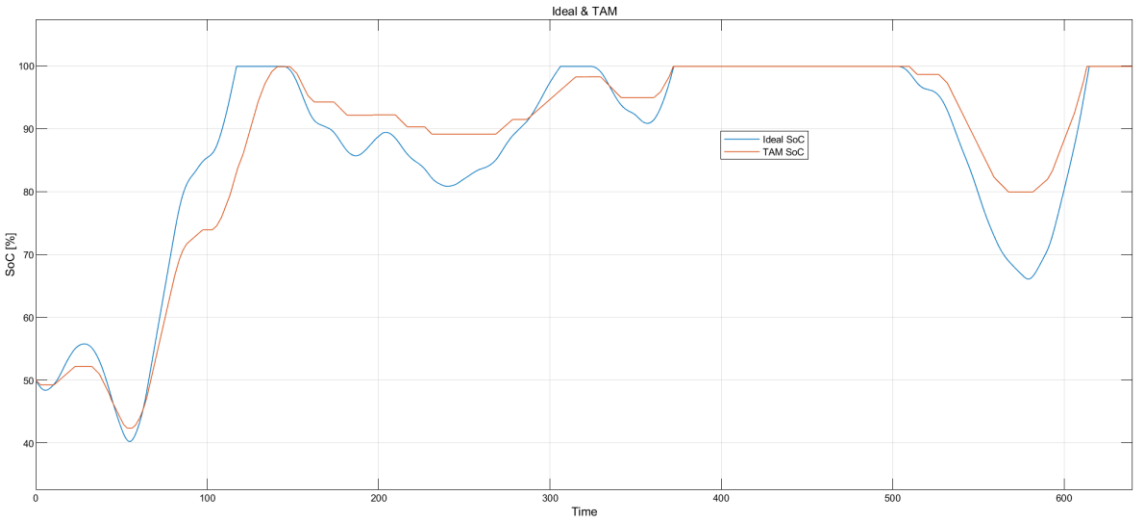

Figure 38 - Comparison between the SoC [%] of the Ideal and the TAM Stack

Figure 39 explains why the TAM SoC profile is not equal to the ideal one. The blue curve represents the mismatch, in this case in not bounded by the constraint of the ±800 kW limit. The red curve represents the electrical power exchanged while the yellow one represents the hydraulic power exchanged. When the mismatch is positive, the red line is above the yellow one: the electricity produced by the wind turbines is used to pump the water inside the battery. Nevertheless, losses are present so just a fraction of the electricity coming from the wind park is converted in hydraulic power therefore the red line displays a greater value than the yellow line. On the other hand, when the mismatch is negative, the water is firstly turbined to produce electricity which will be later delivered to the grid. Also in this process there are losses which visible by noticing that, in this case, the absolute value of the yellow curve, the hydraulic power, is greater than the absolute value of the red curve, the electric power.

The power exchanged to and from the battery correspond to the yellow line when the battery is charging and to the red line when the battery is discharging.

This disquisition is valid for all the following figures presenting the power flows of the stack; hence it will not be repeat unless something essential needs to be underlined.

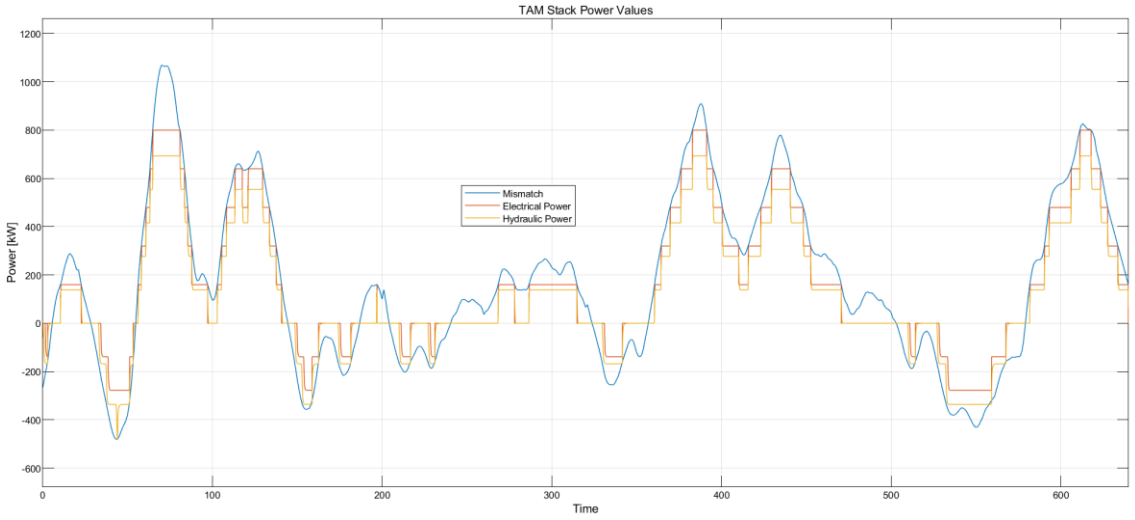

Figure 39 – Power profiles of the TAM Stack

4.1.3. DC SoC

The second comparison is the one between the Ideal and DC stack. In this case, as can be seen in Figure 40, the red line never crosses the blue line, thing that happened more than once in the first comparison. The slops of the red line are very different because the DC stack can deliver power also not in a "quantized" way.

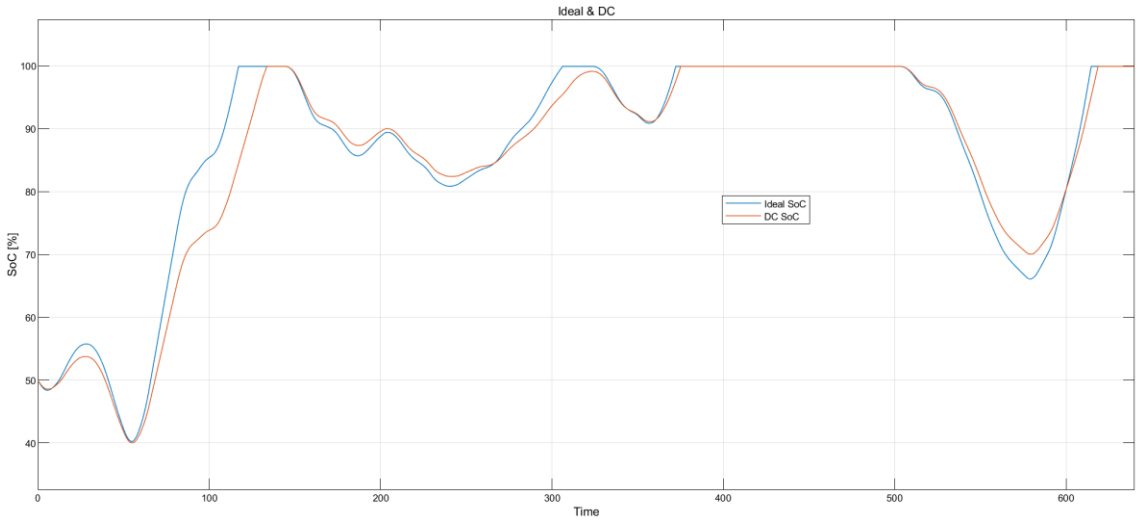

Figure 40 - Comparison between the SoC [%] of the Ideal and the DC Stack

Figure 41 shows the power curves exchanged by the DC stack: the fact that the blue line, corresponding to the mismatch, is always over imposed by the red line when positive and by the yellow line when negative means that this particular system does not have engagement and dispatch protocol losses. The same explanation as for the TAM stack is valid: red line equal electrical power while the yellow one represents the hydraulic power exchanged. System losses are visible by looking at the difference between the red and yellow line.

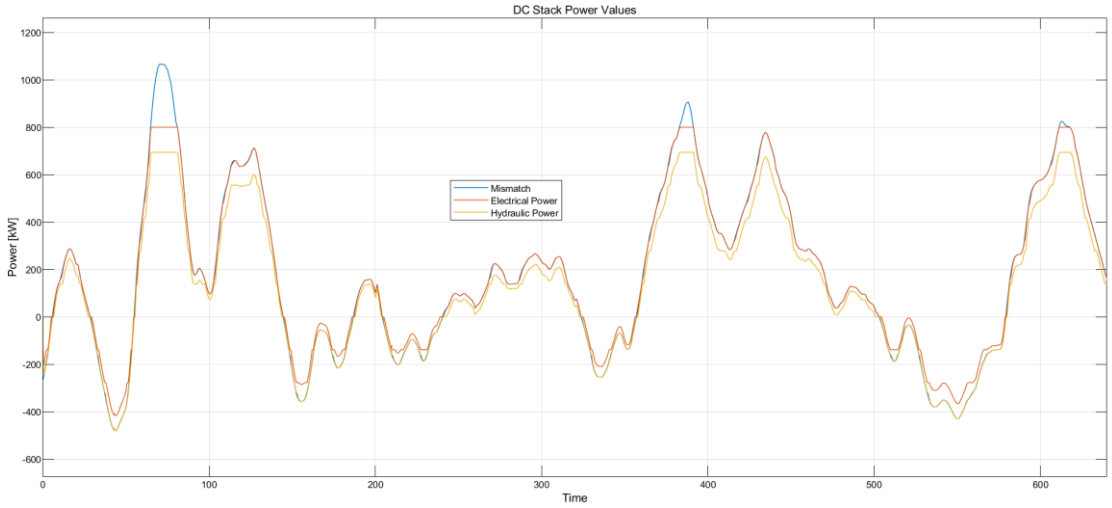

Figure 41 - Power profiles of the DC Stack

4.1.4. Mixed SoC

When analyzing Figure 42, it is possible to notice more fluctuations. This is because the only DC machine present has to go from a situation where it is delivering almost full capacity to another situation when it has to deliver almost zero power since the next in line TAM has been activated. The rationale behind Figure 43 is the same as in the previous cases.

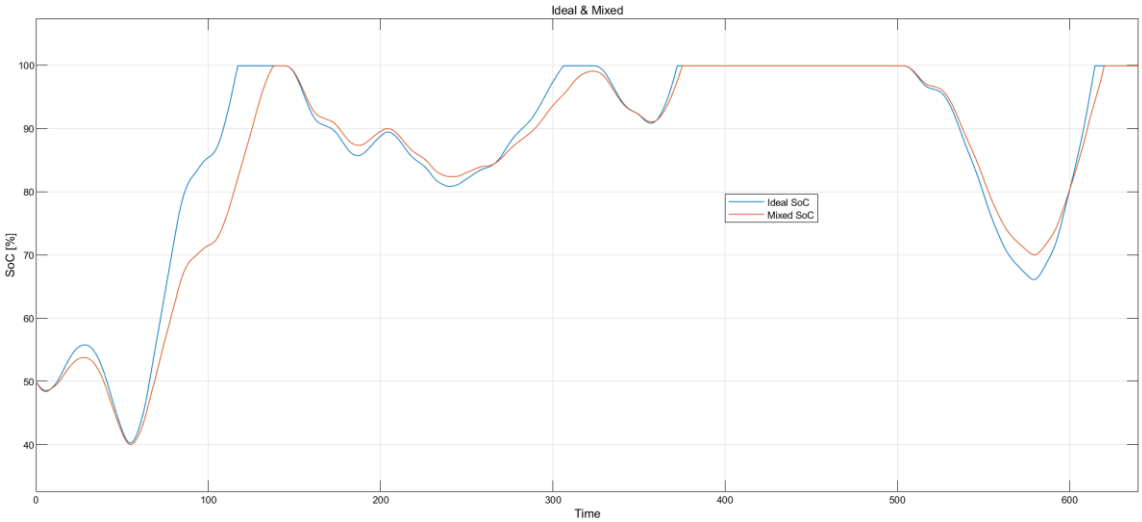

Figure 42 - Comparison between the SoC [%] of the Ideal and the Mixed Stack

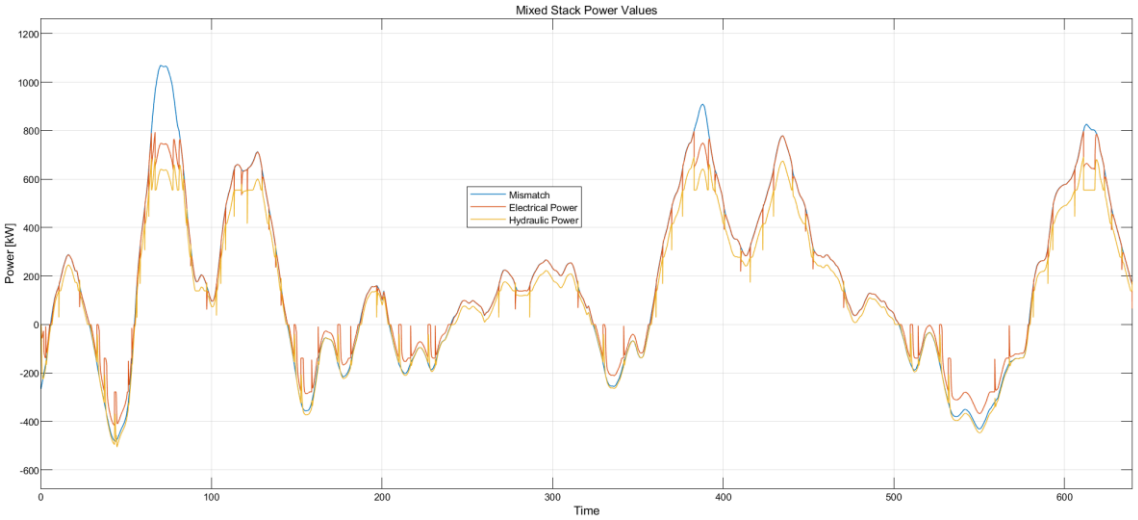

Figure 43 - Power profiles of the Mixed Stack

4.1.5. Split DC SoC

When the system works at low partial load, the efficiency of this configuration is very low, as can be noticed in Figure 45. When the system works in nominal conditions or extremely close to it this configuration is as good as the DC stack. This behavior can be seen when the mismatch is greater than the nominal power of the system, for instance, looking at Figure 45, between t = 50s and t = 80s.

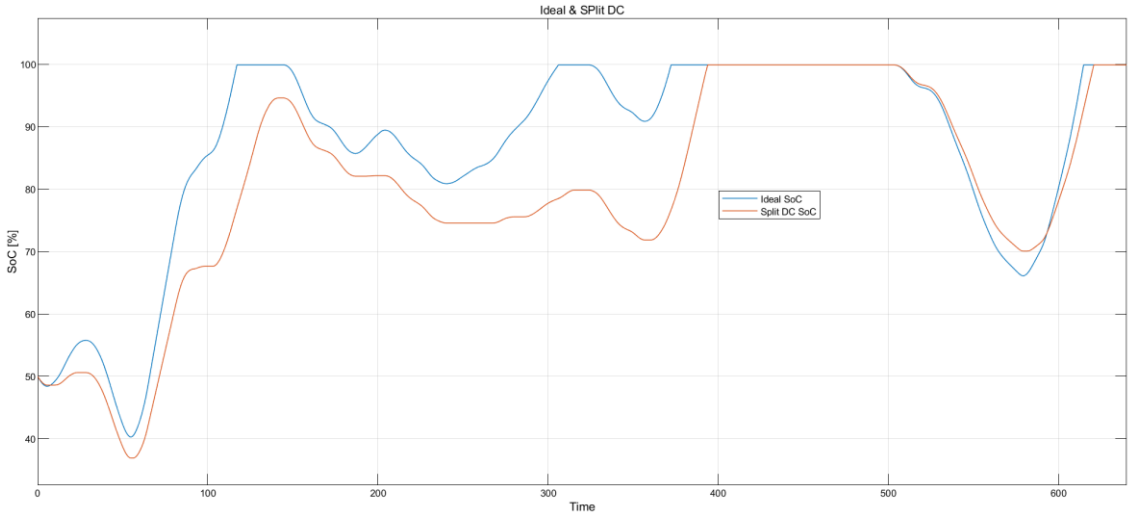

Figure 44 - Comparison between the SoC [%] of the Ideal and the Split DC Stack

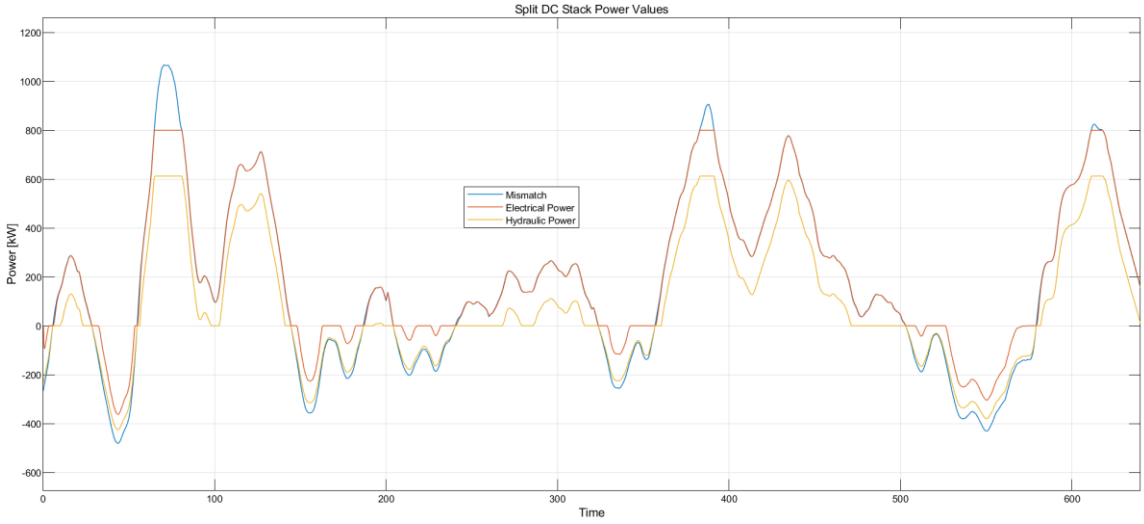

Figure 45 - Power profiles of the Split DC Stack

4.1.6. 125% Power output DC SoC

For this configuration, the SoC behavior is close to the one of the DC, as can be seen in Figure 50. The advantage is that the nominal power can be exceeded as can be seen in Figure 46 in the period between t = 50s and t = 80s. The fluctuations are due to the fact that if the mismatch exceeds the 125% power output of one machine, then it will have to decelerate down to its nominal power output. Also, from Figure 47, it can be noticed that the efficiency of the system is quite high most of the time, in fact the red and yellow line are close to each other.

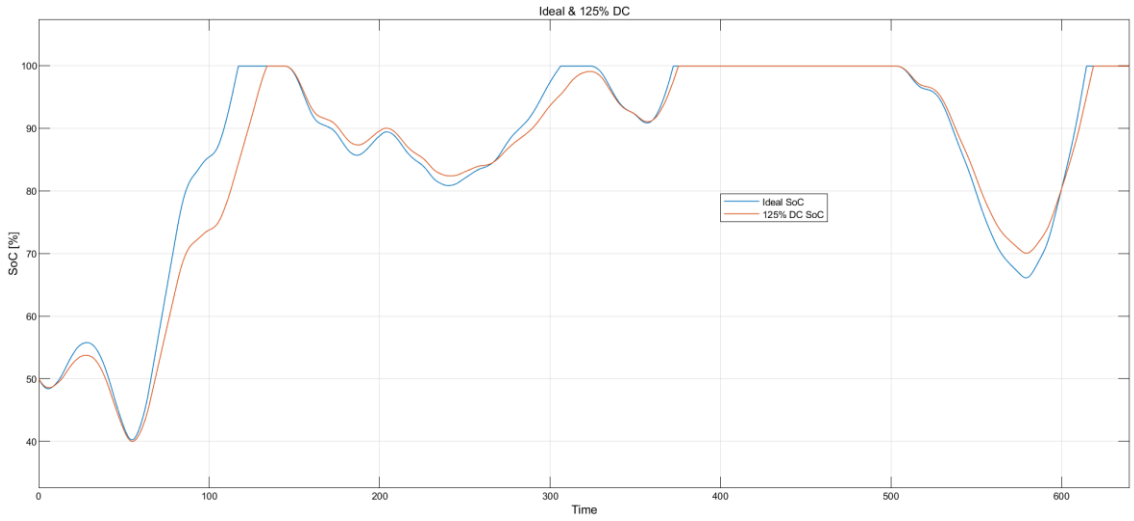

Figure 46 - Comparison between the SoC [%] of the Ideal and the 125% Power Output DC Stack

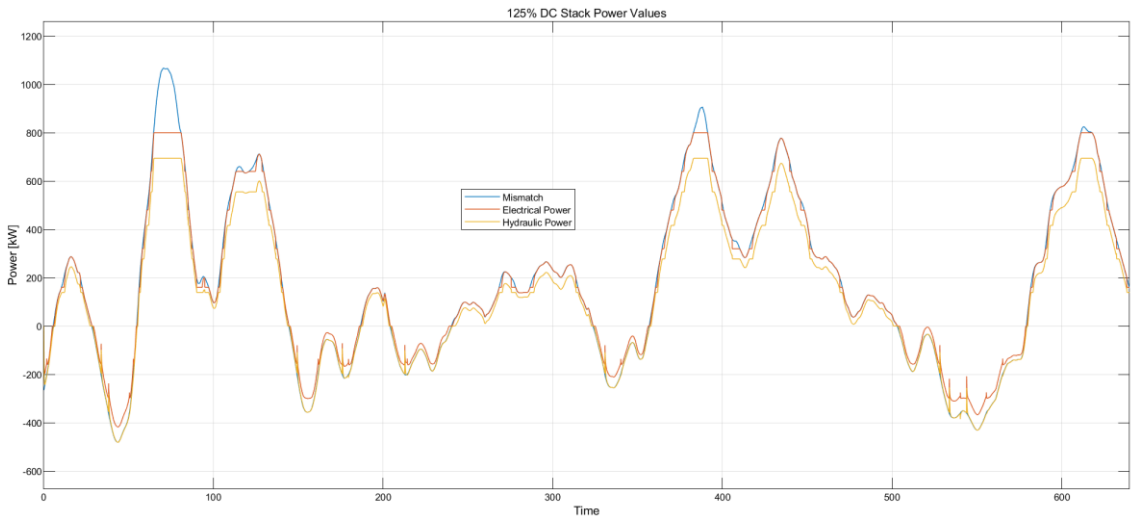

Figure 47 - Power profiles of the 125% Power Output DC Stack

4.1.7. 50% TAM SoC

As can be seen in Figure 48, the SoC curve produced by this configuration sticks to the Ideal SoC curve well. Similarly to the curve explained in section 4.1.2., the red curve crosses the blue curve more than once.

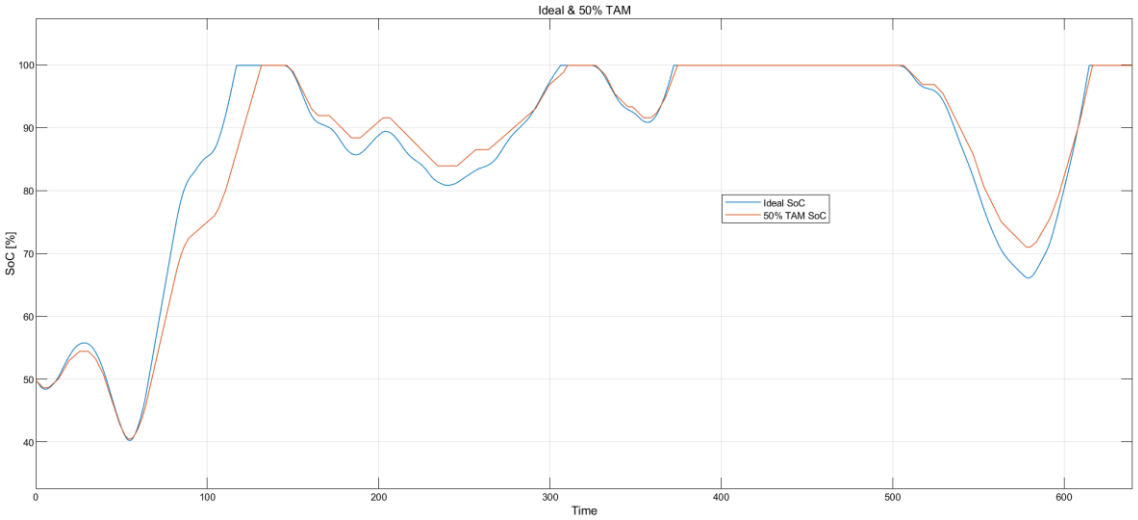

Figure 48 - Comparison between the SoC [%] of the Ideal and the 50% TAM Stack

In Figure 49 can be noticed how the first module of the stack is activated earlier, indeed when the mismatch is equal to 50% of the rated power of the TAM. The aim of this configuration is to avoid switching the TAMs on and off when the mismatch fluctuates around a certain value: this benefit can be observed in the period between t = 200s and t = 230s in Figure 49.

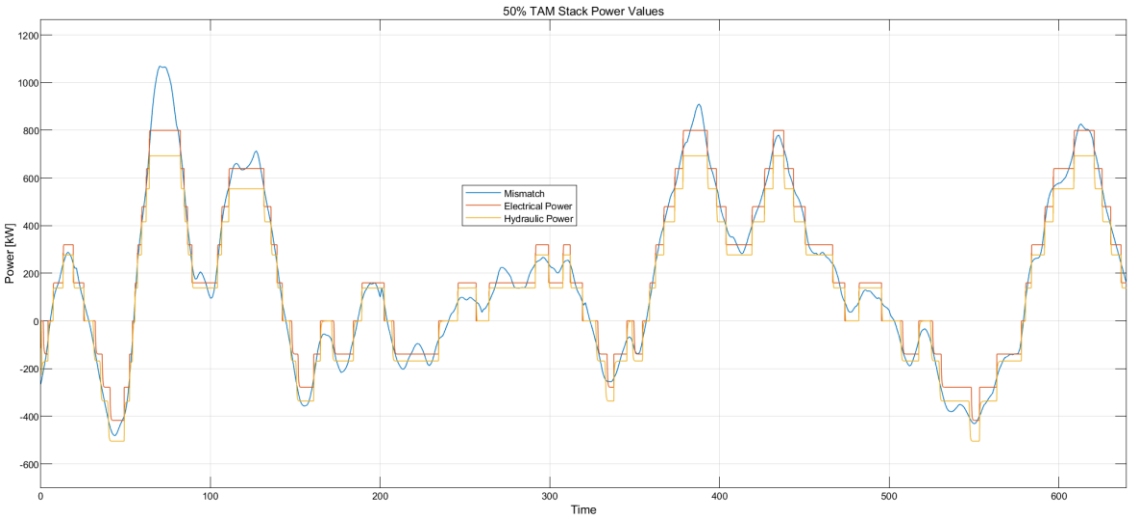

Figure 49 - Power profiles of the 50% TAM Stack

4.1.8. 10 seconds TAM SoC

The relevance of this simulation has been explained in section 3.5.7. As expected, the red curve in Figure 50 looks delayed with respect to the blue one. The red curve is more stable and less fluctuating than the red curves of the other simulations. Figure 51 in the next page shows the same delay in the behavior.

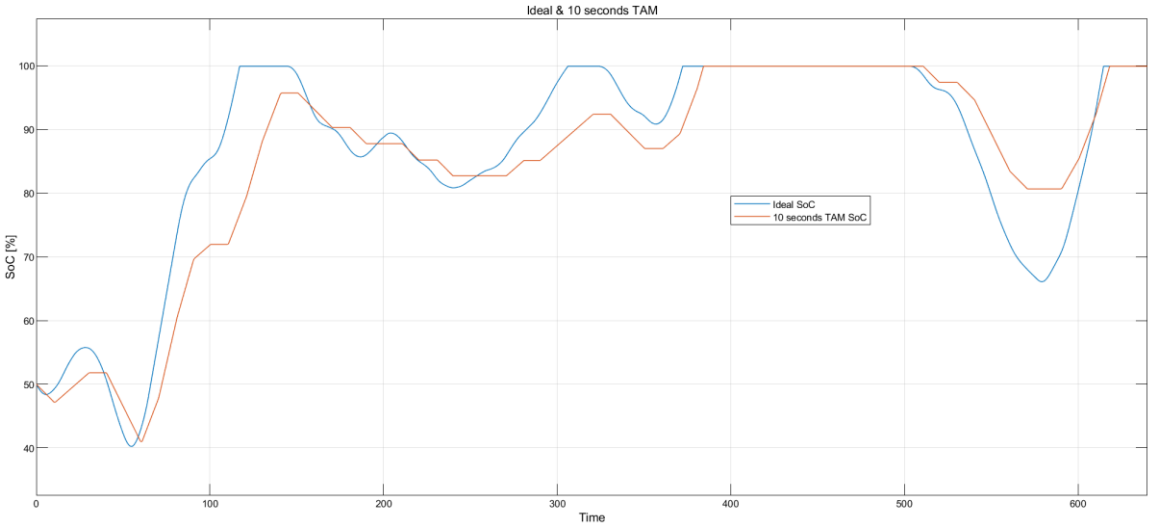

Figure 50 - Comparison between the SoC [%] of the Ideal and the 10 seconds TAM Stack

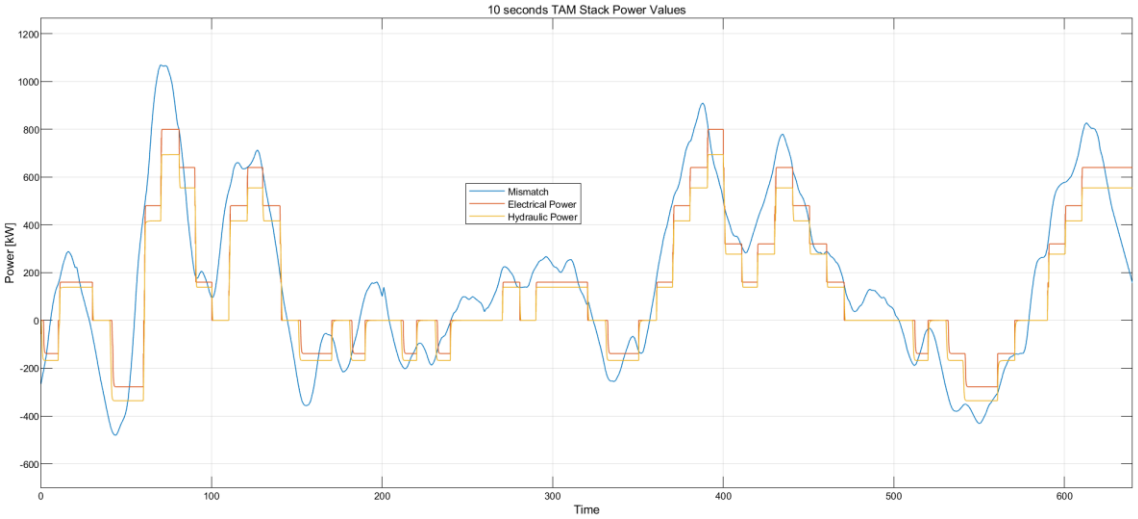

Figure 51 - Power profiles of the 10 seconds TAM Stack

4.2. Results

The goal of this project is to develop different engagement and dispatch protocols for the Battery Management System and to study how they affect the efficiency and the performance of the system, so that a suitable configuration of the hydraulic and electric components used to charge and discharge the Ocean Battery can be designed for a further installation. It is important to always keep in mind that the cost of such components is outside the scope of this research. To compare all the different configurations, the results of all the simulations that have been run need to be analyzed.

4.2.1. Round-Trip Efficiency simulation results

The first results that are going to be analyzed are the ones relative to the RTE. As explained and remarked many times throughout this work, efficiency is the ratio between the energy output and the energy input. What this project is concerned with, since the subject of the research is a battery, is the Round-Trip Efficiency of the Ocean Battery. The ideal battery should have very low losses regardless the power demand it is subjected to. section 3.6. shows how the RTE varies for every configuration when the battery is fully charged and then discharged using different configurations. How can be stated whether one configuration is more efficient than another? The RTE curves are different to one another, but the way it is possible to address their efficiency is by calculating the average of each curve, finding so the Average Round-Trip Efficiency (ARTE). The higher the average is, the more efficient the configuration is regardless the power percentage it is working at. It is important to consider while looking at these results that every configuration presents situations of very low and null RTE. Figure 52 shows such comparison:

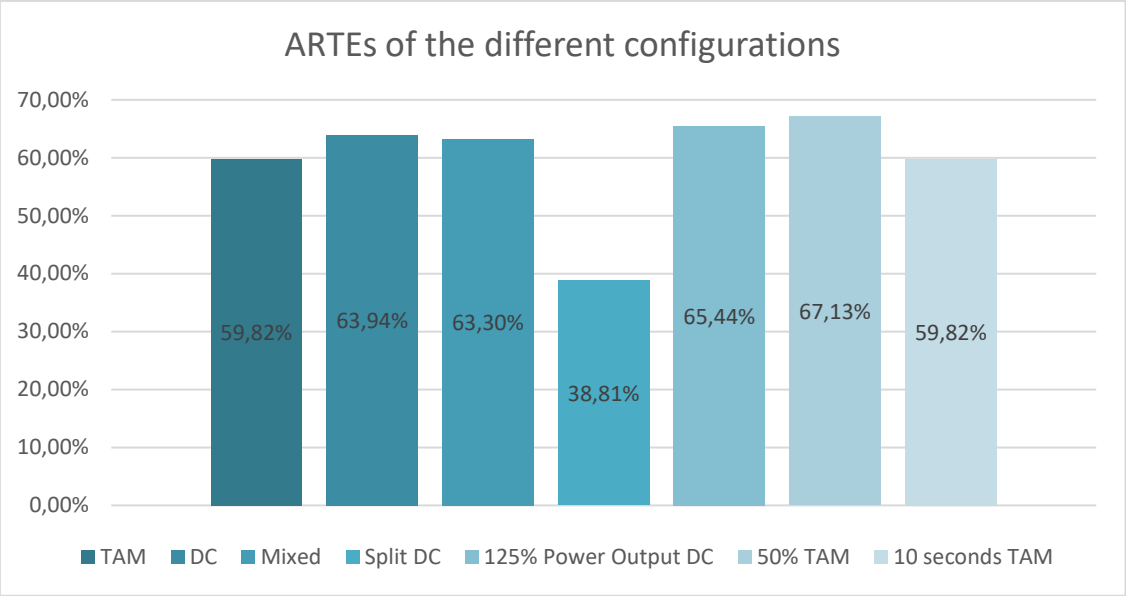

Figure 52 – Comparison of the ARTEs of the different configurations of the system

As expected, the configuration with the lowest ARTE with the value of 38.81% is the Split DC configuration. Being this configuration so far from the other configurations' ARTEs, it can already be discarded as possible candidate for the optimal configuration. All the other stacks have comparable ARTE values. By only considering this graph, the optimal configuration appears to be the 50% TAM with an ARTE of 67.13%. Nevertheless, there are others results that need to be taken into consideration and are presented in the next sections. Table 12 ranks the ARTEs of the configurations from best to worst.

Ranking	Configuration	Value of the ARTE [%]
1	50% TAM	67.13
2	125% Nominal Power Output DC	65.44
3	DC	63.94
4	Mixed	63.30
5	TAM	59.82
6	10 seconds TAM	59.82
7	Split DC	38.81

Table 12 - Ranking of the ARTEs of the configurations

4.2.2. Closeness to the Ideal SoC curve

The simulations run concerning the behavior of the various configurations' SoC will now be analyzed. As explained in section 4.1., the goal of those simulations was to understand which configuration has a closer behavior to the Ideal one. Figure 53 shows all the configurations' SoC curves compared.

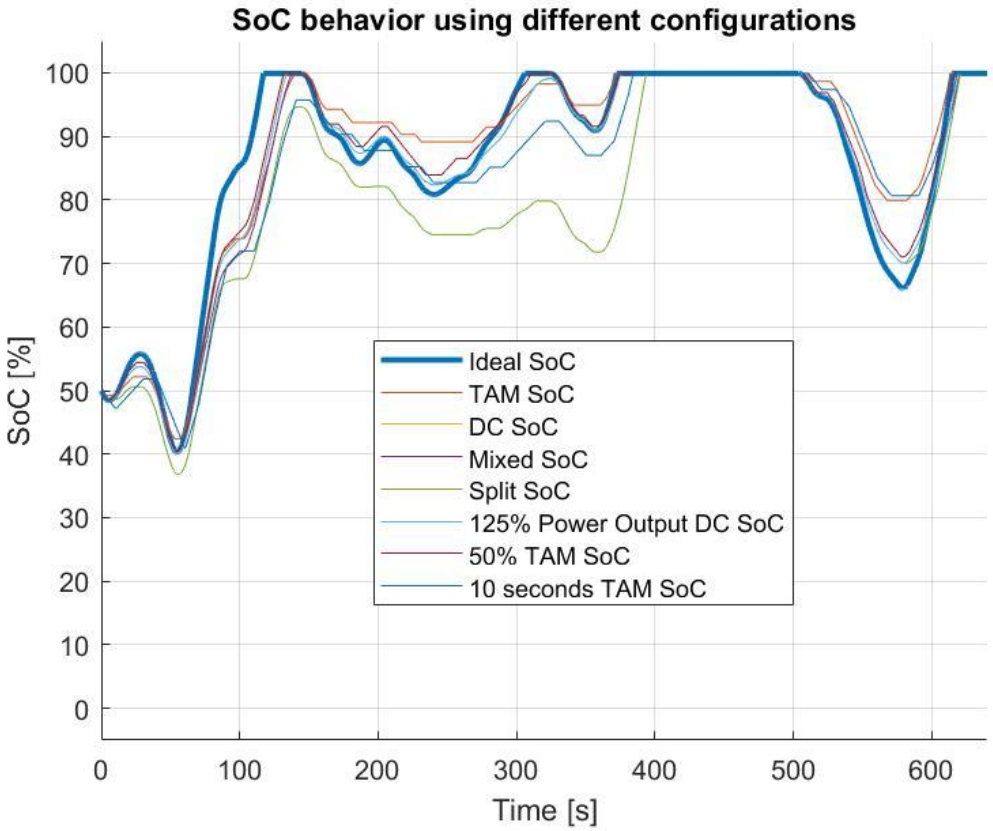

Figure 53 – Comparison between the SoC curves

The thick blue curve represents the ideal behavior of the SoC, which is the behavior of the SoC of the Ocean Battery if all the power available and demanded would be given to the battery and delivered to the grid respectively, without any losses or delay. This behavior is the one desired, unfortunately though, losses and delays are present and, in some cases, very relevant. Nevertheless, the optimal configuration's SoC curve should strive to resemble the Ideal one as much as possible. To mathematically state the "closeness" between the curves the following method has been used.

The objective curve can be higher or lower than the Ideal one, hence the interest is in the absolute value of the difference in height between the two. The absolute value of a difference can be obtained either by elevating to the second power and then taking the square root of

such result, or by extracting the absolute value using the block “abs” in Simulink which gives the module of a given signal. The latter has been preferred due to its simplicity in the calculation. This signal is later integrated over the time of the simulation to find the parameter “Cumulative Distance to the Ideal Curve”, abbreviated in CDIC. The unit of the CDIC is kWh since a power difference is being integrated over time. Comparing the CDICs at the end of the simulation the closeness to the Ideal behavior of the SoC one can be evaluated. The lower this value is, the closer to the Ideal curve the configuration will be.

Figure 54 compares the CDICs. The Split DC CDIC’s CDIC and the 10 seconds TAM’s CDIC are out of scale, confirming for the first one that this type of protocol should be avoided. This result is a signal that the second engagement and dispatch protocol, the 10 seconds TAM, is not worth being further investigated.

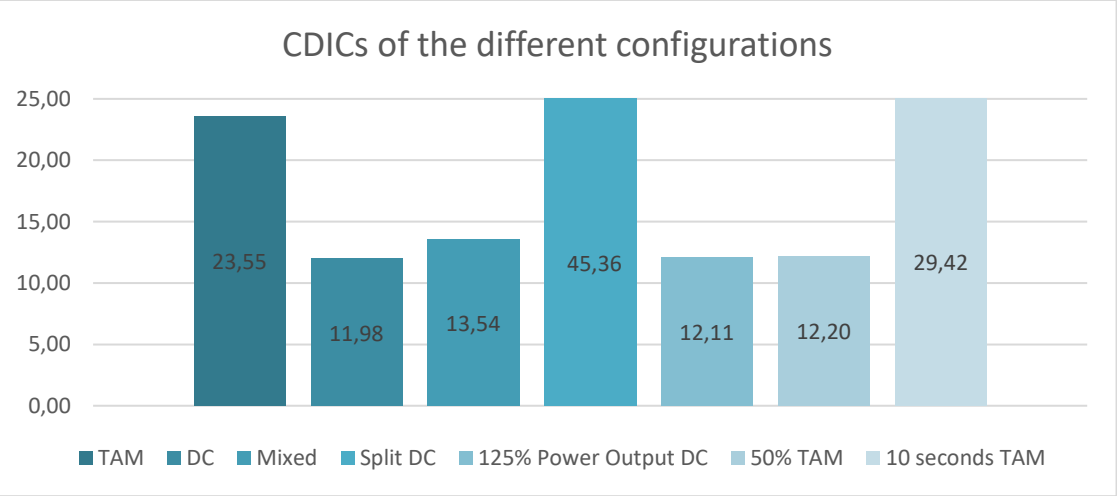

Figure 54 - Comparison of the CDICs of the different configurations of the system

Table 13 ranks the CDICs of the configurations from best to worst.

Ranking	Configuration	Value of the CDIC [kWh]
1	DC	11.98
2	125% Power Output DC	12.11
3	50% TAM	12.20
4	Mixed	13.54
5	TAM	23.55
6	10 seconds TAM	29.42
7	Split DC	45.36

Table 13 - Ranking of the CDICs of the configurations

4.2.3. Efficacy of the configuration

Efficacy is a parameter that is related to the efficiency, but the terms involved in the division are different.

The idea of studying this parameter comes from company experience and needs. While discussing on the various systems' characteristics with the company, it was highlighted that although the TAM stacks seem to be a good option, the fact that they are limited in delivering energy under certain conditions cannot remain unexplored. If the machines that are activated by a certain mismatch value for a consistent amount of time are not producing enough energy to cope with the requirements of the mismatch, then this represents a failure mode. This type of failure mode can be studied and quantified by the parameter efficacy.

The efficacy is calculated by dividing the energy that has been effectively either stored in the battery during the charging process or delivered to the grid during the discharging process, by the energy that should have been ideally exchanged. In other words, it is the multiplication between two terms: the first one is the ratio, when the mismatch is positive, between the energy stored in the battery and the energy made available by the mismatch; the second one is the ratio, when the mismatch is negative, between the energy actually delivered to the grid, and the energy demanded by the mismatch.

Referring to Figures 39, 41, 43, 45, 47, 49 and 51 the efficacies of those systems are calculated by multiplying the ratio between the integral of the yellow curve over the blue curve when the battery is charging (positive mismatch), and the ratio between the integral of the red curve over the blue curve when the battery is discharging (negative mismatch).

The values of the efficacies are presented in Figure 55.

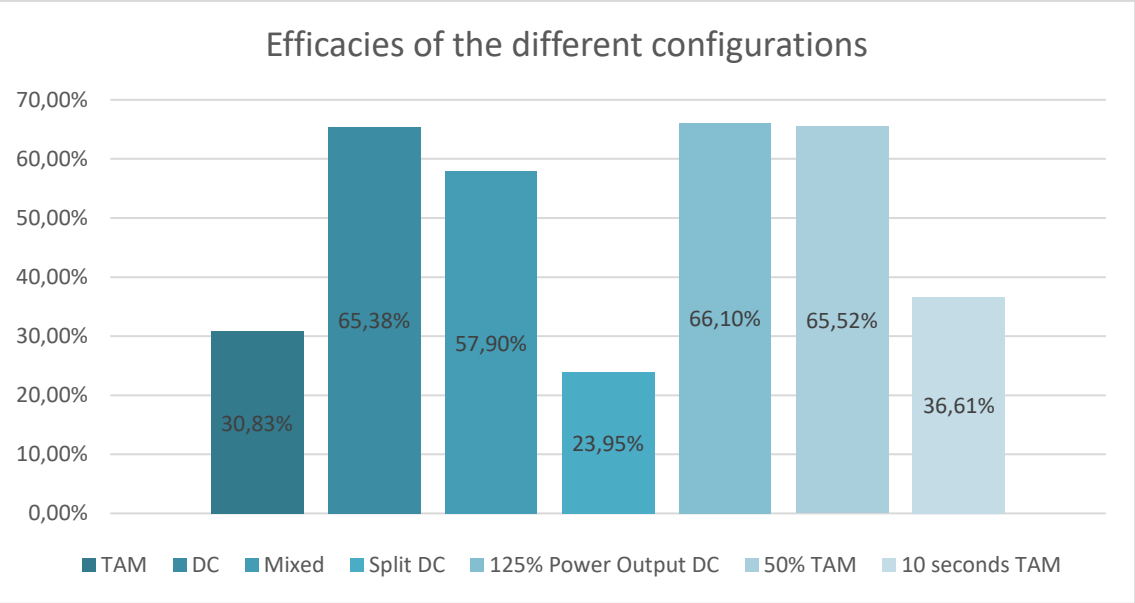

Figure 55 - Comparison of the Efficacies of the different configurations of the system

Table 14 ranks the efficacies of the configurations from best to worst with the respective values. I this case, the higher the efficacy, the better the configuration.

Ranking	Configuration	Value of the Efficacy [%]
1	125% Power Output DC	66.10
2	50% TAM	65.52
3	DC	65.38
4	Mixed	57.90
5	10 seconds TAM	36.61
6	TAM	30.83
7	Split DC	23.95

Table 14 - Ranking of the Efficacies of the configurations

The TAM stack, as expected, is strongly penalized by this parameter since it can be said that the activation of a new TAM is “quantized”. The 50% TAM configuration though, shows very promising results since their efficacy is the second to best one.

4.2.4. Selection of the best configurations

From the previous simulations it is straight-forward to understand that some configurations are not a viable option to be installed in the Ocean Battery.

The Split DC system is always the worst performing one with great distance to the others, hence proceeding with this choice would be substantially wrong. There are basically no advantages coming from this configuration: it can be discarded.

The 10 seconds TAM engagement and dispatch protocol and the TAM configuration have also shown discouraging results, always ranking between 5^{th} and 6^{th} place with quite a substantial margin from the better performing ones. The advantages of these two configurations can also be found in the 50% TAM configuration, so they can both be discarded as well.

The Mixed configuration shows good results, but it is always ranked 4^{th}, meaning that there are three other configurations that are better performing than that one. Therefore, this configuration can also be discarded.

The choice of the optimal configuration and BMS engagement and dispatch protocol falls between the three best performing configurations which are: the DC stack, the 125% Nominal Power Output DC stack and the early activated 50% TAM stack. Among these three configurations, there is one that needs further investigation: the 50% TAM. In section 4.3. it is explained why.

4.3. Early activation TAMs

From the previous simulations, it is possible to notice that the 50% TAM stack is always in the top three performing configuration. The idea of early activating one unit came from the impossibility of the TAMs to work in partial load, hence in many cases some power cannot be exchanged. Early activating these machines leads to a better performing configuration. Nevertheless, the value 50% was chosen without any base of evidence, but just because it is the mean value between 100% (situation corresponding to the TAM stack) and 0% early activation. In the case of 0% early activation, a new unit is activated as soon as the power demand is above the previous rated step. E.g.: if the mismatch is 321 kW, three machines are activated to cope with such a mismatch, similarly, if the mismatch is 10 kW, one machine is activated. All the fractions between 0% and 100% should be analyzed to find the best performing one and, eventually, compare it to the DC and the 125% Nominal Power Output DC.

It is important now to choose wisely the value of the percentage of the mismatch at which a new TAM should be activated. To deicide the value of the early activation, the same three parameters calculated in the previous sections are calculated via simulations and compared among them.

It is important to keep in mind, as benchmarks, the values of the two other direct candidates: the DC stack and the 125% Nominal Power Output DC Stack.

First, the ARTEs of the different early TAMs is presented in Figure 56:

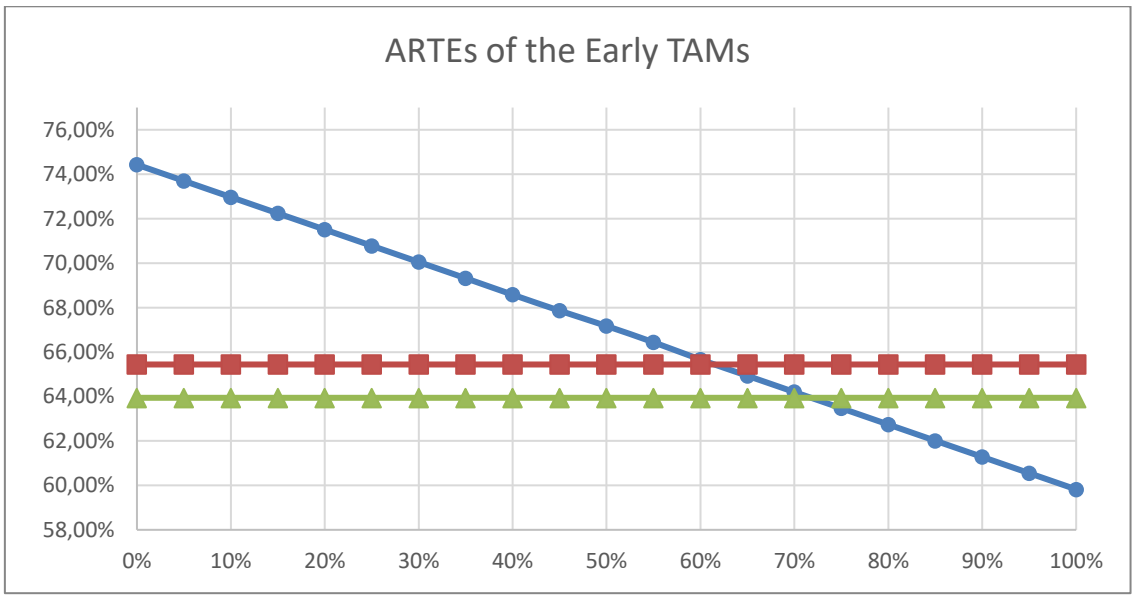

Figure 56 - ARTEs of the early TAMs

The red line represents the ARTE of the 125% Nominal Power Output DC, and the green one represents the ARTE of the DC machine. From this graph it is possible to understand that any value for the early activation below or equal 60%, would be a better choice, ARTE-wise, than the previous two options.

So, the first condition that needs to be given to the percentage of early activation is: early percentage ≤ 60%.

The second parameter considered is the Cumulative Distance to the Ideal Curve. The benchmarks that need to be taken into considerations are the following: the CDIC of the DC stack, which is equal to 11.98, and the one of the 125% Nominal Power Output DC stack which is equal to 12.11. In order to better perform than these two stacks, the value of the CDIC of the early activated TAMs has to be lower than the previous.

Figure 57 shows the behavior of this curve and the two benchmarks. Again, the red line represents the CDIC of the 125% Nominal Power Output DC, and the green one represents the CDIC of the DC machine.

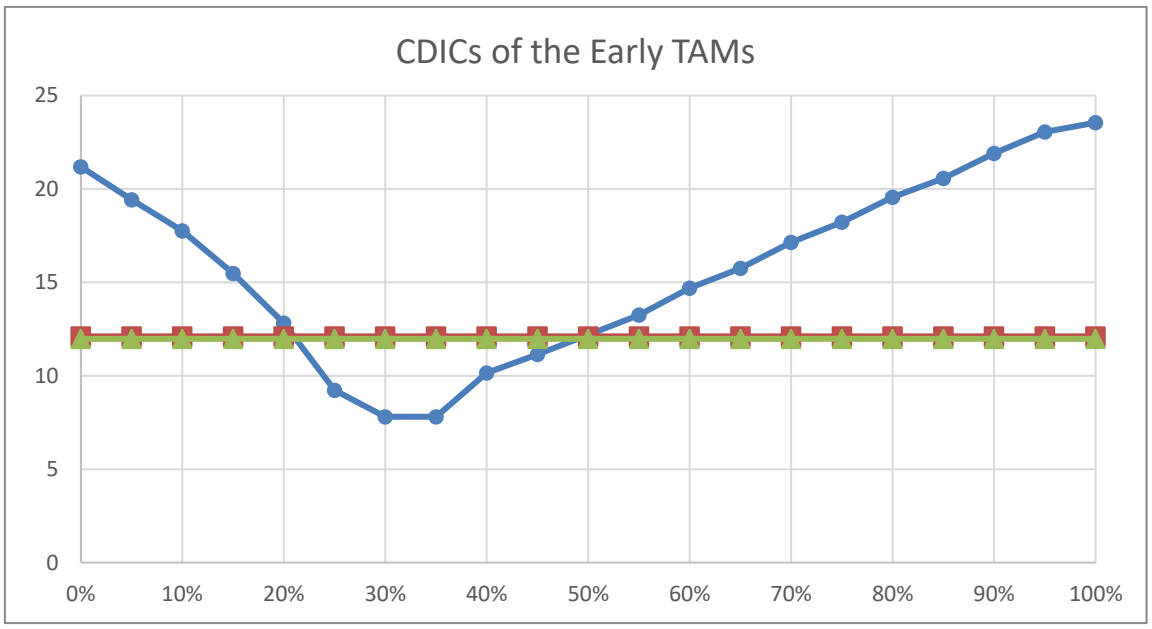

Figure 57 – CDICs of the Early TAMs

So, the second condition that needs to be given to the percentage of early activation is: 22% ≤ early percentage ≤ 50%. This second condition is more restrictive than the previous one.

The last parameter considered to perform such comparison is the Efficacy of the system. The benchmarks that need to be taken into considerations are the following: the Efficacy of the DC

stack, which is equal to 65,38%, and the one of the 125% Nominal Power Output DC stack which is equal to 66,10%.

In order to better perform than these two stacks, the value of the Efficacy of the early activated TAMs has to be greater than the previous.

Figure 58 shows the behavior of this curve and the two benchmarks. Again, the red line represents the Efficacy of the 125% Nominal Power Output DC, and the green one represents the Efficacy of the DC machine.

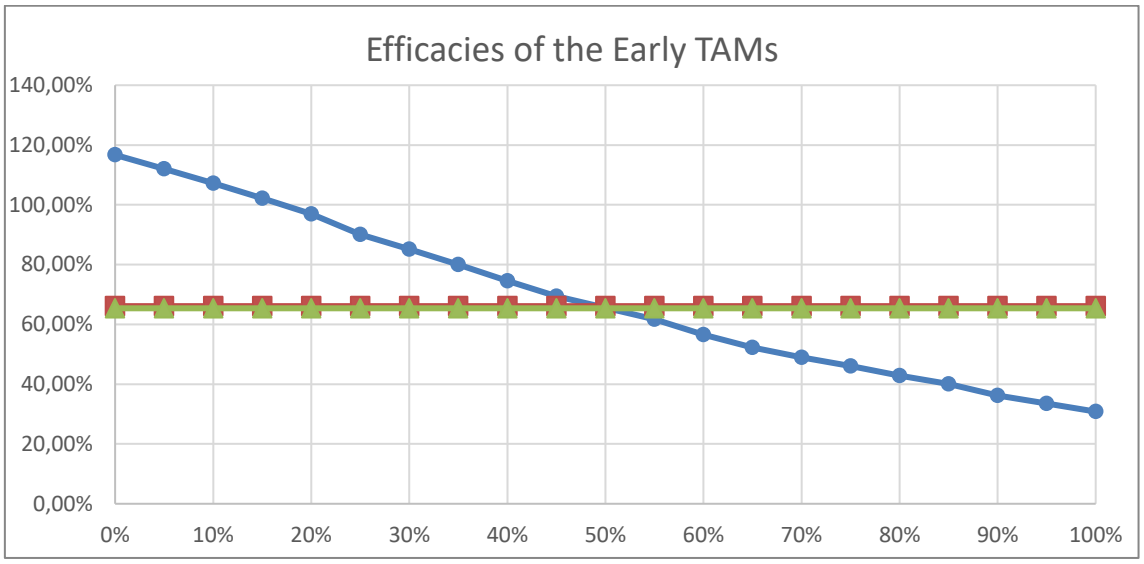

Figure 58 - Efficacies of the Early TAMs

So, the last condition that needs to be given to the percentage of early activation is also include in the previous one and it is: early percentage ≤ 50%.

From these simulations, it appears that the best configuration to be installed is the 22% Margin TAM whose parameters are: ARTE = 71,23%, CDIC = 11,21 and Efficacy = 93,88%.

4.4. Security of supply

One drawback that needs to be mentioned when using the early activation TAM engagement and dispatch protocol for the system, is the fact that the demand-response is not immediate nor precise. In other words, the power extracted from the wind turbines might not be fully used to charge the storage system; similarly, the power withdrawn from the battery and delivered to the grid does not thoroughly matches the behavior of the demand. The security of supply if using this installation is not guaranteed.

Referring to Figure 59, when the mismatch is positive, sometimes more power than what it is available is needed to run all the necessary TAMs and, on the contrary, when the mismatch is negative, sometimes more power than what is requested from the grid is generated by the Ocean Battery and delivered.

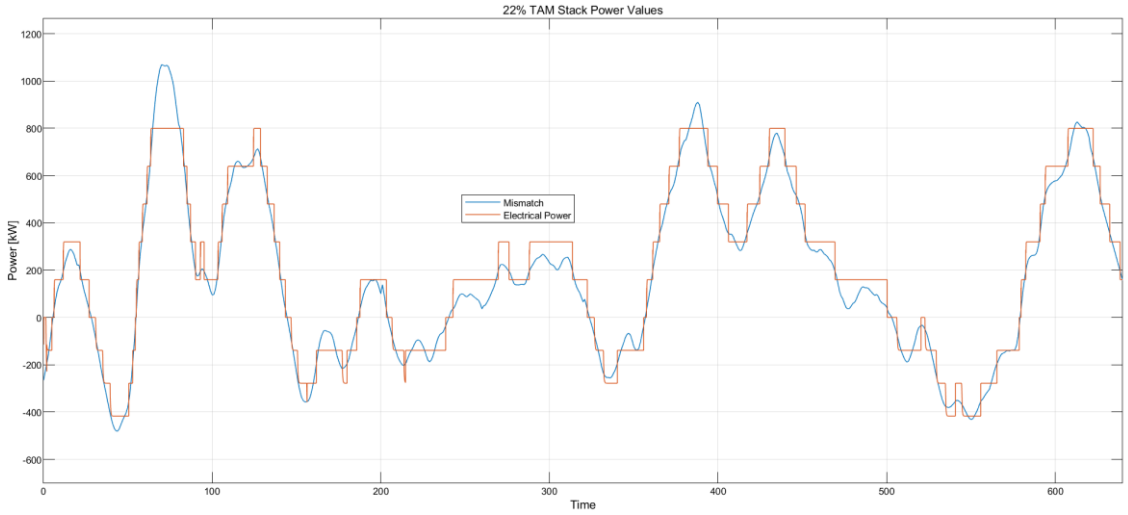

Figure 59 - Power profiles of the 22% TAM Stack

The positive mismatch situation is considered first. When the red line is above the blue one, more power than what is being produced by the wind turbines is needed to charge the battery. Such power would have to be retrieved in some other way, for instance by buying it from the grid itself. If the red line is below the blue line, simply not all the available power is not used to charge the battery. This power surplus will be simply delt with by the grid management system.

When the mismatch is negative, sometimes more power than what is needed by the grid is delivered by the storage system. The grid management system would have to deal with this energy surplus coming from battery. In some other situation, less power than what is needed is being supplied.

Among the four situations described, two of them, as explained, are a grid management system's concern, the other two instead can be problematic for the Ocean Battery.

It is very important to state that one more time that several Ocean Batteries will be connected and working as a cluster. The system is not supposed to serve the purposes of a microgrid storage system therefor the above-described behavior of the system is acceptable by the company. Nevertheless, it is interesting and useful for the company to quantify the flaws of this situation.

Using the early TAM stack the system reacts as follow.

As can be seen in Figure 60, the earlier a new TAM is activated, the more energy needs to be bought from the grid during the charging phase. For the chosen situation, the 22% Early activated TAM, around 10% of the whole energy that has been used throughout the simulation to charge the battery, has to be bought from the grid or retrieved in a somehow different manner than extracting it form the wind turbines.

Figure 61 shows the security of supply being the percentage of the energy demanded by the grid that was possible to deliver. The sooner a new TAM is activated, the more reliable the system is. The 22% Early activated TAM is able to deliver 88.4% of the needed energy.

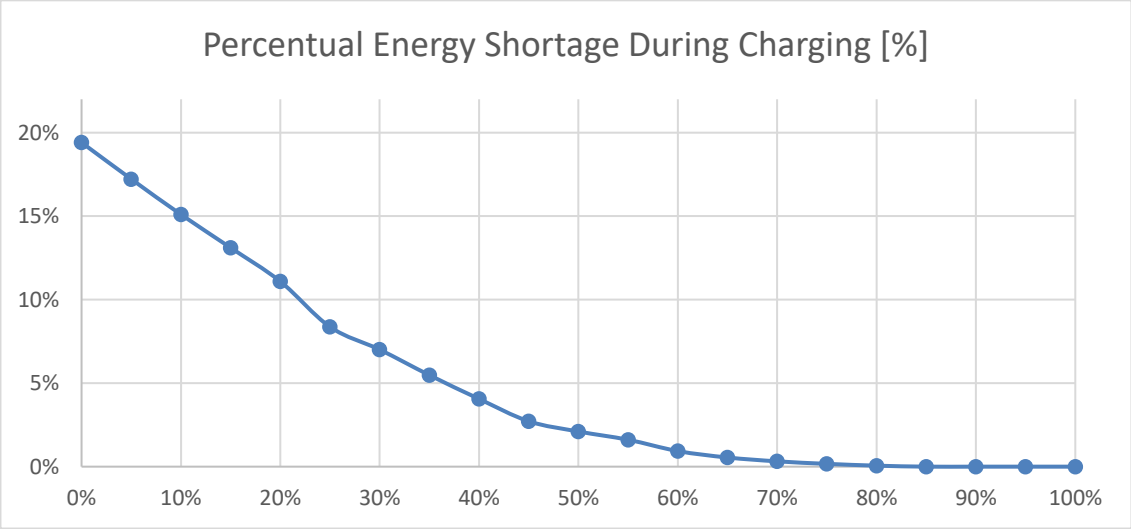

Figure 60 - Percentual of the energy used to charge the Battery during the simulation that cannot be retrieved from the wind turbines

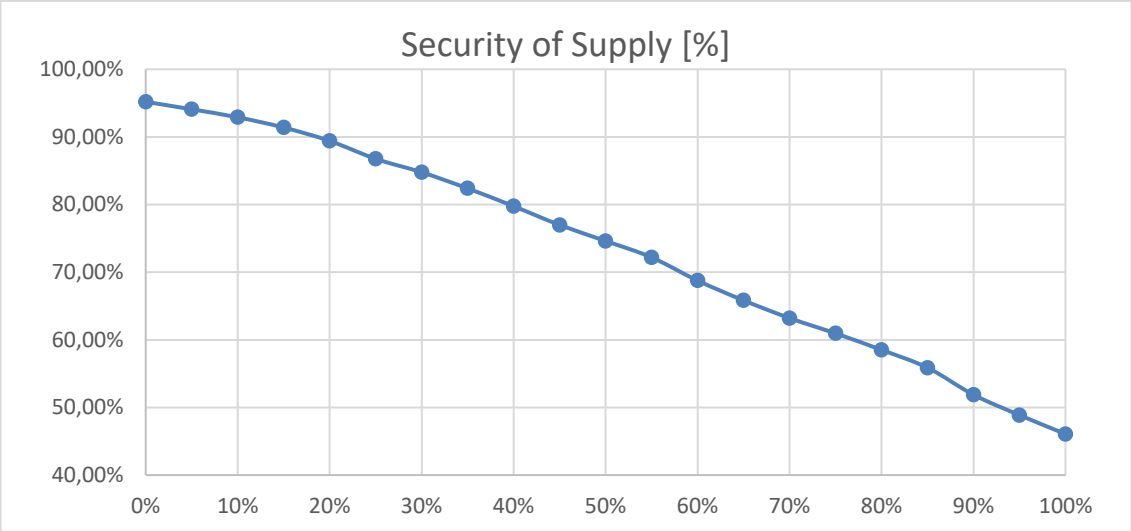

Figure 61 – Security of power supply instantly delivered to the grid

The fact that the energy shortage is not equal to zero and that the security of supply is not 100% with the proposed configuration might seem a great weakness of the system. It is not so. It is important to know that this storage technology is not meant to serve the purposes of an isolated microgrid [22] where power exchanges with the central energy grid are not possible. From this consideration it is possible to state that the performance of this technology are acceptable.

5. Conclusion and further recommendations

The goal of this thesis was to find how the efficiency and the performance change when changing the engagement and dispatch protocol of the Battery Management System of the Ocean Battery. This study has been carried out and, restricting the scope of the research to the situation where only one Ocean Battery unit is used, with the above explained mismatch considered and limited to the configurations presented. Such study has been performed running simulations in Simulink. The Simulink program, which is also on the deliverable of this thesis, responded well to all the simulations run and it is suitable to simulate the behavior of the system used to charge and discharge the Ocean Battery.

Having run all the simulations, the strengths and weaknesses of every engagement and dispatch protocol is now known and can be kept in consideration for future purposes. It has been understood that in this situation having units that run always in nominal condition rather than variable speed operation units results in a better performing and efficient system. Nevertheless, some protocols featuring the variable speed operation units are competitive with the fixed operation ones. It has been understood that the main drawback of using variable speed operation units is the fact that their efficiency can be very low when operated in partial load. On the other hand, using a fixed operation unit has the drawback of not being able to withdraw and deliver the exact amount of power that is needed to charge and discharge the Ocean Battery. This problem can be overcome, as it has been done, by studying what is the best engagement and dispatch protocol to implement in the system such that a compromise between all the considered parameters can be achieved.

It is possible to state that among the presented configurations, the 22% Margin TAM is the optimal configuration; since it is the configuration with the highest Average Round Trip Efficiency equal to 71,23%, it is the configuration whose behavior is the closest to the ideal one and its Efficacy is the best possible one with a value of 93.88%.

Having such an early activated TAM could result in more energy delivered to the grid than needed during the discharging process, and, vice versa, more energy bought from the grid when it comes to charging the battery. This could either be a negative drawback or a possibility to a further implementation. It is important to remember that the primary aim of

this technology is not to serve the purposes of a microgrid with 100% reliability of supply and no power exchanges with the main grid therefore such result is acceptable.

There will be more Ocean Batteries connected as a cluster and hence, the energy surplus produced while discharging one unit, could also be used to activate the PM systems of a different unit to charge it if its SoC is very low. Also, other solutions could be studied and implemented to use that energy production surplus. Vice versa, referring to the charging process, it is possible that an energy deficit happens, and some energy needs to be bought to effectively charge the battery. To activate more Pump-Motor systems in one Ocean Battery unit there might be need of more energy than what is being produced by the wind turbine connected to it. In this situation there would be the need to purchase more energy from the grid to cope with this situation or to see if a different wind turbine unit could generate the needed electricity.

All these situations that have been mentioned can be studied in the future by simulating scenarios where more batteries are connected, and the demand can be split among those. The Simulink system that has been produced throughout this thesis project is viable to conduct such simulations and further studies.

Furthermore, in the battery logic is not present a control mechanism that prevents the storage system from being fully discharged. For this work such implementation was not necessary, but when more batteries come to play it might be a good idea to insert such control mechanism.

Appendices

A. Hydraulic dimensioning

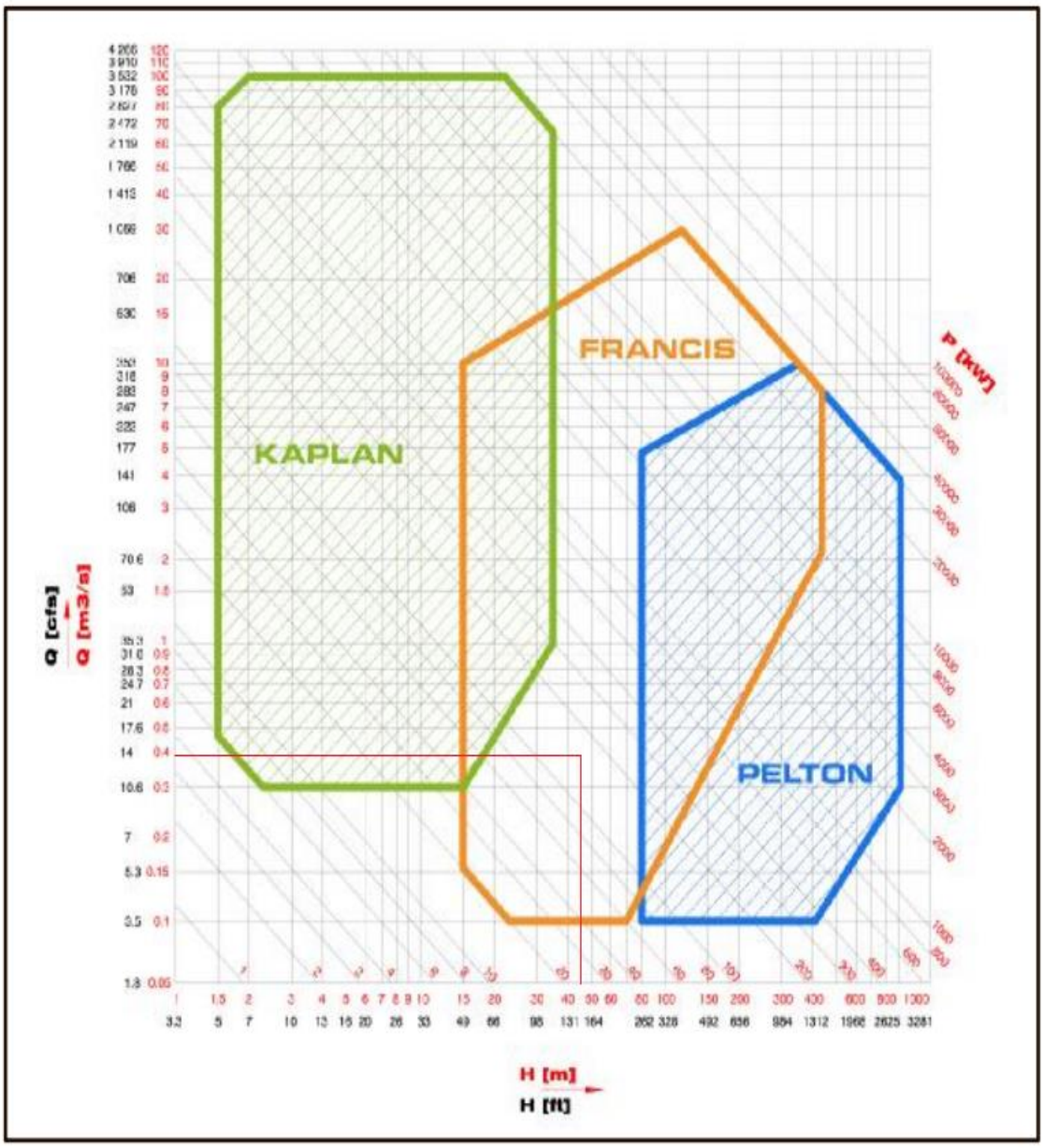

Figure 62 - Pump model chart selection [3]

To start the dimensioning the pump and turbine another parameter decision had to be taken: the nominal angular velocity. From the Simulink asynchronous motor, I could see that the nominal angular velocity at which the chosen motor runs is n_{motor}=1487 RPM. I assumed that no gearbox was needed so $n_{motor} = n_{pump}$ =1487 RPM. The reason I wanted to avoid the use of a

gearbox is because it is one of the most common failure causes in many other power generation applications like wind turbines [5].

From this, it was possible to calculate the pump specific speed n_{sp} using this formula:

$$n_{\mathrm{sp}} = \frac{n_{\mathrm{pump}} * (Q)^{0.5}}{(H)^{0.75}} \tag{9}$$

so, n_{sp} = 48.4 m^3/s.

Using the graph on Figure 63 [4] I could esteem the parameter Φ. Φ is the velocity ratio, meaning the ratio between the peripheral and the spouting velocity. This is important to calculate the impeller diameter D_1.

From the graph it could be read Φ = 1.09. In Figure 63 is also present the formula showing the relation between Φ and the impelled diameter D_1.

Reversing the formula and solving for D_1 I obtained an impeller diameter of 0.41 m.

Once the impeller diameter was calculated, following the paper instructions it was also possible to calculate the turbine moment of inertia J using the following formula:

$$J = 115 * (D)^{4.5} \tag{10}$$

The moment of inertia of the pump is J = 2.23 kg*m^2. It is rather important to specific that, given the known geometry of the rotating element, the obtained value for the moment of inertia is comprehensive of the mass of water inside the rotor itself so no further calculation is needed.

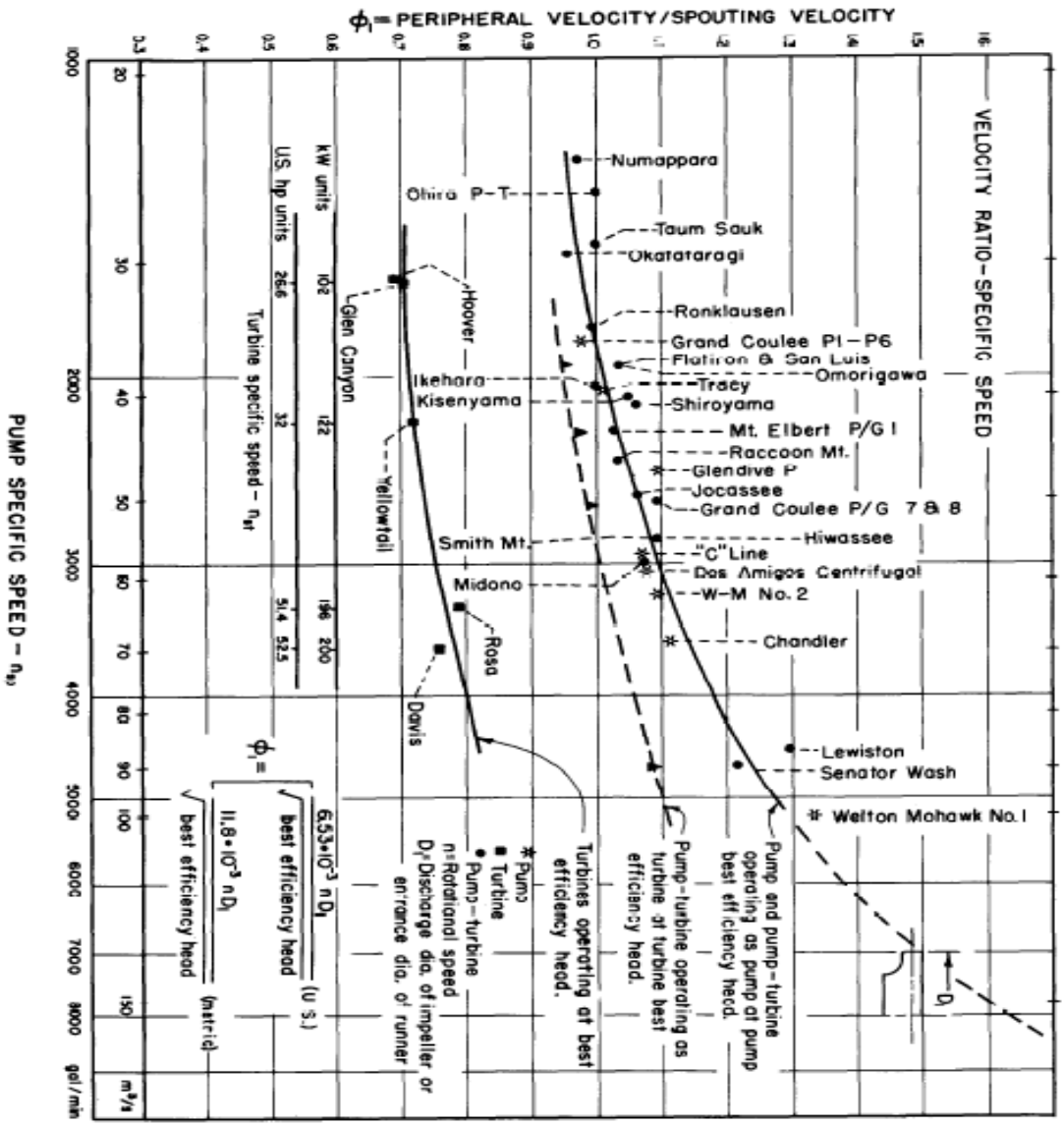

Figure 63 - Velocity ratio and specific speed graph [4]

Performing the exact same steps, it was possible to calculate the same specifics for the turbine instead of the pump.

B. Linear Extrapolation

To extrapolate precise values from a graph a method called linear extrapolation was used. Such mathematical method is now explained. As can be seen in Figure 64, the x-axis has an accuracy of 10%: the graph maximum value is 100 and it is possible to distinguish only the multiples of 10 in the graph by looking at the vertical lines. In order to read more values on the graph, one must manually increase the precision of the graph from 10 to 100 performing a linear extrapolation. This process is conceptually simple, yet quite time consuming if not performed with a computer.

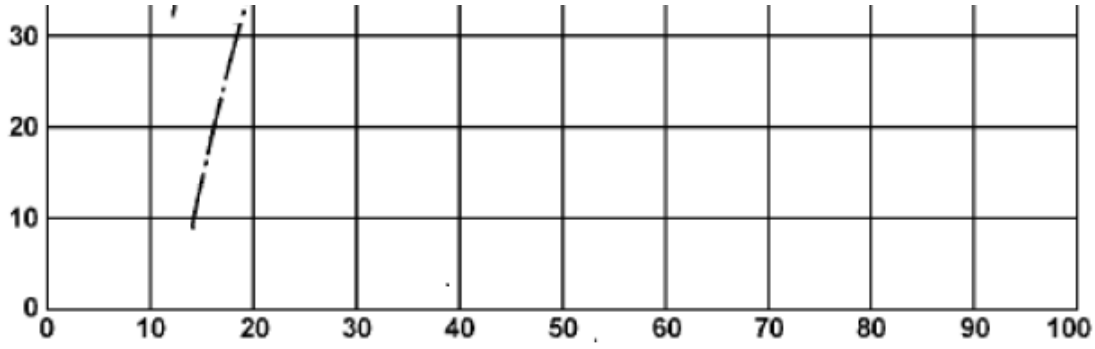

Figure 64 - Graph with precision 10

In order to perform a linear extrapolation on this graph, the first thing that needs to be done is to draw an oblique line from point (0, 10) to point (100, 30) as can be seen in Figure 65. Doing so, it is possible to extrapolate all the integer values between 10 and 20 in the y-axis.

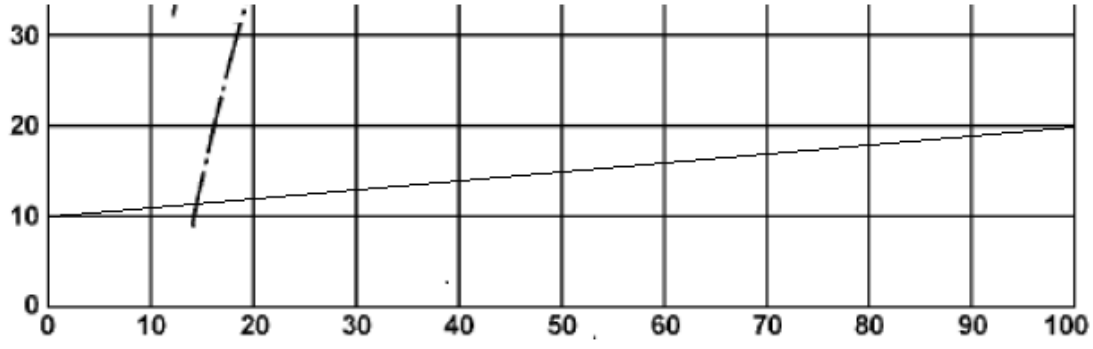

Figure 65 - Step 1 of the linear extrapolation method

The second step to perform, is to draw lines parallel to the x-axis any time the oblique line crosses the vertical lines of the pre-existing grid as shown in Figure 66. It is possible to notice

that the y-axis between 10 and 20 is now divided into 10 equally spaced segments. Each intersection between the line y-axis and the just drawn horizontal lines represents an integer value between 10 and 20.

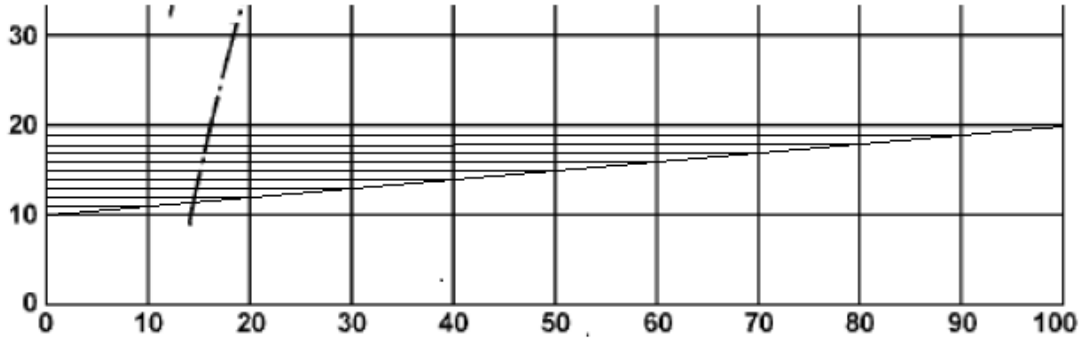

Figure 66 - Step 2 of the linear extrapolation method

All the previous steps need to be performed again in the other direction, therefore increasing the precision of the x-axis. Once done that, it is possible to read with more accuracy the graph pairing to every flowrate value, 100 in total, the corresponding value of the efficiency of the machine. Reading the y-value at the intersection between the vertical lines and the curve number two, gives the accurate value of the efficiency at a given operational point. As shown in Figure 3: η(Q=14%) = 10%; η(Q=15%) = 14%; η(Q=16%) = 20%.

As above mentioned, this process is as simple as time consuming if manually performed since the previous steps need to be done for every value in the range of zero to 100.

Once done that, it was possible to insert these values in Matlab and work with them. To further increase the precision of this function, the Matlab command “Interp” was used to have 1000 values, hence higher precision in the calculation.

C. Centrifugal machine load characteristic

To couple the two machines, it is needed to find the relationship between torque and angular velocity of the rotating element, being the pump and the turbine, that will later be coupled to the motor characteristic graph. In other words, also the characteristics of the hydraulic elements need to be determined and later represented in the same graph of the motor and generator.

The characteristic of the hydraulic components is explained in "*Fondamenti di macchine, Turbopompe"* [6].

As explained in section 2.1., the power needed by a centrifugal pump (or turbine) is equal to:

$$P * \eta = \rho * g * H * Q \tag{11}$$

Rewriting that equation, it can be said that:

$$P = \mathrm{K}_1 * H * Q \tag{12}$$

Where K_1 is a constant equal to $\frac{\rho * g}{\eta}$. Moreover, as shown in Equation 3, the power delivered is equal to the torque times the angular velocity.

In the previously mentioned paper [6], it is explained that the flowrate is directly proportional to the angular velocity of the pump (or turbine) and that the Head (H) that can be supplied, is directly proportional to the square of the angular velocity of the pump (or turbine):

$$Q \; \alpha \; \omega \quad ; \quad H \; \alpha \; \omega^2 \tag{13}$$

Substituting these two correlations into the second equation we get:

$$P = \mathrm{K}_2 * \omega^2 * \omega = \mathrm{K}_2 * \omega^3 \tag{14}$$

Where K_2 is a different constant than K_1.

From Equation 3, it is possible to understand that the value of the torque can be obtained by dividing the power by the angular velocity. Doing so, one can get a relation between the torque and the angular velocity of a centrifugal pump that looks as follow:

$$\frac{P}{\omega} = \frac{\mathrm{K}_2 * \omega^3}{\omega} \tag{15}$$

So,

$$\mathrm{T} = \mathrm{K}_2 * \omega^2 \tag{16}$$

This result is confirmed by the PDF "*Dynamic of Motor-load*" [7], where it is stated that, usually, centrifugal pumps' load increases quadratically with the increase of angular velocity, resulting in a parabola when plotted in a ω-T plane.

Now, to be able to fully describe the behavior of the centrifugal element, the value of the constant K2 needs to be calculated.

Calculating this value is quite a straightforward process: knowing the nominal power (160 kW) and the nominal angular velocity (155.7 rad/s) and using equation 3, the nominal torque can easily be calculated.

$$T = \frac{P}{\omega} = \frac{160000\ \mathrm{W}}{155.7\ \frac{rad}{s}} = 1027.6\ N * m$$

Using Equation 16 also the value of K2 can be calculated.

It is important to say that, the pump characteristic will be symmetric to the x-axis to the turbine characteristic since the pump receives power from the motor, and the turbine delivers power to the generator. Hence, a distinction between K_{pump} and the $K_{turbine}$ needs to be made.

$$\mathrm{K_{pump}} = \frac{T_{\mathrm{pump}}}{\omega^2} = \frac{1027.6\ \mathrm{N} * \mathrm{m}}{\left(155.7\ \frac{rad}{s}\right)^2} = 0.042388\ \frac{N * m}{\left(\frac{rad}{s}\right)^2}$$

$$\mathrm{K_{turbine}} = \frac{T_{\mathrm{turbine}}}{\omega^2} = \frac{-1027.6\ \mathrm{N} * \mathrm{m}}{\left(155.7\ \frac{rad}{s}\right)^2} = -0.042388\ \frac{N * m}{\left(\frac{rad}{s}\right)^2}$$

So, finally, for this centrifugal machine, it can be said that:

$$\mathrm{T} = \pm 0.042388 * \omega^2$$

D. Transient behavior of the system

The variation of any state variable, (being position, speed, temperature etc.) for every real system is not instantaneous, but it does require some time to reach steady state. In this section the transient behaviors of both the pump-motor (PM) system and that of the turbine-generator (TG) system will be explained and analyzed. The following explanation is backed up by the PDF "*Dynamic of motor-load*" [7].

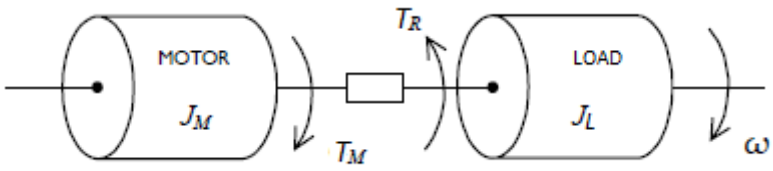

Figure 67 - Mechanical system, motor and load coupling [7]

Figure 67 shows a schematic of a mechanical system where a driving element, the motor, is coupled to a dragging element that needs to be accelerated, the load.

The equation of dynamic balance can be written as follow:

$$T_M - T_L = \frac{d(J\omega)}{dt} = J\frac{d\omega}{dt} + \omega\frac{dJ}{dt} \tag{17}$$

Where T_M and T_L and the motor and the load torque and J is the sum of moments of inertia of the motor and the load. Supposing that the pump and the turbine will always be filled by the same amount of water, therefore their mass nor dimensions change, the moment of inertia of the system can be assumed constant. Hence, the previous equation becomes:

$$T_M - T_L = J\frac{d\omega}{dt} \tag{18}$$

From this equation, it is trivial to notice that when $T_M > T_L$ the system is accelerating, vice versa when $T_M < T_L$ the system is decelerating and if $T_M = T_L$ the system is in steady state.

In the PM system the the TAM is the motor and the pump is the load, while in the TG system, the turbine is the motor and the generator is the load.

To study these two systems in Simulink, it is important to use a transfer function that can be obtained by perform a Laplace transform:

$$T_{\mathrm{M}}(t) \overset{L}{\Rightarrow} T_{\mathrm{M}}(s) \tag{19}$$

$$T_{\mathrm{L}}(t) \overset{L}{\Rightarrow} T_{\mathrm{L}}(s) \tag{20}$$

$$J\frac{d\omega(t)}{dt} \overset{L}{\Rightarrow} J[s\omega(s) - \omega(t=0)] \tag{21}$$

From which:

$$T_{\mathrm{M}}(s) - T_{\mathrm{L}}(s) = J\omega s \tag{22}$$

Assuming that $\omega(t=0) = 0$.

By definition, the transfer function relates the output or response of a system, in this the angular velocity to its input or stimulus, the difference between the motor and the load torque. So, writing the transfer function of this system we obtain as follow:

$$G_{\mathrm{M}}(s) = \frac{\omega(s)}{T_{\mathrm{M}}(s) - T_{\mathrm{L}}(s)} = \frac{1}{Js} \tag{23}$$

As explained in the previous sections, the torque of the TAMs is provided by the output of the Simulink block, while the torque of the pump and turbine is given by the previously deducted quadratic formula.

The moment of inertia of the two systems is different since the pump and the turbine have different dimensions. Summing the values of the moments of inertia in Tables 1, 2 and 3, we obtain:

$$J_{\mathrm{PM}} = J_{\mathrm{motor}} + J_{\mathrm{pump}} = 2.9 + 2.23 = 5.13\ [kg * m^2]$$

$$J_{\mathrm{TG}} = J_{\mathrm{generator}} + J_{\mathrm{turbine}} = 2.9 + 0.51 = 3.41[kg * m^2]$$

So, the Simulink part of the program representing the two systems looks as follow:

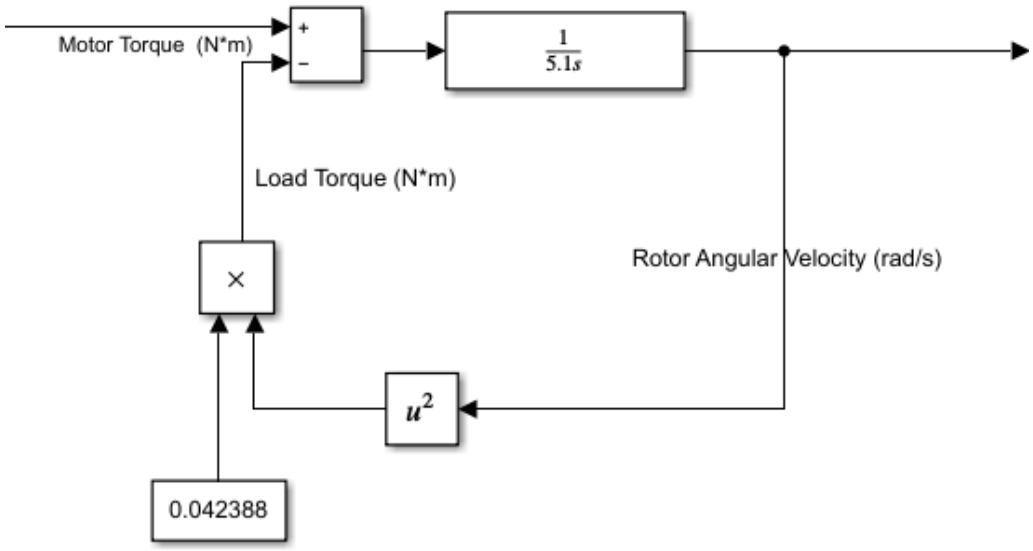

Figure 68 – Pump-motor system's transfer function

Please notice that in the PM system in Figure 68, the motor torque is positive, and it is the driving torque; the load torque is the torque required by the pump, which is subtracted to the motor torque, hence negative. On the contrary, in the TG system represented in Figure 69, the load torque, the one delivered to the generator is negative (as explained in section 2.3.), and the turbine torque, which in this case is the driving torque is positive since is a negative value that is being subtracted.

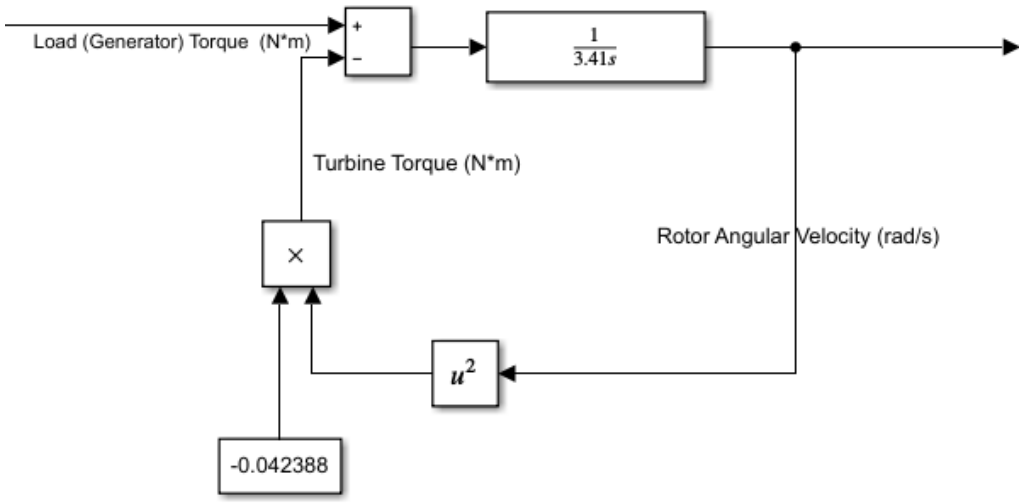

Figure 69 - Turbine-generator system's transfer function

The angular velocity transient that is obtained from this transfer function is described by the following exponential function:

$$\omega(t) = \omega_{\text{nom}} * (1 - e^{-\frac{t}{\tau}}) \tag{19}$$

Everything is known in this equation except for the time constant τ.

The time constant represents the time it would take to the system to reach steady state if the difference between the motor torque and the load torque would be constant. In other words, τ is the time it would take the rotating mass to reach nominal velocity starting from rest, if a constant acceleration was applied to it. So, rewriting the second equation of this section, it is possible to obtain the following equation:

$$T_{\text{M}} - T_{\text{L}} = J\frac{d\omega}{dt} = J * \frac{\omega_{\text{final}} - \omega_{\text{initial}}}{\tau} \tag{20}$$

Assuming that $\omega_{\text{final}} = \omega_{\text{nominal}}$ and $\omega_{\text{initial}} = 0$; recognizing that $\frac{T_{\text{M}} - T_{\text{L}}}{J}$ is the angular acceleration *a.* It is possible to write the following equation to calculate the system time constant which simply comes from the definition of acceleration:

$$\frac{T_{\text{M}} - T_{\text{L}}}{J} = \frac{\omega_{\text{nominal}}}{\tau} \tag{21}$$

So:

$$\tau = \frac{\omega_{\text{nominal}} * J}{T_{\text{M}} - T_{\text{L}}} \tag{22}$$

Where $T_{\text{M}} = 1027.6\, N * m$, the nominal torque; $T_{\text{L}} = 0$, since we supposed the initial condition is $\omega_{initial} = 0$ and load torque depends on the angular velocity, $\omega_{\text{nominal-pump}} = 155.7\, rad/s$ $\omega_{\text{nominal-turbine}} = 158.5\, rad/s$ and J has been previously calculated. Therefore:

$$\tau_{\text{pump}} = 0.777\, seconds \quad ; \quad \tau_{\text{turbine}} = 0.517\, seconds$$

To validate the calculation of the time constants, I also used the energy conservation principle. The nominal kinetic energy of the system is:

$$E_{\text{k-nominal}} = \frac{1}{2} * J * \omega_{\text{nominal}}{}^2 \tag{23}$$

While the initial is equal to zero since the system is at rest. If constant power of 160 kW is supplied to said system at rest, the time it will take to reach that value of kinetic rotational energy corresponds to the system time constant.

$$P * \tau = \frac{1}{2} * J * \omega_{\text{nominal}}{}^{2} \tag{24}$$

Substituting the correct values in Equation 24, the same time constants as with the other method are obtained.

E. The working principle of the DC Machine

As for the three-phase asynchronous machine, the explanation of the working principle of the DC machine will be concise, just to make the reader understand how it works and how some results are calculated.

One definition and explanation of a DCM can be given as follows: “DC machines include dc motors and dc generator. Machine operation is based on two fundamental electromagnetic interaction: a conductor moving in a magnetic field will have an electromotive force induced in it and a conductor carrying current and lying in a magnetic field will have a mechanical force acting on it” [11].

Figure 70 shows a representation of a schematic of the DC machine:

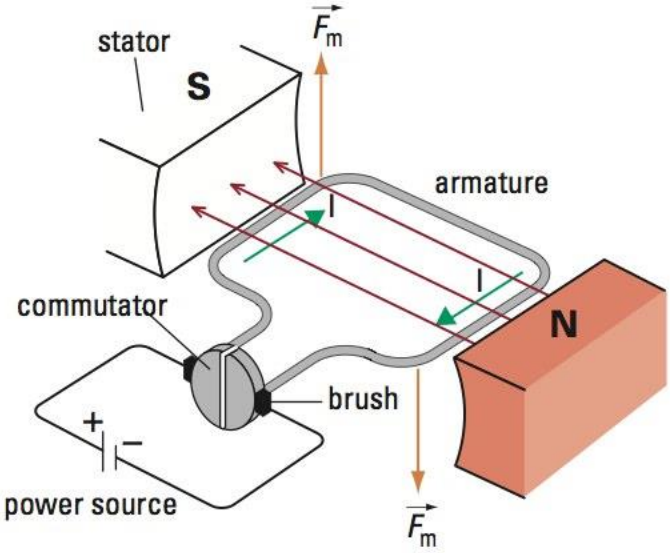

Figure 70 - DC machine working principle schematic [12]

This machine too is divided into two main parts: the stator and the rotor. The function of the stator is to produce a constant and uniform magnetic field, represented by the red arrows. This can be achieved either with two permanent magnets, as in the figure or with wire windings conducting current, in both cases, put one in front of the other. The rotor consists of a winding made of a conducting material called the armature. In motor configuration a power source connected to the rotor by two brushes generates a current that passed through the armature. A wire conducting current inside a magnetic field is subjected to the Lorentz force. This force is what induces motion in the rotor. When the armature passes the perpendicular position with respect to the magnetic field, the direction of the Lorentz force changes, and the

rotor would be forced to rotate in the opposite direction. The commutator ring is the element that does not allow this direction change to happen: it changes the polarity inside the armature making possible for the Lorentz force to always be directed in the same direction and, therefore, having the rotor rotating the same way. The more the windings in the rotor, the smoother will be the rotation.

In generator mode, the thing that differs is the fact that a driving external force makes the armature, which also in this configuration are conducting current, rotate inside the magnetic field generating an electromotive force (EMF) which is what produces electric power.

The generated EMF depends on the sine of the angle between the magnetic field and the direction of the current inside the armature. If only one armature is present, the EMF will have the shape of a sine function over time. Due to the commutator ring, the shape the EMF will have over time, is of the absolute value of a sine function EMF =|sin(θ)|. If more armatures are present, the EMF will be represented by the maximum EMF value produced by every armature at any instant in time as shown in Figure 71 by the red curve:

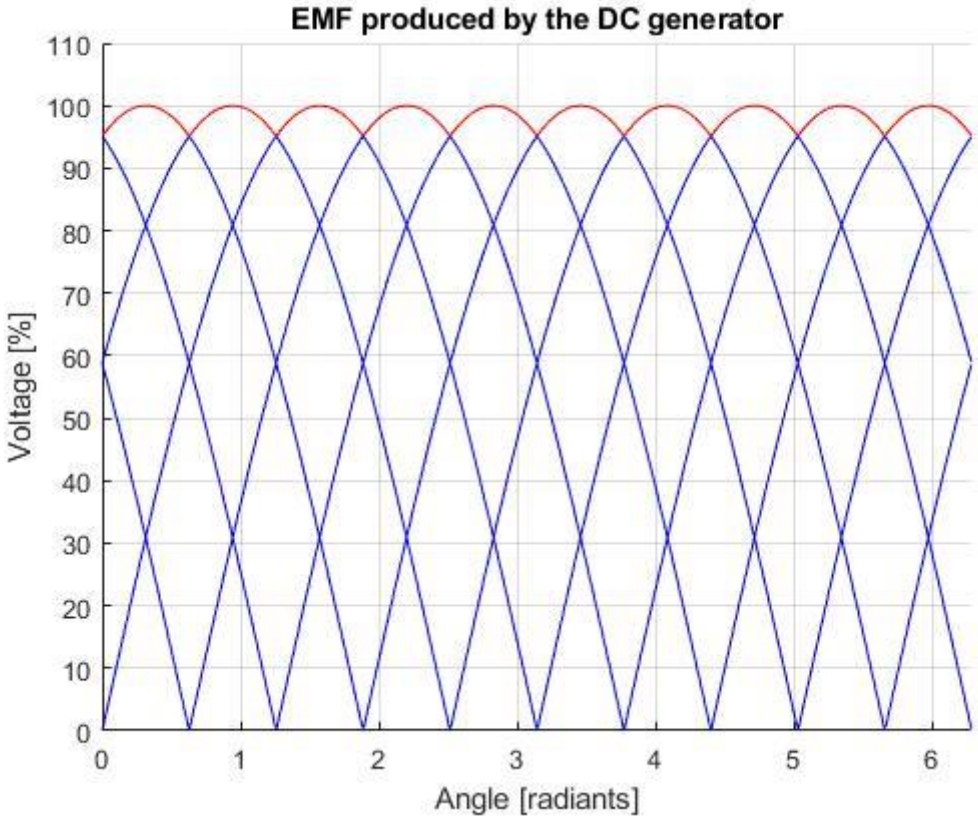

Figure 71 - Red line representing how the DC voltage is produced

According to this principle, more armature windings are present, the less the EMF produced is fluctuating. In the limit case where the number of armatures is infinite, the EMF produced is constant. This is why this type of machines are DC machines: the EMF, and hence the current produced, is constant and not fluctuating.

There are two crucial aspects about this machine that need to be addressed: the first is the fact that, since the machine is powered by a constant voltage source and, in generator mode, as just explained, it produces a constant voltage, in order to connect these machines to the grid the use of, respectively, a rectifier and an inverter is needed. These additional devices bring losses that, even if small, need to be accounted for in the model. The efficiency of the rectifier is assumed to equal to that of the inverter and equal to 98% [13].

The second issue that needs to be solved are the friction losses caused by the brushes connected to the commutator ring. Since the brushes are always touching the rotor, the friction between the two elements is a counterplayer in the power exchange process. Due to this problem, the efficiency of this type of motors is quite low compared to the other electric motors, and equal to 74% [14].

The most common practice to overcome this problem, is to use a variant to above-described type of machine: the Brushless DC machine (BLDC). The working principle of the BLDC is basically the same, what changes is the fact that “the rotor is a permanent magnet; the coils (armature) do not rotate but are instead fixed in place on the stator. Because the coils do not move, there is no need for brushes and a commutator” [15], one just needs to excite one coil at the time with the right frequency. “To change the rotation speed, you change the voltage for the coils” [15]. As you would change the armature voltage (as later will be better explained) in a Brushed DC machine. The efficiency of this type of machines can be considered equal to 98.4% [16].

Unfortunately, Simulink does not have a pre-set model for the BLDC machine that could be suitable to be inserted in my system. Since the working principle of the two machine is substantially the same, so is the way the speed control is performed and the machines’ characteristic are extremely similar to one another, I decided to use the Brushed DC machine block in my Simulink model considering, though, the better efficiency of the BLDC machine when it comes to calculating the process efficiency.

F. Implementation and confirmation of the model with the DC machine

As previously mentioned, the main limitation of TAMs is the fact that these machines are meant to work at constant speed, so velocity variations are not desirable. This peculiarity could be a limitation for the optimal behavior of the ocean battery; hence it would be useful to this study to add and study a variable speed motor and generator so to give more possibilities to the engagement and dispatch protocols of the Battery Managment System. If results coming from the Simulink model are consistent and similar to the ones of the TAM machine, this is a confirmation of the fact that the SImulink model works properly.

It has been decided to use the DC Machine (DCM). The reason why this was picked, is because it is a commonly used variable speed machine. It is also one of the pre-set models in Simulink, so all the electrical components are dimensioned with reliable values. If the implementation of another machines applied to the Simulink model leads to similar results, then the system itself can be considered reliable. Furthermore, if in a later stage there is need to study the behavior of the system with a different machine, the model should work with any type of motor and generator.

Nevertheless, there are some similarities between the two machines that, for simplicity's sake will not be explained again but just mentioned. The similarities are:

- Referring to Figure 5, the energy flows are the same for both machines.
- When the torque delivered by the machine is negative, then the machine is working in generator mode.
- The external characteristics of the pump and the turbine are the same.
- Stability is to be considered only on the pump-motor coupling.
- The inertia effects are accounted in the same way using the same transfer function. It only changes the value of the moment of inertia of the machines' rotor which are respectively $J_{DCmotor} = J_{DCgenerator} = 0.92$ kg/m^2.
- In the Simulink model everything remains the same except for the TAM blocks (which are, of course, substituted by the DCM blocks.
- The way the process efficiency is calculated is the same.

This section is not meant to compare the two machines since, being different elements, they cannot be compared. The meaning of this section is to introduce a variable speed motor and generator and to explain the characteristic of the DCM. Furthermore, this section is meant to explain that the proposed Simulink model works and could be used in the future with any

other electric machine model if the integration of the DCM in the model leads to the same behavior of the system as for the TAM.

a. Variable speed operation of the DCM

Once explained in Appendix E the working principle of the DCM, the motor and generator characteristic can be evaluated. To do so, it has been extrapolated the torque value delivered by the machine while working at speeds ranging from 0 to 200 rad/s with precision of 0.1 rad/s (speed = [0:0.1:200] in Matlab). It was done so, using the pre-set Simulink model which requires a constant field voltage of 300 V and an armature voltage of 500 V. This pre-set is meant to deliver a nominal power of 167 kW when working at angular velocity of 183 rad/s. The characteristic of this machine is shown in Figure 72:

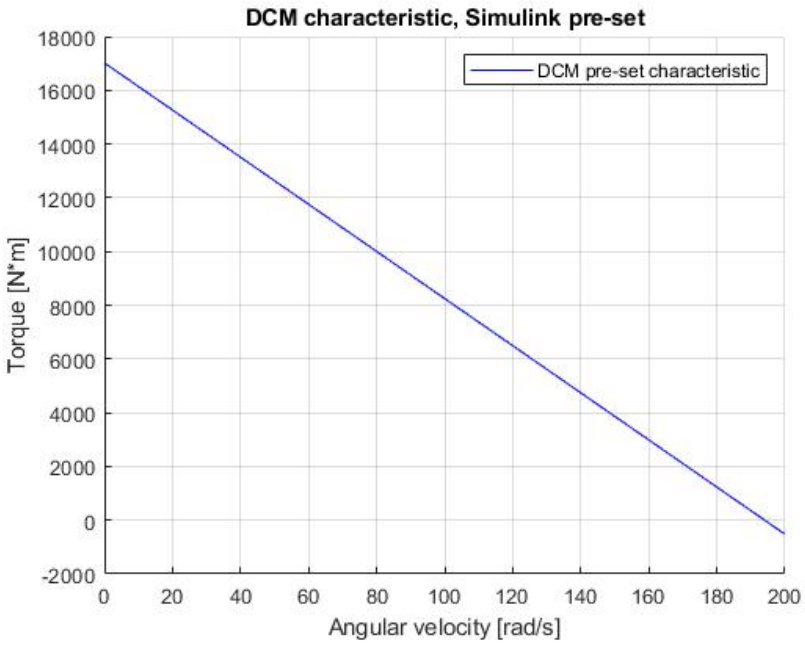

Figure 72 - DCM characteristic of the pre-set Simulink model

The DCM characteristic is represented by a straight decreasing line.

It is important to dimension the DCM in such a way that the nominal condition of this machine corresponds to the nominal condition of the TAM. In other words, it is important to change the DCM characteristic in such a way that at the TAM rated speed, 155.7 rad/s, or very close to it, corresponds the torque value that will deliver the rated power of 160 kW.

Changing the DCM characteristic is an easy and controllable process: changing the armature voltage (*Va*) is enough to substantially change the characteristic. Therefore, DCMs are extremely suitable for variable speed operations. When varying the *Va*, the slope of the

decreasing straight line will remain the same, while the thing that will change is the intercepts at the origin, making the whole curve shift down.

After a trial-and-error process, the *Va* value that corresponds to the desirable nominal condition is *Va* = 430.93 V. Appling this *Va*, it is possible to obtain an angular velocity of 155.72 rad/s and a torque value of 1025 N*m, which lead to a power output of 160 kW. Which is the same as the TAM nominal condition. Figure 73 shows the coupling of the pump and DCM working in nominal condition:

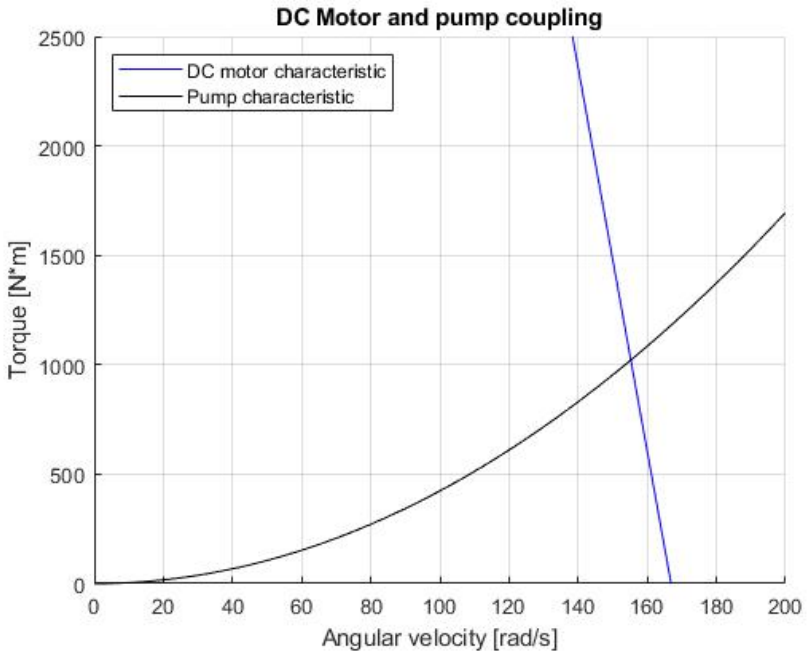

Figure 73 - DC Motor and pump coupling in nominal conditions

Once the nominal working condition has been represented, it is important to show how, varying the *Va*, also the DCM characteristic changes in order to show the different working points. Figure 74 shows the coupling of the two elements for different working conditions:

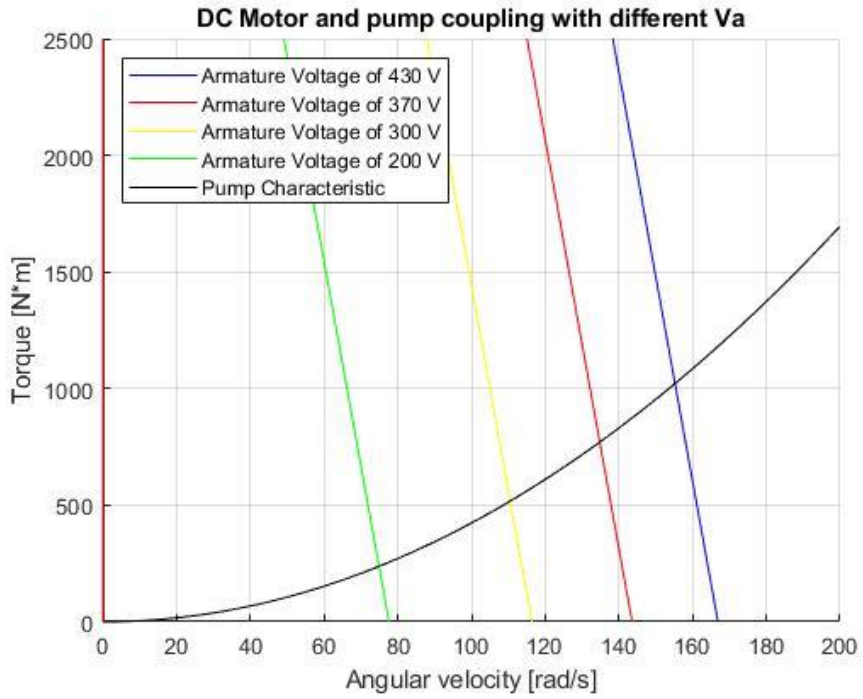

Figure 74 - Operational points with different applied armature voltage

Figure 74 confirms the reason why this type of machine is very versatile for variable speed operations: changing the armature voltage is practically an easy thing to do and the output is the desired one.

One last very important thing that is worth mentioning is the linearity of the dependence between the applied *Va* and the intercepts to the origin (that I will refer as "*q*" from now on) of the DCM characteristic. The slope of all the DCM lines is the same since it does not depend on the *Va*, what changes, as previously mentioned, is the interception with the y-axis, *q*. The value of *q*, and therefore the DCM's characteristic at a given *Va*, can be easily found in this way: *q* increases linearly as *Va* increases. If *Va* = 0, then also *q* = 0, when *Va* = 430 V then *q* = 14635 N*m. These values have been extrapolated from Matlab. In a very simple but effective way it was possible to calculate that the line representing the intercepts to the origin in function of *Va* is:

$$q = 34.0349 * Va \tag{5}$$

Furthermore, it has been calculated doing simulation that to every angular velocity of the pump characteristic corresponds one and only one power output. So, the logic behind the determination of the working *Va* is as follows:

- The power required is the degree of freedom: what is imposed and needs to be delivered.
- To any power requirement corresponds one and only one working point on the pump characteristic.
- To any working point corresponds one and only one DCM characteristic crossing it, that has a fixed slope.
- To any DCM characteristic corresponds one and only one *q.*
- Once having determined the value of *q,* using Equation 5 it is straight forward to calculate the *Va* that needs to be applied to the DCM in order to operate at a certain working condition.

The main conclusion that can be withdrawn from this disquisition is that to any given power demand corresponds one and only one armature voltage that needs to be applied to the DCM.
As last remark it is important to say that, even though the previous explanation has been carried out only for the PM system, everything that has been said it is also valid for the TG system. By lowering the armature voltage, it is possible shift the DCM characteristic in such a way that the operational point is a negative one. Again, also in this case, when running the DCM in generator mode, stability is not a concern.

References

[1] Usman, A. A., & Abdulkadir, R. A. (2015). Modelling and simulation of micro hydro power plant using matlab simulink. *International journal of advanced technology in Engineering and Sciences*, *3*, 260-272.

[2] Sala, R. (2012). *Impianti Idroelettrici e Turbine Idrauliche*, in: http://www-3.unipv.it/webidra/materialeDidattico/mdidattico.htm [visited on 20/04/2020].

[3] Mavel, a.s. (2015). *Mavel Turbines,* in: https://mavel.cz/turbines/ [visited on 20/04/2020].

[4] Stelzer, R. S., & Walters, R. N. (1977). *Estimating reversible pump-turbine characteristics* (No. 39). Department of the Interior, Bureau of Reclamation, Engineering and Research Center.

[5] Chen, L., & Lam, W. H. (2015). A review of survivability and remedial actions of tidal current turbines. *Renewable and Sustainable Energy Reviews*, *43*, 891-900.

[6] Poggio, A. (2017). *Fondamenti di macchine, Turbopompe.* Unpublished manuscript – Politecnico di Torino, Turin, Italy.

[7] Petrella, R. (2014). *Dynamic of Motor-load,* in: http://www.diegm.uniud.it/petrella/Azionamenti%20Elettrici%20(PN)/Complementary%20stuff%20chapter%202.pdf [visited on 12/05/2020]. Unpublished manuscript – Uniud, Udine, Italy.

[8] DOE, U. (2008). Improving Motor and Drive System Performance: A Sourcebook for Industry.

[9] Dijkstra, H., Barradas-Berglind, J., Meijer, H., van Rooij, M., Prins, W., Vakis, A., & Jayawardhana, B. (2016, November). Revenue optimization for the Ocean Grazer wave energy converter through storage utilization. In *Proc. of the RENEW2016 Conference* (pp. 207-213).

[10] Diyoke, G. C., Okeke, C., & Aniagwu, U. (2016). Different Methods of Speed Control of Three-Phase Asynchronous Motor. *American Journal of Electrical and Electronic Engineering*, *4*(2), 62-68.

[11] Keream, S. S., Mohammed, K. G., & Ibrahim, M. S. (2018). Analysis study in principles of operation of DC machine. *Journal of Advanced Research in Dynamical and Control Systems*, *10*(02), 2323-2329.

[12] *BBC Science (2020). Electromagnetism and magnetism,* in: http://sph3u1-0.blogspot.com/2013/06/jun-10-class-dc-motor-and-induction.html

[13] Mozzato, A. (2013). Rendimenti delle macchine elettriche e lo sviluppo dei motori ed inverter ad alta efficienza.

[14] Digilander (2020). *Indirect efficiency of the DC motor,* in: https://digilander.libero.it/riz30/miositolimonta/rendimento_indiretto_del_motore.htm#:~:text=Il%20rendimento%20del%20motore%20in,diretto%20oppure%20il%20metodo%20indiretto.&text=In%20questo%20caso%20il%20rendimento,erogata%20diviso%20la%20potenza%20assorbita [visited on 11/07/2020].

[15] Reneas Electronics Corporation. (2020). *Brushless DC Motors,* in: https://www.renesas.com/us/en/support/technical-resources/engineer-school/brushless-dc-motor-01-overview.html [visited on 11/07/2020].

[16] Atmaca, E. (2015). Energy management of solar car in circuit race. *Turkish Journal of Electrical Engineering & Computer Sciences*, *23*(4), 1142-1158.

[17] Homerenergy. (2020). *Battery Round-trip Efficiency*, in: https://www.homerenergy.com/products/pro/docs/latest/battery_roundtrip_efficiency.html [visited on 15/09/2020].

[18] TU Delft. (2019). *SET3815 System Integration Project. Per-minute load profile.* Unpublished manuscript.

[19] TU Delft. (2019). *SET3815 System Integration Project. Wind speed data.* Unpublished manuscript.

[20] Niekolaas, K. (2020). *Revenue maximization of distributed Ocean Battery systems through Model Predictive Control* (Doctoral dissertation).

[21] Ng, T. B. (2007). *Unsteady operation of the Francis turbine* (Doctoral dissertation, University of Tasmania).

[22] Electropedia. International Electrotechnical Commission. [visited on 20/12/2020].